Stochastic Differential Equation Theory Applied to The Modeling of Wireless Channels

Stochastic Differential Equation Theory Applied to The Modeling of Wireless Channels

By

Tao (Stephen) Feng, M.Eng, B.S.

A Thesis

Submitted to the School of Graduate Studies

in Partial Fulfilment of the the Requirements

for the Degree

Doctor of Philosophy

McMaster University

Doctor of philosophy (2008) McMaster University

(Electrical Engineering) Hamilton, Ontario

TITLE:	Stochastic Differential Equation Theory Applied to The Modeling of Wireless Channels
AUTHOR:	Tao (Stephen) Feng, M.Eng. (McMaster University), B.S. (Univ. of Sci. & Tec. of China)
SUPERVISOR:	Dr. Tim Field
CO-SUPERVISOR:	Dr. Simon Haykin
NUMBER OF PAGES:	xiv, 137

Abstract

Ever faster data transmission in wireless communication is desired to satisfy emerging markets for various media services, such as voice, picture and video calls, multimedia messaging, music and video downloads, and even television. With the explosive increase in the use of mobile devices such as cellular phones, PDAs, GPS, and laptop computers, power consumption has become a prime consideration in the design of mobile communication systems. In order to reliably maintain a high rate of transmission and low power consumption, it is imperative that the receiver obtains as much knowledge as possible about the current state of the channel. A more accurate model of wireless communication channels will indisputably help in obtaining more knowledge about the transient channel state, providing a more accurate and efficient reproduction of the transmitted signal, and decreased power consumption by the receiver. With careful choice and consideration of the channel model, systemic optimization based on the selected channel model will improve the system performance of the transmitter and receiver through better encoding and decoding, as well as through better control of transmitted signal's power level. This thesis focuses on understanding the physical and statistical characteristics of wireless

channels, and investigates how to represent wireless channels using simple mathematical models.

This thesis initially studied a simple time-varying stationary channel, i.e. a multipath flat fading channel without terminal motion, which is typically used for indoor wireless communication. With an introduction of stochastic differential equations, we derived a first-order AR stochastic process to represent this stationary channel. For a general multipath flat fading channel with terminal motion, the traditional Clarke's model was then extended by incorporating the effects of fluctuations in the component phases and analyzed statistically.

The resulting theoretical power spectrum was shown to fit practical measured spectra, in contrast to the traditional theoretical flat fading channel spectra (*Jakes' spectrum* in [19]).

Finally, we developed a state-space model that represents a wireless channel using these modified spectral characteristics. This was achieved by developing a relationship between the state-space model and the theory of a rational transfer function. A novel method for designing a rational transfer function for linear systems was then proposed. In this method, the rational transfer function is represented via the *Observable Canonical Form* (OCF) to obtain the state-space model, which can be used to represent and simulate a flat fading wireless channel. The presented state-space approach is simple and provides rapid computation. The present AR and state-space models provide valuable contributions that can be integrated with other algorithms for better system optimization of wireless communication networks.

Acknowledgment

Completing my Ph.D. has been a special period in my life. I have experienced trials and tribulations, along with success and happiness. Writing a dissertation would obviously not be possible without the personal and practical support of many people.

Firstly, I would like to express my gratitude to my supervisor, Dr. Tim Field, for his support and belief in my abilities. With his enthusiasm, his inspiration, and his exceptional clarity of explanation, he helped my research become first-class publications. He provided encouragement, sound advice, good teaching, good company, and plenty of good ideas. I would also like to thank my co-supervisor, Dr. Simon Haykin, for his financial and intellectual support. With his patient and insightful guidance, I have learned how to think carefully as a researcher.

I would like to thank my committee members, Dr. Sui Feng and Dr. T. Kiruba, for their helpful comments on my research and thesis, and Dr. Jian-Kang Zhang for his helpful suggestions on my research path and pleasant company on the badminton court. I am also grateful for the friendship extended by Ke (Kevin) Zhang, Yu Wu, Yanbo Xue.

Lastly, and most importantly, I wish to thank my parents, Ru-An Feng and Dao-Qing Xu. They bore me, raised me, supported me, taught me, and loved me. To them I dedicate this thesis.

Contents

List of Figures

Preface

Portions of this thesis relate to published material co-authored by the candidate, as listed below:

- T. Feng, T.R. Field, and S. Haykin, Stochastic Differential Equation Theory Applied To Wireless Channels, IEEE Trans. on Communication, Volume 55, Issue 8, Aug. 2007, pp. 1478 - 1483 .
- T. Feng, T.R. Field, Statistical Analysis of Mobile Radio Reception – an Extension of Clarke's Model, IEEE Trans. Comm., accepted for publication, August 2007 (in production)
- T. Feng, T.R. Field, A State-Space Model for Flat Fading Channels with a Novel Method of Rational Function Filter Design, submitted to IEEE Trans. Wireless Comm. (accepted for publishing with minor revision)
- T. Feng, T.R. Field, Novel PSD Function for Multipath Flat Fading Channels, accepted for PIERS 2008 in Cambridge, USA. (presentation)
- T. Feng, T.R. Field, State-space Model for Multipath Flat Fading Channels, accepted for PIERS 2008 in Cambridge, USA. (presentation)

Chapter 1

Introduction

1.1 Motivation for The Problem

The term wireless normally refers to any type of electrical or electronic operation accomplished in space without the use of a "hard wired" connection, though this may be accomplished using wires if desired. Wireless communication is the transfer of information over a distance using wireless methods, i.e. without “wires”; often, is simply shortened to "wireless". The distances involved may be short (a few meters, such as a television remote control) or very long (thousands or millions of kilometers for radio communications). As a branch of telecommunications, wireless communications is rapidly developing and intimately connected with every day life.

Wireless technology is ubiquitous in daily life, such as cellular telephones, personal digital assistants (PDAs), and wireless local area networking (wireless LAN), bluetooth networking (mice, keyboards, headsets, etc), global position-

ing systems (GPS), satellite television, cordless telephones, keyless entry, and many others. In effect, there too many wireless applications to list here.

Generally speaking, wireless communication involves three types of communication:

* radio frequency communication

* microwave communication, for example long-range line-of-sight via highly directional antennas, or short-range communication

* infrared (IR) short-range communication, for example from remote controls.

Applications may involve point-to-point communication, point-to-multipoint communication, broadcasting, cellular networks, and other wireless networks.

Sometimes the term "cordless" is confused with the term “wireless”; while the former terminology generally refers to powered electrical or electronic devices that operate from a portable power source (e.g., a battery pack) without cables to limit their mobility, such as cordless telephones, these devices are also wireless in the sense that information is transferred from the device to a base unit via some type of wireless communication link.

With the developments of semiconductor technology, information theory, signal processing, practical electromagnetism, computer software, and others, wireless communication is now becoming more complicated and powerful. Faster data transmission in wireless communication is required to satisfy the demands of emerging media markets, such as video calls, multimedia messaging, music and video downloads, and even television. Whether market driven or technology pushed, current trends in our society incite people to de-

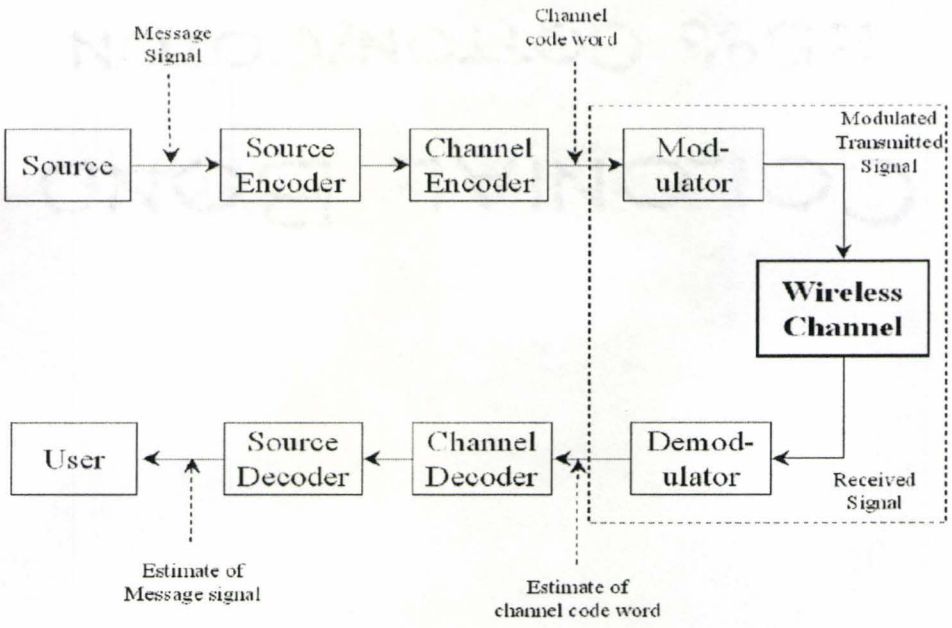

Figure 1.1: Wireless communication system

sire instantaneous information delivery, regardless of time or location. These demands necessitate continually improving performance from wireless communication networks.

A typical wireless communications system is shown in Figure 1.1. Compared to wired communication, the design of wireless communications system is considerably more complicated, and requires much more effort to reliably transmit data in noisy wireless environments. As the core of wireless communication systems, the channel coder/decoder and channel estimator have to be well designed and implemented to compensate for random interference from wireless channels and to be able to restore transmitted information. A more accurate representation, or model, of a wireless communication channel will

lead to more appropriate transmitter and receiver designs for encoding and decoding data, as well as better control over the power level of the transmitted signal and choice in the transmission rate and modulation schemes. Transmission rates and power consumption are very important factors designing mobile receivers for consumers. With due consideration and careful selection of the channel model, as well as optimization of other channel model dependent components of the wireless system, more accurate and efficient reproduction of the transmitted signal by the receiver will be possible.

For most everyday applications, wireless communication is a multiuser environment, such that the signals transmitted by users could interfere each other. Known as jammers, or inter-symbol interference technically, this must be accounted for in the system design. If the receiver knows the channel characteristics of the other users and has information about their transmitted signals, these signals can be subtracted from the total signal to improve the performance of the estimated transmitted data intended for that receiver. Thus, better characterization and modeling of the wireless channel may help to minimize inter-symbol interference from other users.

1.2 Overview of Channel models

From a simple introduction of wireless communication, it's clear that modeling a wireless communication channel is one of the most fundamental components on which transmitters and receivers are designed and optimized. The transmitted signal arrives at a receiver from different directions, having traveled via

different paths and undergone different attenuations, phase shifts and time delays, leading to random fluctuations in the signal strength. As well, the strength of the received signal decreases as the distance from the transmitter increases.

Reductions in the power of the received signal, which experiences time-variation caused by changes in the transmission medium or path (channel), is referred to as *fading*. Based on different fading environments, two channel models are classified for characterizing the statistical properties of the received signal. One is short-term fading, also called multipath fading, which corresponds to severe signal envelope fluctuations that occur in densely built-up areas over short distances or periods of time. The other is the so called *Log-normal shadowing*, or large-scale fading, corresponding to less severe mean signal envelope fluctuations that occur in larger and less populated suburban areas, where transmitter-receiver separation distances are larger (several hundred or thousands of meters).

Ossanna [55] was the pioneer who characterized the statistical properties (waveforms, power spectra, frequency power spectra, etc.) of the received signal produced by a set of interfering waves reflected from the planar surfaces of buildings and houses in the vicinity of a mobile station. His model was better suited to describing fading occurring mainly in suburban areas. Clarke [26] produced a model that characterized interfering signals as a set of random azimuthal waves, each having a random phase and arbitrary azimuth. This scattering model was the first comprehensive scattering model to predict time and frequency domain channel characteristics, which was suited to describing

the short-term fading that occurs mainly in urban areas (see also [57, 56]). The short-term models can provide various distributions for the received signal amplitude (Rayleigh, Ricean, etc.), as well as information on the power spectrum (Doppler spectral density) of the wireless channel. The log-normal shadowing model can predict the average power loss due to distance and power loss due to signal reflection from surfaces. When measured in dB, the power loss coefficient fits a log-normally distribution, from which the log-normal shadowing model is named (see also [58, 59, 60]). Besides the large-scale and small-scale fading phenomena, the channel may contain impulsive noise occurring in short bursts originating from e.g. car engines, jet engines, machines in factories etc.. In this thesis, the impulsive noise will be ignored in the modeling of wireless channels.

For small-scale / multipath fading channels, the amplitude of the received signal can be viewed as a continuous-time stochastic process in terms of its rapid fluctuations. Stochastic differential equations (SDEs) have been applied in the study of radio communications in the literature, dating back to the work of Stratonovich [1] and Rytov [2, 3]. The SDE approach was further applied to the system analysis for synchronization problems by Lindsey in [4]. Recently, Primak and Kontorovich published a series of results (in English) on the application of SDEs to the synthesis of a stochastic process with given statistical characteristics [5, 6]. The results developed by Primak et al. are applied to the modelling of various communication channels, radar signals, etc. [5, 7, 8]. Comparing with these SDE applications, most of the research work described in the current thesis deals with the constructive approach,

i.e. that of deriving an SDE for the dynamics of the multipath channel, from first principles, from which all of its statistical characteristics can be deduced [27, 28].

This thesis is primarily concerned with the short-time statistical characteristics and modeling of wireless channels (i.e. multipath fading channel), which are closely interconnected with the techniques implemented in wireless systems, such as channel coding / decoding, channel estimation, channel equalization, etc. These techniques are used to remove the effects of noisy channels on the performance of transmission. The original contributions in this work may be found in the presentation of an advanced statistical analysis (stochastic differential equation) of the traditional Clarke's model, in the provision of a new scattering multipath model as an extension of Clarke's work, and in a state-space dynamic representation of an arbitrary flat fading channel that provides very good performance.

1.3 Thesis Overview

This thesis includes six chapters, organized as follows. The thesis begins with a review of previous work and provides an introduction. Chapter 2 of this thesis provides a background in wireless channel propagation, including various channel models, giving some basic conception and necessary information for subsequent discussions of more advanced channel models.

Chapter 3 introduces stochastic differential equations (SDE) as a very useful mathematical tool in statistical analysis. Readers are assumed to have

basic knowledge of statistics, such as probability, distribution, random variables, stochastic process, etc. The contents of this chapter are not intended to provide a complete discussion of the associated mathematical theory and analysis, though a tutorial is provided for use of SDEs in solving simple research problems, as well as to facilitate comprehension in the ensuing chapters.

Chapter 4 reviews a simple scattering model for a wireless multipath channel without Doppler frequency shift. The novelty of this simple scattering model focuses on fluctuations in the component phases, which are often treated as a time-invariant random variable in the literature; however, it has been presented in [12, 13] for a discussion of statistical characteristics of sea-clutter. Advanced mathematics (SDE) is used for a strict analysis of the presented scattering model, as well as to provide a solution of the simple dynamic model. While long assumed to be true in the literature with minimal reasoning, the first-order AR process as a discrete SDE was proven to be an appropriate model for the presented scattering model.

Chapter 5 adopts the same fluctuation considerations in the component phases for Clarke's well known scattering model. With further statistical analysis of this extended Clarke's model, we obtained a novel autocorrelation expression and the power spectrum for a flat wireless fading channel. The traditional *Jakes' spectrum*, which results from Clarke's model, is unlimited when frequency components are near the positive or negative maximum Doppler shift, and is zero when the frequency component is larger than the maximum positive Doppler shift or smaller than maximum negative shift. For any measured power spectral density, its curve always reaches a vertex around

the maximum Doppler shift and rapidly decreases to zero. Compared with the traditional Jakes' U-shape spectrum, the presented novel power spectrum curve more closely approximates the measured power spectrum for a real wireless channel, and is more flexible in shape control. To build a dynamic model for an arbitrary measured power spectrum, or the presented theoretical spectrum, we used knowledge of linear systems to design a transfer function with a standard Gaussian noise input to achieve the desired output power spectrum. As a special rational function (filter) design, this novel method is fast and stable. Correspondingly, state-space models can be used to describe the linear system with an arbitrary rational transfer function. One of these state-space models is called *Observable Canonical Form* (OCF), which was used to generate wireless channel data in the time domain with desired power spectrum. The presented state-space model approached the desired power spectrum with very small relative error (see also on page 103), providing a fast and simple channel simulator that can be easily implemented in both software and hardware.

Chapter 6 summarizes the work contained in this thesis and discusses potential future lines of investigation.

Chapter 2

Wireless Channel Propagation and Noise

2.1 Introduction

The mobile radio channels[1] are an important factor in the performance of wireless communication systems, making it necessary to have a firm understanding of their functioning. The transmission path between the transmitter and the receiver can vary from a small distance (simple line-of-sight) to a large distance, such as one severely obstructed by buildings, mountains, and foliage. Unlike stationary wired channels, radio channels are extremely random and cannot be easily analyzed mathematically; even the speed of relative motion between the transmitter and receiver impacts how rapidly signal level changes. Modeling radio channels has historically been one of the most difficult parts

[1] A *channel* refers to the impulse response between the transmitted and the received signal.

of mobile radio system design, and is traditionally done in a statistical fashion based on measurements made specifically for an intended communication system or spectrum allocation.[39]Some novel methods of modeling channels are based on advanced mathematical analysis and reasoning, including stochastic differential equations.[27, 28]

The mechanisms behind electromagnetic wave propagation are diverse, but can generally be attributed to reflection[2], diffraction[3], and scattering[4].[39] Most current cellular radio systems operate in urban areas where there is no direct line-of-sight path between the transmitter and the receiver, and where the presence of high-rise buildings causes severe diffraction loss. Due to multiple reflections from various objects, the electromagnetic waves have to travel along numerous paths of varying length before arriving at the receiver. The total effect of the interaction between these waves causes multipath fading at a specific location, and the strength of the received signal waves decreases as the distance between the transmitter and receiver increases.[39]

[2] *Reflections* occur when an electromagnetic wave impinges on a surface with dimensions larger compared to the wavelength of the propagating wave.

[3] *Diffraction* is due to the initiation and propagation of secondary wavelets from the main wavefront in the presence of an obstacle or an obstruction. These secondary wavelets combine to form a new wave front allowing the main wave to propagate in shadowed regions or behind obstructions. The field strength of such wave decreases rapidly as the receiver moves further into the shadowed regions.

[4] *Scattering* (where the term is borrowed from the particle theory of light) occurs when an electromagnetic wave impinges on a surface with dimensions smaller compared to the wavelength of the propagating wave.

2.2 Large-Scale Path Loss

The general term fading is used to describe fluctuations (mostly irregular) in the envelope of a radio signal arriving at the receiver. When such fluctuations are discussed, it must be considered whether a short observation interval (or small distance), or a long observation interval (or large distance) has been taken. Different propagation models apply to different distances of propagation from the transmitter to the receiver.

In the literature, two classes of modes are used for radio propagation. Propagation models that characterize signal strength over large transmitter-receiver (T-R) separation distances (hundreds or thousands of meters), known as *large-scale* propagation models, are useful in estimating the radio coverage area of a transmitter. On the other hand, propagation models that characterize the rapid fluctuations (mostly irregular) of the received signal strength over very short travel distances (a few wavelengths) or short time durations (on the order of seconds) are called *small-scale* or fading models.[39]

2.3 Small-Scale Fading and Multipath

For wireless communication, the amplitude of a radio signal changes rapidly over a short period of time or travel distance. This is known as small-scale *fading*. Radio signals travel through two or more paths to arrive at the receiver at slightly different times, resulting in a combined signal at the receiver with random fluctuations in amplitude and phase. This phenomenon is referred to as *multipath* propagation / fading.

Radio waves coming from different directions with different propagation delays causes the received signal by a mobile at any point in space to contain a large number of plane waves having randomly distributed amplitudes, phases, and angles of arrival. These multipath components cause the signal at the mobile receiver to distort or fade. When the mobile receiver is moving, each multipath radio wave experiences a shift in frequency due to the Doppler effect, called Doppler shift, which is proportional to the velocity of the receiver and the angle between the mobile receiver's direction and the arrival direction of the received multipath wave. At any instant in time, radio waves travelling over different multipaths have different Doppler shifts with different amplitudes, creating a random-like total received signal wave. Even when the mobile receiver is stationary, i.e. no Doppler shift on the multipath wave, the received signal still fluctuates due to the motion of scatterers within the channel (i.e. the scattering properties of the radio propagation medium). The mathematical descriptions of these fluctuations in radio (flat) channels for a stationary or non-stationary receiver are discussed in chapters 4 & 5.

2.3.1 Flat & Frequency Selective Fading

If a mobile radio channel has a constant gain and linear phase response over a bandwidth that is greater than the bandwidth of the transmitted signal, then the received signal will undergo *flat fading*, i.e. a channel passes all spectral components of transmitted signal with approximately equal gain and linear phase.[39]When a transmitted signal passes through a flat channel, the

received signal is represented as:

$$r(t) = h(t)s(t), \tag{2.1}$$

where $r(t)$ is the received signal, $s(t)$ is the transmitted signal, and $h(t)$ is a flat channel, which is a stationary stochastic process.

If the channel possesses a constant-gain and linear phase response over a bandwidth that is smaller than the bandwidth of transmitted signal, then the received signal will undergo *frequency selective fading.*[39] For such a channel, the received signal includes multiple copies of the transmitted waveform that are attenuated (faded) in amplitude and delayed in time. When a transmitted signal passes through a flat channel, the received signal is represented as:

$$r(t) = \sum_{n=1}^{L} h_n(t)s(t - \frac{n}{w}),$$

where $s(t)$ is the transmitted signal, $r(t)$ is the received signal, L is the number of copies of the transmitted waveform at receiver, w is the bandwidth of the transmitted signal, and $\{h_n(t)\}$ are stationary stochastic processes.

2.4 Statistical Models for Multipath Fading Channels

In the literature, several multipath models have been suggested to explain the observed statistical nature of a wireless communication channel. One model

in particular, Clarke's model based on scattering, is the most widely applied.

In 1968, Clarke developed a mathematical model to represent a channel fading from scattering. The model assumes a fixed transmitter and N incident multipath waves with arbitrary relative phases, arbitrary azimuthal angles of arrival, and equal average amplitude.

For the kth path signal wave arriving at an angle ψ_k (measured by the direction of wave radiation and the terminal motion), the component Doppler shift is given by:

$$f_k = \frac{v}{\lambda} \cos \psi_k \tag{2.2}$$

where v is the speed of the receiver, and λ is the wavelength of the incident wave. With a relative phase $\varphi^{(k)}$ assumed as uniformly distributed on the interval $[0, 2\pi)$ and an amplitude x_k for the kth path signal wave, Clarke's model is defined as follows:

$$\varepsilon_t = \sum_{k=1}^{N} x_k \exp[j(2\pi f_k t + \varphi^{(k)})]. \tag{2.3}$$

The autocorrelation of the envelop ε_t at the receiver is given by [26]:

$$\begin{aligned} R_\varepsilon(\tau) &= \mathbf{E}[\varepsilon_t \varepsilon^*_{t+\tau}] \\ &= P_0 J_0(2\pi f_D \tau), \end{aligned} \tag{2.4}$$

where f_D is the maximum Doppler frequency shift (equal to v/λ), P_0 is the average amplitude ($= \mathbf{E}[x_k]$), and $J_0()$ is a zeroth-order Bessel function of the first kind. The channel autocorrelation defined in Eq. (2.4) is plotted in

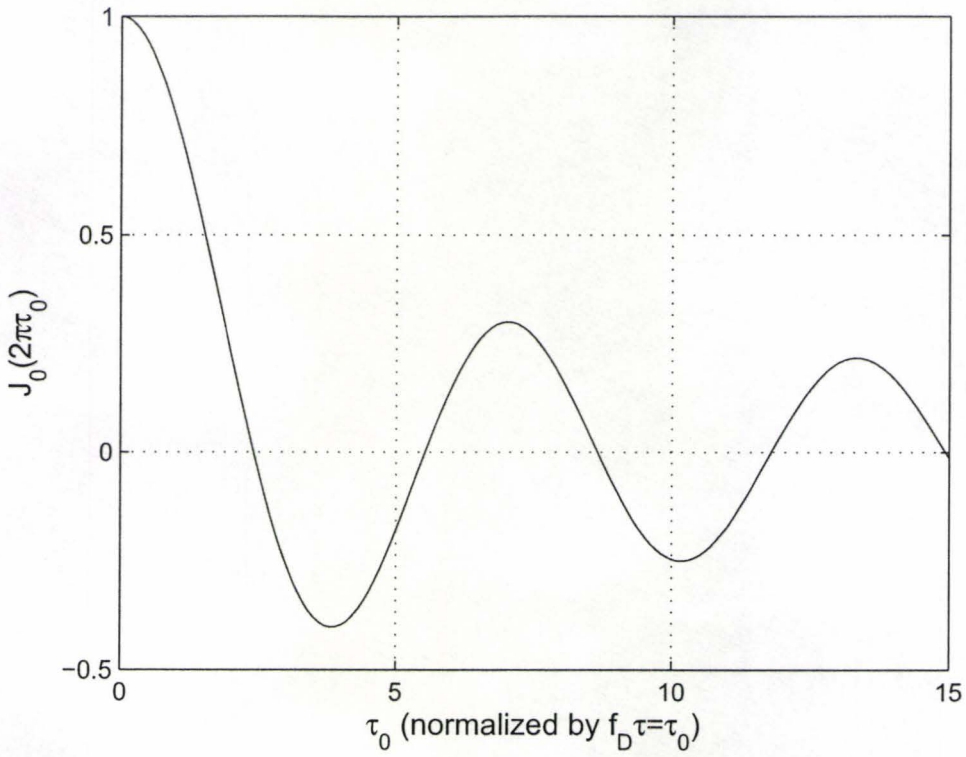

Figure 2.1: Autocorrelation of channel from Clarke's model with $P_0 = 1$ and $f_D\tau = \tau_0$

Figure 2.1. We know that for a stationary channel, the power spectrum can be obtained from the Fourier transform of the autocorrelation function:

$$\begin{aligned} S_\varepsilon(f) &= \mathcal{F}\{R_\varepsilon(\tau)\} \\ &= P_0\mathcal{F}\{J_0(2\pi f_D\tau)\} \\ &= \begin{cases} \frac{P_0}{\pi f_D\sqrt{1-(f/f_D)^2}} & |f| < f_D \\ 0 & |f| > f_D \end{cases} \end{aligned} \tag{2.5}$$

where $\mathcal{F}\{\cdot\}$ is the Fourier transform operator. A plot of the power spectrum

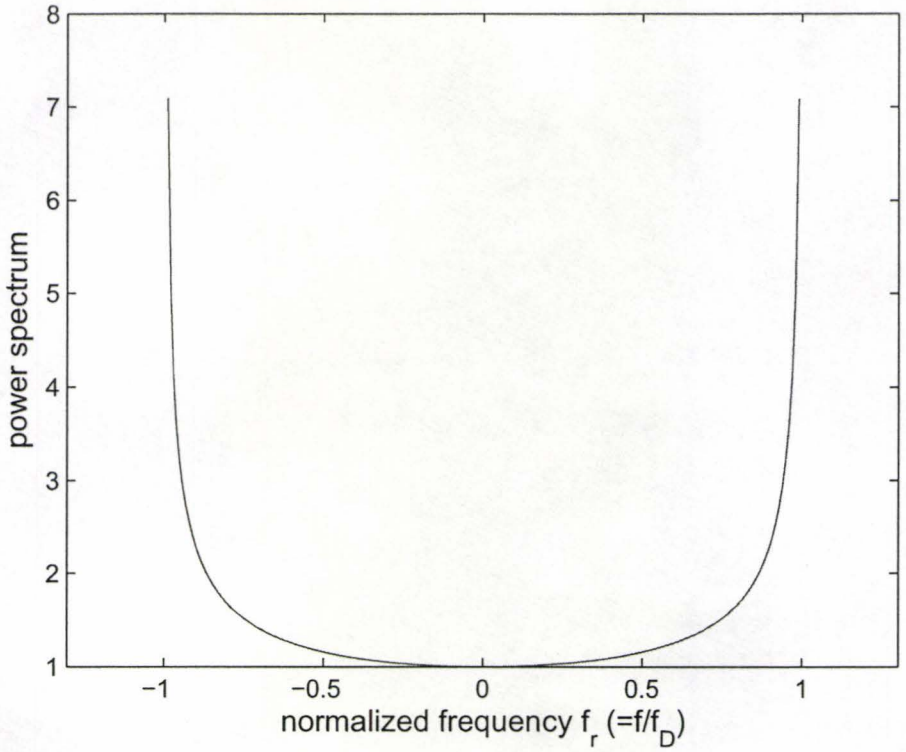

Figure 2.2: Model of power spectrum for a mobile radio channel based on Clarke's model

for a mobile radio channel, represented as $S_\varepsilon(f)$ in Eq. (2.5), is shown in Figure 2.2.

The power spectrum in Eq. (2.5) was initially developed by Gans [41] as a spectrum analysis for Clarke's model. In 1974, W. C. Jakes, Jr. [19] published his book, "Microwave Mobile Communications", in which he included Clarke's model and Gan's results. Since Jake's book became famous, Clarke's fading channel model and Gan's results on power spectrum are also referred to as Jakes' model or Jakes' spectrum in the literature.

Although Clarke's model and Jakes' spectrum are suggested for many international communication standards, such as International Mobile Telecommunications-2000 (IMT-2000), the global standard for third generation (3G) wireless communications, it has some limitations in representing the measured flat fading channel, such that the Clarke's model cannot describe channel fluctuation when the mobile receiver is stationary. Similarly, Jakes' spectrum cannot specify the peak value and has a fixed spectral width, $2f_D$, whereas the real measured spectrum will reach a peak near the maximum Doppler frequency and then decay to zero (see Figure 5.3 in section 5.2.2). These shortcomings in Clarke's model and Jakes' power spectrum can be overcome by introducing fluctuations in the relative component phases, i.e. $\varphi^{(k)}$ in Clarke's original model (2.3). A comprehensive discussion of extending Clarke's model, including detailed mathematical reasoning, can be found in section 5.2, Chapter 5.

2.5 Summary

The objective of this chapter is to introduce general knowledge of wireless channels, and their characteristics and associated models, so that the readers will possess sufficient background knowledge to read and understand the remainder of this thesis.

In this chapter, we discussed wireless radio propagation, focusing on multipath and small-scale fading, and the statistical modeling of multipath fading channels. With the exception of the last paragraph of the final section, this

knowledge can be traced back more than thirty years in the literature. However, research on radio propagation continues to develop, benefitting from advanced mathematical knowledge such as stochastic differential equations and new statistical channel models. My contribution to the radio propagation is discussed in chapter 5. Comparing to the traditional Clarke's channel model, the new channel model approximates more closely the real measured wireless channels in both the time and frequency domains (power spectrum).

Chapter 3

Stochastic Differential Equations

3.1 Introduction

A stochastic differential equation (SDE) is a differential equation in which one or more of the terms is a stochastic process. The solution of SDE is also a stochastic process. In mathematics, an equation of the form

$$dx_t = b(t, x_t)dt + \sigma(t, x_t)dB_t \tag{3.1}$$

is called a stochastic differential equation (SDE), where x_t denotes a stochastic process, $b(t, x_t)$ and $\sigma(t, x_t)$ are functions of t and x_t, B_t denotes a Wiener process (standard Brownian motion, see 3.2). The Wiener process is non-differentiable and requires its own rules of calculus. Thus the interpretation of the SDE expression in (3.1) requires additional background of mathematics, which is to be introduced in the following sections.

The SDE theory is traditionally used in physical science and financial math-

ematics. Recently, more researcher has been conducted in the application of SDE theory to various areas of engineering. SDEs have been successfully used to model and analyze K-distributed electromagnetic scattering in [12]. A first-order stochastic autoregressive model for a flat stationary wireless channel based on SDE theory is introduced in [27]. Stochastic channel models based on SDEs for cellular networks have been presented in [15].

This chapter is organized as follows. Firstly in section 3.2, we introduce the concept of *Brownian Motion*, which is fundamental to the SDE theory. Then, in section 3.3, we explain the Ito's calculus, relating it to the traditional Riemann integral, which is more familiar to engineers. The notion of stochastic differential equation is based on the Ito's calculus. Finally, we summarize the tools of Ito calculus in section 3.4.

3.2 Brownian Motion

Brownian motion, named after the botanist Robert Brown, refers to either the random movement of particles suspended in a fluid or the mathematical model used to describe such random movements, often called a Wiener process.

Brownian motion is among the simplest continuous-time stochastic processes, and it limits both simpler and more complicated stochastic processes. This universality is closely related to the universality of the normal distribution. In both cases, it is often mathematical convenience rather than model accuracy that motivates their use.

In mathematics, the Wiener process is a continuous-time stochastic pro-

cess named in honour of Norbert Wiener, an American theoretical and applied mathematician. He was a pioneer in the study of stochastic and noise processes, contributing work relevant to electronic engineering, electronic communication, and control systems. The Wiener process plays an important role both in pure and applied mathematics. Specifically, it plays a vital role in stochastic calculus, diffusion processes, and even potential theory. In applied mathematics, the Wiener process is used to represent the integral of a white noise process, and so is useful as a model of noise in electronics engineering, instrument errors in filtering theory, and unknown forces in control theory.

3.2.1 Mathematics Definition of Brownian Motion

A stochastic process is a phenomenon which evolves over time in a random way. Thus, a stochastic process is a family of random variables X_t, indexed by time (or in a more general framework by a set T). A realization of a sample function of a stochastic process $X = (X_t; t \in T)$ is an assignment, where $t \in T$, of a possible value of X_t. Thus, we obtain a random "curve" referred to as the *trajectory* or *path* of X. A basic but very important example of a stochastic process is the *Brownian motion process.*

A one-dimensional standard *Brownian motion* or *Wiener process* is a real-valued stochastic process $\{B_t; t \geq 0\}$, satisfying the following:

1. $B_0 = 0$.

2. For any $t_0 < t_1 < \cdots < t_n$, the random variables B_0, $B_{t_1} - B_{t_0}$, $\cdots$, $B_{t_n} - B_{t_{n-1}}$ are independent variables.

3. For any $t_1 < t_2$, the probability distribution of $B_{t_2} - B_{t_1}$ is a Gaussian distribution with zero mean and a variance of $(t_2 - t_1)$, i.e., $B_{t_2} - B_{t_1} \sim N(0, t_2 - t_1)$.

4. B_t is almost surely continuous.

These properties stipulate that the motion is continuous but nowhere differentiable. Intuitively, the displacement $B_{t_2} - B_{t_1}$ over the time interval $t_2 - t_1$ can be regarded as the sum of a large number of small independent displacements. The central limit theorem is applicable, and it is reasonable to assume that $B_{t_2} - B_{t_1}$ is normally distributed (in fact, it is also necessary to assume the continuity of the trajectories). Similarly, it seems reasonable to assume that the distributions of $B_{t_2} - B_{t_1}$ and $B_{t_2+h} - B_{t_1+h}$ are the same for any $h > 0$, if we assume the medium to be in equilibrium. Finally, the displacement $B_{t_2} - B_{t_1}$ should clearly depend only on the length $t_2 - t_1$ and not on the time at which the observation begins. A natural extension of B is the d-dimensional Brownian motion defined by d independent copies $B^1, B^2, \cdots, B^d$ of B. Figure 3.1 shows a trajectory example for 2-dimensional Brownian motion.

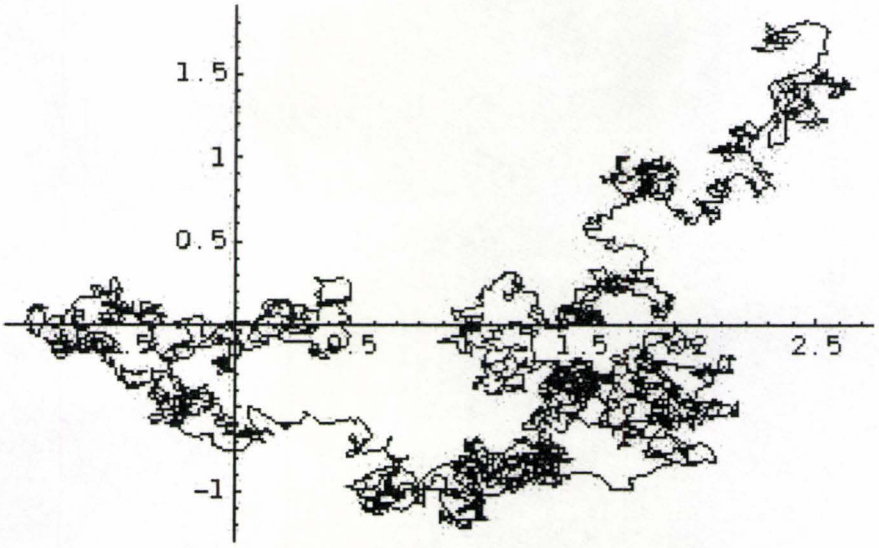

Figure 1: Trajectory of a 2-D Brownian motion

Figure 3.1: trajectory of a 2-dimension Brownian motion

3.3 Ito's Calculus

3.3.1 Ito's Stochastic Integration

Supposing we have a function of Brownian motion (or Wiener process) $f(B_t)$, let's check the change in this function after a brief period δt:

$$f(B_{t+\delta t} - B_t).$$

By Taylor's theorem, we have

$$f(B_{t+\delta t} - B_t) = (B_{t+\delta t} - B_t)f'(B_t) + \frac{1}{2}(B_{t+\delta t} - B_t)^2 f''(B_t) + \cdots . \quad (3.2)$$

For Brownian motion B_t, we have (from the definition of Brownian motion, see 3.2.1)

$$\mathbf{E}(B_{t+\delta t} - B_t)^2 = \delta t.$$

If we define the following,

$$S(t) = f(B_t), \quad (3.3)$$

Eq. (3.2) can be rewritten by introducing the above equation,

$$dS_t = f'(B_t)dB_t + \frac{1}{2}f''(B_t)dt. \quad (3.4)$$

Rewriting Eq. (3.4) in integrated form, we have:

$$S_t - S_0 = \int_0^t f'(B_s)dB_s + \int_0^t \frac{1}{2}f''(B_s)ds, \quad (3.5)$$

where the first item in the right hand side of Eq. (3.5), i.e., $\int_0^t f^{'}(B_s)dB_s$, is called a *stochastic integral.* This integral is defined in 1950's by Ito (Kiyoshi Ito, (born September 7, 1915), a Japanese mathematician whose work is now known as *Ito calculus*) :

$$\int_0^t f^{'}(B_s)dB_s \triangleq \lim_{n\to\infty} \sum_{j=0}^{n} f^{'}(B_{t_j})(B_{t_{j+1}} - B_{t_j}), \tag{3.6}$$

where the integral time period $[0, t]$ is separated into n slots, i.e., $0 = t_0 < t_1 < \cdots < t_{n+1} = t$, with the property

$$\max\left\{|B_{t_{j+1}} - B_{t_j}|\right\} \to 0, \text{ when } n \to \infty \text{ for } 0 \leqslant j < n. \tag{3.7}$$

Moving the second item in the right side of Eq. (3.5), i.e., $\int_0^t \frac{1}{2} f^{''}(B_s)ds$ to the left side of Eq. (3.5) , and switching both sides of Eq. (3.5), we have:

$$\int_0^t f^{'}(B_s)dB_s = S_t - S_0 - \int_0^t \frac{1}{2} f^{''}(B_s)ds. \tag{3.8}$$

Substituting Eq. (3.3) into the above Eq. (3.8), we obtain:

$$\int_0^t f^{'}(B_s)dB_s = f(B_t) - f(B_0) - \int_0^t \frac{1}{2} f^{''}(B_s)ds. \tag{3.9}$$

Now, using Eq. (3.9), we can calculate some simple stochastic integrals. For example, let's calculate the integral below:

$$\int_0^t B_s dB_s = ? \tag{3.10}$$

If we define the following:

$$f(B_s) = \frac{1}{2}B_s^2, \tag{3.11}$$

then we have

$$\begin{aligned} f'(B_s) &= B_s \\ f''(B_s) &= 1. \end{aligned} \tag{3.12}$$

Substituting Eqs. (3.11) and (3.12) into (3.9), we obtain:

$$\begin{aligned} \int_0^t B_s dB_s &= \frac{1}{2}B_t^2 - \frac{1}{2}B_0^2 - \int_0^t \frac{1}{2}ds \\ &= \frac{1}{2}\left(B_t^2 - B_0^2 - t\right) \\ &= \frac{1}{2}\left(B_t^2 - t\right). \end{aligned} \tag{3.13}$$

With the result in (3.13), we thus obtain the solution of the stochastic integral in Eq. (3.10).

To explain the stochastic integral, i.e. (3.10), we use an approach which expresses the concept of Ito's integral as (3.6). In the stochastic integral (3.10),we may express the integral as the limit of summation in a Riemann integral, such

as:

$$\int_0^t B_s dB_s = \lim_{n\to\infty} \sum_{j=0}^{n} B_{t_j}(B_{t_{j+1}} - B_{t_j}), \tag{3.14}$$

and,

$$\int_0^t B_s dB_s = \lim_{n\to\infty} \sum_{j=0}^{n} B_{t_{j+1}}(B_{t_{j+1}} - B_{t_j}), \tag{3.15}$$

where both above limitations satisfy the property of integral time period separation (Eq. (3.7)).

For a general Riemann integral, the limits of summation, such as (3.14) and (3.15), are the same. However, it must be considered whether or not they are the same for a stochastic process. The answer is revealed below.

Firstly, let's look at the right side of Eq. (3.14) and check the expectation:

$$\begin{aligned} \mathbf{E}\left[\sum_{j=0}^{n} B_{t_j}(B_{t_{j+1}} - B_{t_j})\right] &= \sum_{j=0}^{n} \mathbf{E}\left[B_{t_j}(B_{t_{j+1}} - B_{t_j})\right] \\ &= \sum_{j=0}^{n} \left[\mathbf{E}(B_{t_j})\mathbf{E}(B_{t_{j+1}} - B_{t_j})\right]. \end{aligned} \tag{3.16}$$

In the above we use the Wiener process property that the increment is independent, i.e. $B_{t_j}, (B_{t_{j+1}} - B_{t_j})$ are independent. From the definition of Wiener process (cf. section 3.2.1 on page 22), we know that

$$\mathbf{E}(B_{t_{j+1}} - B_{t_j}) = 0.$$

Incorporating the above in Eq. (3.16), we have:

$$\mathbf{E}\left[\sum_{j=0}^{n} B_{t_j}(B_{t_{j+1}} - B_{t_j})\right] = 0. \tag{3.17}$$

Including (3.14) into the above, we have

$$\mathbf{E}\left[\int_0^t B_s dB_s\right] = 0. \tag{3.18}$$

Now, looking at the right side of Eq. (3.15) and verifying the expectation:

$$\begin{aligned}\mathbf{E}\left[\sum_{j=0}^{n} B_{t_{j+1}}(B_{t_{j+1}} - B_{t_j})\right] &= \sum_{j=0}^{n} \mathbf{E}\left[(B_{t_{j+1}} - B_{t_j} + B_{t_j})(B_{t_{j+1}} - B_{t_j})\right] \\ &= \sum_{j=0}^{n} \left\{\mathbf{E}(B_{t_{j+1}} - B_{t_j})^2 + \mathbf{E}\left[B_{t_j}(B_{t_{j+1}} - B_{t_j})\right]\right\}.\end{aligned} \tag{3.19}$$

From the properties of the Wiener process, we know that

$$\mathbf{E}(B_{t_{j+1}} - B_{t_j})^2 = \mathbf{var}(B_{t_{j+1}} - B_{t_j}) = t_{j+1} - t_j \tag{3.20}$$

Taking Eqs. (3.17) and (3.20) into the above, we obtain:

$$\mathbf{E}\left[\sum_{j=0}^{n} B_{t_{j+1}}(B_{t_{j+1}} - B_{t_j})\right] = \sum_{j=0}^{n}(t_{j+1} - t_j) = t. \tag{3.21}$$

Including (3.15) into the above, we have

$$\mathbf{E}\left[\int_0^t B_s dB_s\right] = t. \tag{3.22}$$

Comparing Eqs. (3.18) and (3.22), we conclude that the right side of (3.14) and (3.15) are not equal. Now, if we choose the limitation expression of the stochastic integral of $\int_0^t B_s dB_s$ as the right side of Eq. (3.14), we arrive at Ito's integral. Generally, for a stochastic integral, Ito's integral is defined as:

$$\int_a^b f(t, B_t) dB_t = \sum_{j=0}^{n} f(t_j, B_{t_j})(B_{t_{j+1}} - B_{t_j}), \tag{3.23}$$

where,

$$a = t_0 < t_1 < \cdots < t_{n+1} = b,$$

with the property,

$$\max\left\{|B_{t_{j+1}} - B_{t_j}|\right\} \to 0, \text{ when } n \to \infty \text{ for } 0 \leqslant j < n.$$

Having now defined the Ito's integral in Eq. (3.23), we have to verify that Ito's integral of $\int_0^t B_s dB_s$ has the same result as in Eq. (3.13). If we define the following:

$$I_n = \sum_{j=0}^{n} B_{t_j}(B_{t_{j+1}} - B_{t_j}), \tag{3.24}$$

thus $\{I_n\}$ is a Cauchy sequence, which will be illustrated below. From Eqs.

(3.14) and (3.24), we have,

$$\int_0^t B_s dB_s = \lim_{n\to\infty} I_n \tag{3.25}$$

We then attempt to identify a random variable I that satisfies the following:

$$\mathbf{var}(I_n - I) \overset{approach}{\rightarrow} 0.$$

First, we know that

$$\begin{aligned}
\mathbf{E}[I_n] &= \mathbf{E}\left[\sum_{j=0}^{n} B_{t_j}(B_{t_{j+1}} - B_{t_j})\right] \\
&= \sum_{j=0}^{n} \mathbf{E}(B_{t_j})\mathbf{E}(B_{t_{j+1}} - B_{t_j}) \\
&= 0,
\end{aligned}$$

where in the above derivation we use property 2 of the Wiener process (see 3.2.1). By introducing the equation,

$$ab = \frac{(a+b)^2 - a^2 - b^2}{2}$$

into equation 3.24, we have

$$\begin{aligned} I_n &= \sum_{j=0}^{n} \frac{(B_{t_j} + B_{t_{j+1}} - B_{t_j})^2 - B_{t_j}^2 - (B_{t_{j+1}} - B_{t_j})^2}{2} \\ &= \sum_{j=0}^{n} \frac{B_{t_{j+1}}^2 - B_{t_j}^2 - (B_{t_{j+1}} - B_{t_j})^2}{2} \\ &= \frac{1}{2}\sum_{j=0}^{n}(B_{t_{j+1}}^2 - B_{t_j}^2) - \frac{1}{2}\sum_{j=0}^{n}(B_{t_{j+1}} - B_{t_j})^2 \\ &= \frac{1}{2}B_t^2 - \frac{1}{2}\sum_{j=0}^{n}(B_{t_{j+1}} - B_{t_j})^2 \end{aligned}$$

From Eqs. (3.17), (3.19) and (3.21), we obtain:

$$\mathbf{E}\left[\sum_{j=0}^{n}(B_{t_{j+1}} - B_{t_j})^2\right] = t$$

Thus,

$$\mathbf{E}(I_n) = \frac{1}{2}B_t^2 - \frac{1}{2}t$$

Now, assuming the following:

$$I = \frac{1}{2}B_t^2 - \frac{1}{2}t = \mathbf{E}(I_n). \tag{3.26}$$

Then,

$$I_n - I = -\frac{1}{2}\left[\sum_{j=0}^{n}(B_{t_{j+1}} - B_{t_j})^2 - t\right]$$

Therefore, if we want to show $\{I_n\}$ converges to I, we have to show that

$\mathbf{var}(I_n - I) \stackrel{?}{\rightarrow} 0$:

$$\begin{aligned}
\mathbf{var}(I_n - I) &= \frac{1}{4}\mathbf{var}\left[\sum_{j=0}^{n}(B_{t_{j+1}} - B_{t_j})^2 - t\right] \\
&= \frac{1}{4}\sum_{j=0}^{n}\mathbf{var}\left[(B_{t_{j+1}} - B_{t_j})^2\right] \\
&= \frac{1}{4}\sum_{j=0}^{n}\left\{\mathbf{E}(B_{t_{j+1}} - B_{t_j})^4 - \left[\mathbf{E}(B_{t_{j+1}} - B_{t_j})^2\right]^2\right\} \\
&= \frac{1}{4}\sum_{j=0}^{n}\left\{3(t_{j+1} - t_j)^2 - (t_{j+1} - t_j)^2\right\} \\
&= \frac{1}{2}\sum_{j=0}^{n}(t_{j+1} - t_j)^2 \qquad (3.27)
\end{aligned}$$

In above derivation, we use the properties of a random variable x having a Gaussian distribution with zero mean and variance σ^2. We then obtain:

$$\mathbf{E}[x^4] = 3\sigma^4.$$

We also have,

$$\begin{aligned}
\sum_{j=0}^{n}(t_{j+1} - t_j)^2 &\leq \max_j |t_{j+1} - t_j| \sum_{j=0}^{n}(t_{j+1} - t_j) \\
&= t \cdot \max_j |t_{j+1} - t_j| \\
&\rightarrow 0 \qquad (3.28)
\end{aligned}$$

Substituting (3.28) into (3.27), we instantly obtain:

$$\mathbf{var}(I_n - I) \rightarrow 0, \text{ for } n \rightarrow \infty. \qquad (3.29)$$

From the above Eqs. (3.29), (3.26) and 3.25, we finally verify that:

$$\int_0^t B_s dB_s = I = \frac{1}{2}B_t^2 - \frac{1}{2}t.$$

This is the same result as that obtained with Eq. (3.13. From the above discussion of a detailed calculation of a special stochastic integral defined by Ito, we can see that the Taylor's expansion is applicable to Ito's integral.

3.3.2 Stochastic Differential Equation and Ito's Formula

After we simply explain the stochastic integration (Ito's integral), we can now define the essence of a stochastic differential equation (SDE).

If a stochastic process $x(t)$ satisfies the following Ito's stochastic integral equation as

$$x_t - x_0 = \int_0^t b(t, x_t)dt + \int_0^t \sigma(t, x_t)dB_t,$$

then we say the stochastic process $x(t)$ obeys the Ito's stochastic differential equation,

$$dx_t = b(t, x_t)dt + \sigma(t, x_t)dB_t. \tag{3.30}$$

Note: In the following part of this thesis, we use w_t to represent Wiener process, which is to replace B_t as a Brownian motion in previous part of this thesis.

An informal sketch of the proof of Ito's formula is provided here. Suppose x_t is an Ito stochastic process that obeys a stochastic differential equation

(Ref. (3.30)):

$$dx_t = b \cdot dt + \sigma \cdot dw_t \tag{3.31}$$

Let $f(t, x_t)$ be a function of t and x_t, and consider the differential of $F_t(t, x_t)$. Observe (cf. Taylor's theorem):

$$dF_t = \frac{\partial f}{\partial t} \cdot dt + \frac{\partial f}{\partial x_t} \cdot dx_t + \frac{1}{2}\frac{\partial^2 f}{\partial x_t^2} \cdot dx_t^2 + \frac{1}{2}\frac{\partial^2 f}{\partial t^2} \cdot dt^2 + \frac{\partial^2 f}{\partial x_t \partial t} \cdot dx_t dt + \cdots \tag{3.32}$$

We also know (Ref. Oksendal [14]),

$$\begin{aligned} dw_t^2 &= dt \\ dw_t dt &= 0 \\ dt^2 &= 0. \end{aligned} \tag{3.33}$$

Substituting (3.31) into (3.32) with (3.33) yields only the first three non-zero terms of (3.32):

$$dF_t = \frac{\partial f}{\partial t} dt + \frac{\partial f}{\partial x_t} dx_t + \frac{1}{2}\frac{\partial^2 f}{\partial x_t^2} dx_t^2 \tag{3.34}$$

In essence, we only take the first three terms on the right hand side of (3.32) to obtain this result, i.e. (3.34), since $dw_t^2 = dt$, and terms of $O\left(dt^{\alpha}\right), \alpha > 1$, contribute nothing to stochastic integrals (Ref. Oksendal [14]). Substituting (3.31) into (3.34) with (3.33) yields Ito's formula:

$$dF_t = \left(\frac{\partial f}{\partial t} + b\frac{\partial f}{\partial x_t} + \frac{\sigma^2}{2}\frac{\partial^2 f}{\partial x_t^2}\right) \cdot dt + \sigma \frac{\partial f}{\partial x_t} \cdot dw_t \tag{3.35}$$

3.4 Summary

This chapter provides sufficient mathematical background knowledge for the readers understand the remainder of this thesis. Here, we are not in pursuit of the completeness and rigour of the mathematical theory of Ito's calculus, and we focus on the elucidation of the essential difference of Ito's integral and the traditional Riemann integral and corresponding the statement of rules and formula of Ito's calculus (SDE theory) so that readers are able to apply the knowledge stated in this chapter to the practical application at hand and solve the related problems. The next two chapters are examples of applying SDE theory to the traditional multipath wireless channels, where some novel results are presented.

Chapter 4

Multipath Flat Fading Channel Without Doppler Frequency

4.1 Introduction

Modeling wireless channels is essential to wireless communication systems. An auto-recursive (AR) process of order one for wireless flat fading channel has long been assumed, but without a rigorous mathematical/physical basis. In this chapter, we firstly analyze the statistics of the flat fading wireless channel for a stationary receiver; then we derive a stochastic differential equation as a dynamic model for such channel through rigorous mathematical reasoning; finally we obtain a first-order stochastic AR model for the flat fading wireless channel with stationary receiver from discretizing the dynamic SDE. The resulting AR model describes more of the origin of multi-path fading channels than traditional AR models in literature and it can efficiently model and gener-

ate Rayleigh-distributed stationary fading channels. The Markovian property of the AR model is inherited through the SDE approach.

Experiments with mobile communication at VHF frequency began in the 1920s. Results of these experiments show that signal quality varies from "excellent" to "no signal". The signal incoming to the receiver contains a large number of reflected radio waves, which are characterized by "multipath reception". Thus, the wireless channel behaves in a random-like fashion.

The purpose of this chapter is to develop a dynamic model of a stationary wireless channel, in the case that the receiver is not moving, thus zero Doppler shift. Jakes' description pertains to a wireless channel with Doppler shift and random component phases, but with deterministic temporal evolution. In contrast we are concerned with the case that the component phases fluctuate in time, whereas in Jakes' model they are assumed to be constant in time. For a stationary (i.e. zero Doppler shift) channel, Jakes' model results in a constant (one) as the autocorrelation, that is inappropriate for long time periods because the stationary channel is still time-varying due to the relative phase fluctuations. This article presents an SDE / AR-1 model to describe the dynamical behavior of such stationary channels. The SDE / AR-1 model is obtained through systematic mathematical reasoning starting from the (random walk) scattered electric field model with multi-path fading characterization, i.e. Eq. 4.3. We are not concerned with non-stationary channels with Doppler shift.

The random behavior of a wireless channel can be viewed as a stochastic process. Stochastic differential equations (SDEs) are a powerful mathemat-

ical tool to analyze such processes. Traditional statistical analysis of p.d.f., autocorrelation, etc. of stochastic processes cannot describe the random behavior of these in the time domain, in contrast to SDEs which capture all the continuous time statistical properties.

Several papers have been presented on the application of SDEs to the research of Radar scattering and wireless communications. Field & Tough ([12, 13]) have successfully used SDEs to analyze K-distributed noise in electromagnetic scattering. Charalambous & Menemenlis ([17]) addressed SDEs to model multipath fading channels. In this chapter, we will derive a simple SDE dynamical equation for the time variation of Rayleigh distributed stationary wireless channels (cf. [12]). The underlying assumptions for our SDE model require Rayleigh distributed, stationary, first-order Markovian, multi-path fading wireless channels. An extended dynamical description of electromagnetic propagation including line of sight (LoS) reception, for which the received envelope consists of a superposition of specular and scattered components with resulting Ricean distribution, is provided *inter alia* in Field & Tough (2005) [25]. Rigorous mathematical analysis and computer simulation verify our SDE model. A first-order stochastic AR model is derived directly by discretizing the SDE model in the time-variable.

There are two view points that are traditionally taken in the literature. One is concerned with mathematical tractability in the models of wireless propagation. Another is concerned with the experimental accuracy and design aspects of the problem for which a higher-order of AR model may be more appropriate. In this chapter, we adopt the former point of view, thus preserving the Markov

property and retaining mathematical simplicity and tractability. We derive a first-order AR process for a Rayleigh-distributed stationary wireless channel based on the SDE analysis of multi-path Rayleigh fading. In section 4.2, we discuss the statistical properties of a flat wireless channel without Doppler shift effect. The SDE analysis and a resultant SDE model for multi-path stationary Rayleigh fading channels is presented in section 4.3. A first-order AR model as a discretization of the SDE is discussed in section 4.4. The summary and conclusions for this chapter are drawn in section 4.5.

4.2 Statistical Analysis of a Wireless Flat Channel Without Doppler Frequency

In this section, we will firstly introduce the very basic model based on physics assumption for the multipath flat fading channel without Doppler frequency shift, then we make a rigorous statistical analysis, such as auto-correlation, power spectral density, for such a wireless channel.

4.2.1 Basic dynamic model

The signal incoming to the receiver behaves fluctuations due to the multipath propagation. The Rayleigh distribution has been used for a long time to describe such a received signal, which results in a so-called *"Rayleigh distributed channel"*.

The random walk model for the scattered electric field was developed in the 1980s (see [9]-[11]). These references give statistical description and correlation

functions, while no time dependent models were provided. This was extended in [[12, 13]] to a continuous time description in which the scattered electric field is modeled according to

$$\varepsilon_t = \sum_{k=1}^{N} \exp[j\varphi_t^{(k)}], \tag{4.1}$$

The phase factors $\exp[j\varphi_t^{(k)}]$ are independent and uniformly distributed on the unit circle $\{|z| = 1, z \in \mathbb{C}\}$ ($\mathbb{C}$ is the set of all complex numbers) and $\varphi_t^{(k)}$ has uniform random initialization on the interval $[0, 2\pi)$ and satisfies

$$d\varphi_t^{(k)} = B^{1/2} dw_t^{(k)}, \tag{4.2}$$

in which dw represents infinitesimal increments in a Wiener process w (see e.g. Ref. [14]). Here, B is a constant with the dimension of frequency, which determines the correlation timescale for the component phase process $\varphi_t^{(k)}$.

Considering a general wireless channel, the received signal on each path is random. Thus we consider the following extended time description of the scattered electric field at the stationary receiver for a wireless channel with "multipath reception" characterization:

$$\varepsilon_t = \sum_{k=1}^{N} x_k \exp[j\varphi_t^{(k)}], \tag{4.3}$$

where the "form factor" x_k is the amplitude of the received signal on kth path. The relative phase $\varphi_t^{(k)}$ satisfies the SDE (4.2). Comparing with Jakes' model (see [19]), Eq. (4.3) introduces temporal relative phase fluctuations without

considering Doppler shift. The Chapter 5 will discuss the model of the wireless flat channel considering Doppler frequency shift and temporal relative phase fluctuations. With the assumption of phase fluctuations according to (4.2), Field & Tough [12] successfully applied a random walk model (where Doppler shift is fixed independent of the path/scatterer) to the analysis of radar sea clutter in Ref. [13]. The "multipath reception" ε_t will be a stationary process based on the the assumption of the phase fluctuation properties (cf. (4.2)) and initial condition (cf. Appendix 4.6.1).

4.2.2 Autocorrelation

Given Eq. (4.3) for a multipath flat channel, the autocorrelation of the complex envelope ε_t of the received signal at receiver is written as

$$R_\varepsilon(\tau) = \mathbf{E}[\varepsilon_t \varepsilon^*_{t+\tau}]. \tag{4.4}$$

where the asterisk denotes complex conjugation and τ is a time lag. Before we compute the autocorrelation of the channel, we begin by computing the cross-correlation between a pair of signal rays, which is given by

$$\mathbf{E}[x_k e^{j\varphi_t^{(k)}} \cdot x_m e^{-j\varphi_{t+\tau}^{(m)}}] = \begin{cases} 0 & if \quad m \neq k \\ \mathbf{E}[x_k^2] \cdot \mathbf{E}[e^{j(\varphi_t^{(k)} - \varphi_{t+\tau}^{(k)})}] & if \quad m = k \end{cases} \tag{4.5}$$

in which we neglect the effects of small changes in distance/time-delay on the amplitude $\{x_k\}$ of the component signal rays[1] and assume that any pair of signal rays are independent with each other.

Taking the basic channel model (4.3) and the cross-correlation of any pair of signal rays (4.5) into Eq. (4.4), we obtain

$$\begin{aligned} R_\varepsilon(\tau) &= \\ \mathbf{E}[\sum_{k=1}^{N} x_k e^{j(\varphi_t^{(k)})} \sum_{m=1}^{N} x_m e^{-j(\varphi_{t+\tau}^{(m)})}] &= \\ \sum_{k=1}^{N} \mathbf{E}[x_k^2]\mathbf{E}[e^{j(\varphi_t^{(k)} - \varphi_{t+\tau}^{(k)})}] & \quad . \end{aligned} \tag{4.6}$$

Here, we let

$$P_0 = \sum_{k=1}^{N} \mathbf{E}[x_k^2] \tag{4.7}$$

which is the average received power.

Based on our essential modification that the component phases are Wiener processes, governed by (4.2) rather than mere constants as in the traditional Jakes' model, we obtain

$$\begin{aligned} \varphi_t^{(k)} - \varphi_{t+\tau}^{(k)} &= \int_t^{t+\tau} B^{1/2} dw_t^{(k)} \\ &= -B^{1/2}(w_{t+\tau}^{(k)} - w_t^{(k)}) \end{aligned} \tag{4.8}$$

where $w_t^{(k)}$ is a standard Wiener process as mentioned before. Thus, $w_{t+\tau}^{(k)} - w_t^{(k)}$

[1]Within a tiny period, the phase $\{\varphi_t^{(k)}\}$ behaves fast changes due to high frequency characteristics, while the amplitude $\{x_k\}$ behaves very slow changes because the paths of the radio incoming to the receiver are relatively constant within a tiny period, i.e. the diffusion of the energy is relatively slow than the phase variation.

is Gaussian distributed random variable with zero mean and variance of $|\tau|$, i.e.

$$w_{t+\tau}^{(k)} - w_t^{(k)} \sim \frac{1}{\sqrt{2\pi|\tau|}} \exp(-\frac{x^2}{2|\tau|}) \tag{4.9}$$

Using (4.8) and (4.9), we derive that

$$\begin{aligned} \mathbf{E}[e^{j(\varphi_t^{(k)} - \varphi_{t+\tau}^{(k)})}] &= \mathbf{E}[e^{-jB^{1/2}(w_{t+\tau}^{(k)} - w_t^{(k)})}] \\ &= \int_{-\infty}^{\infty} e^{-jB^{1/2}x} \frac{1}{\sqrt{2\pi|\tau|}} e^{-\frac{x^2}{2|\tau|}} dx \\ &= e^{-B|\tau|/2} \end{aligned} \tag{4.10}$$

From Eq. (4.10), we see that the expectation of two phase factors $\mathbf{E}[e^{j(\varphi_t^{(k)} - \varphi_{t+\tau}^{(k)})}]$ is uncorrelated with the index, i.e. k, of corresponding signal path. Substituting (4.10) into (4.6) and referring the definition of the average received power (4.7), we obtain

$$\begin{aligned} R_\varepsilon(\tau) &= \sum_{k=1}^{N} \mathbf{E}[x_k^2] e^{-B|\tau|/2} \\ &= P_0 e^{-B|\tau|/2}. \end{aligned} \tag{4.11}$$

Eq. (4.11) is the final close form expression for the autocorrelation of the multipath fading channel without Doppler frequency shift. It is obvious that the autocorrelation of the multipath flat fading channel is an exponential-decaying function, which is plotted in Figure 4.1.

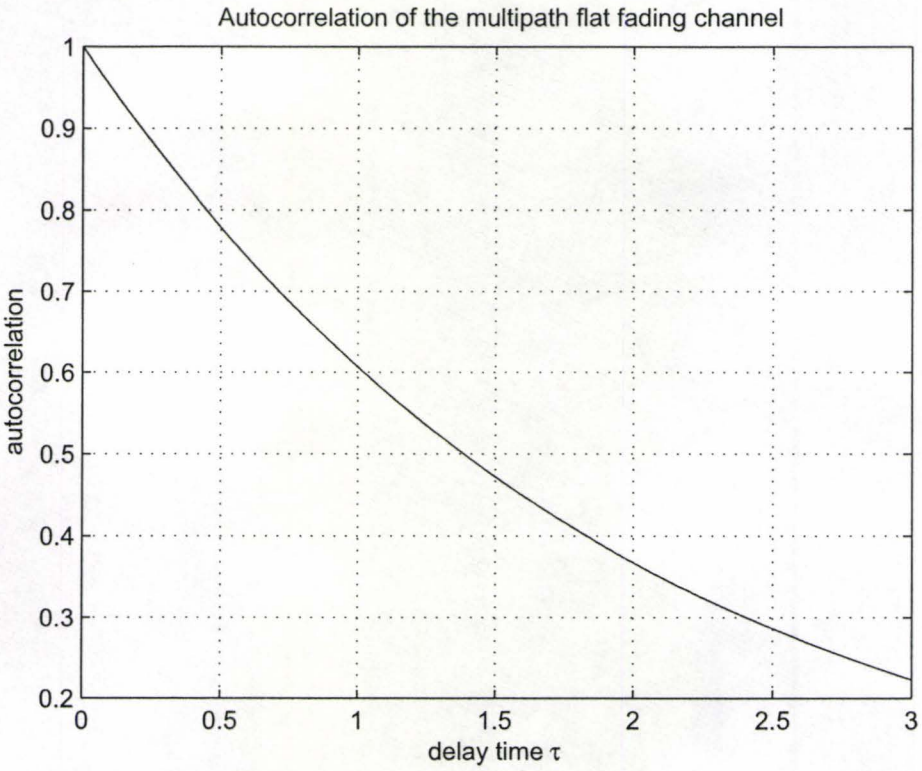

Figure 4.1: Autocorrelation of the multipath fading channel without Doppler frequency shift.

4.3 Dynamic Modeling of a Wireless Flat Channel Without Doppler Frequency

Discussions on the modeling of multi-path fading for stationary wireless channels to date tend to be limited in that no systematic analysis of a dynamic model is provided. Indeed, Jakes' model ([19] cf. Eq. (5.1)) does not describe the dynamics of a stationary channel, viewing its auto-correlation in the absence of Doppler as a constant, i.e. a time-invariant channel. In contrast, in what follows we develop the time-dynamic model of a wireless channel for a stationary receiver and obtain a first order AR model representation based on systematic mathematical reasoning starting from the well-known scattered electric field model with component phase fluctuations and multi-path fading characterization as presented in Eq. (4.3).

4.3.1 Modeling of a Wireless Flat Channel

We start from the fundamental multipath characteristic equation of wireless flat channel (4.3) as the basis for the following mathematical reasoning.

From equation (3.35) (Ito's formula, cf. section 3.3), the Ito differential of (4.3) is (see Appendix 4.6.2)

$$\varepsilon_t^{(N)} = \sum_{k=1}^{N} x_k \left(id\varphi_t^{(k)} - \frac{1}{2}(d\varphi_t^{(k)})^2 \right) \exp[j\varphi_t^{(k)}]. \tag{4.12}$$

When $N \to \infty$, if we introduce Eq. (4.2) into (4.12), after invoking use of Ito

calculus ([14]), we arrive at (see Appendix 4.6.3)

$$d\varepsilon_t^{(N)} = -\frac{1}{2}B\varepsilon_t^{(N)}dt + B^{\frac{1}{2}}\sigma_x d\xi_t \tag{4.13}$$

where $\sigma_x^2 = \sum_{k=1}^{N} x_k^2$, which is the variance of $\varepsilon_t^{(N)}$ (see Appendix 4.6.4). An alternative derivation of the variance involves computation of autocorrelation functions of in-phase and quadrature components that are computed at zero lag to give variance ([[23]]), but yield the same result. We will show that the variance of in-phase / quadrature components is $\frac{1}{2}\sigma_x^2$ in the next section (see Eq. (4.19)). The quantity ξ_t is a complex Wiener process with properties (see Appendix 4.6.3)

$$|d\xi|^2 = dt, d\xi^2 = 0, d\xi \cdot dt = 0. \tag{4.14}$$

For a real received signal $\varepsilon_t^{(N)}$, the variance of $\varepsilon_t^{(N)}$ is always finite for any N, so $\sigma_x < +\infty$ when $N \to \infty$. If we define

$$\Psi_t \triangleq \lim_{N\to\infty} \varepsilon_t^{(N)}, \tag{4.15}$$

then we can rewrite equation (4.13) as

$$d\Psi_t = -\frac{1}{2}B\Psi_t dt + B^{\frac{1}{2}}\sigma_x d\xi_t \tag{4.16}$$

where the random variable σ_x is the square root of variance of Ψ_t. Thus, (4.16) is our SDE model for a flat wireless channel without Doppler frequency.

4.3.2 Solution of a Wireless Channel SDE Model

We have presented a simple SDE model for a wireless channel as characterized by (4.3). In this subsection, we will give some mathematical analysis of the SDE model (4.16), and explore the relationship with the Rayleigh distribution.

Let the amplitude process of (4.16) be expressed in terms of its *in-phase* and *quadrature-phase* components I and Q:

$$\Psi_t = I_t + iQ_t \tag{4.17}$$

where i the square root of -1. Then I_t and Q_t can be described as two independent Ornstein-Uhlenbeck processes e.g.([14]) with SDEs

$$\begin{aligned} dI_t &= -\frac{1}{2}BI_t dt + \frac{\sqrt{2}}{2}B^{\frac{1}{2}}\sigma_x dw_t^{(I)} \\ dQ_t &= -\frac{1}{2}BQ_t dt + \frac{\sqrt{2}}{2}B^{\frac{1}{2}}\sigma_x dw_t^{(Q)} \end{aligned} \tag{4.18}$$

The probability density functions (p.d.f) of I_t and Q_t have the same stationary forms, namely,

$$p(y) = \frac{1}{\sqrt{\pi}\sigma_x}\exp\left[-\frac{y^2}{\sigma_x^2}\right] \tag{4.19}$$

Thus I_t and Q_t are asymptotically Gaussian variables with mean zero and variance $\frac{1}{2}\sigma_x^2$. From (4.17) and (4.19), we find that the p.d.f of $|\Psi_t|$(defined as

Z) will be a Rayleigh distribution as

$$p(z) = \frac{2z}{\sigma_x^2} e^{-\frac{z^2}{\sigma_x^2}} \tag{4.20}$$

Here, the knowledge that the square root of the sum of two squared Gaussian variable is a Rayleigh distributed random variable has been used for (4.20).

4.3.3 The Wireless Channel SDE Model in Polar Form

In this subsection, we will explore the polar representation of the process Ψ_t since it is useful to compute the AR parameter in Eq. (4.27) (cf. section 4.4). In this polar representation the resultant phase fluctuations (4.26) provide a method to calculate the quantity B of (4.16) that is an essential ingredient in these AR parameters.

The complex amplitude process can alternatively be expressed in polar form

$$\Psi_t = R_t \exp(i\theta_t). \tag{4.21}$$

Thus

$$i\theta_t = \log(\Psi_t / R_t), \tag{4.22}$$

so from Ito's formula (cf. section 3.3) we have

$$id\theta_t = \frac{d\Psi_t}{\Psi_t} - \frac{1}{2}\left(\frac{d\Psi_t}{\Psi_t}\right)^2 - \frac{dR_t}{R_t} + \frac{1}{2}\left(\frac{dR_t}{R_t}\right)^2 \tag{4.23}$$

Since the left hand side of Eq. (4.23) is purely imaginary, we can express in

terms of alone as (see [12])

$$d\theta_t = \frac{1}{2i}\left[\left(\frac{d\Psi_t}{\Psi_t} - \frac{1}{2}\left(\frac{d\Psi_t}{\Psi_t}\right)^2\right) - \left(\frac{d\Psi_t^*}{\Psi_t^*} - \frac{1}{2}\left(\frac{d\Psi_t^*}{\Psi_t^*}\right)^2\right)\right]. \tag{4.24}$$

From (4.14) and (4.16), we have

$$\frac{d\Psi_t}{\Psi_t} - \frac{1}{2}\left(\frac{d\Psi_t}{\Psi_t}\right)^2 = -\frac{1}{2}Bdt + \frac{B^{\frac{1}{2}}\sigma_x}{\Psi_t}d\xi_t. \tag{4.25}$$

Notice that we have $\left(\frac{d\Psi_t}{\Psi_t}\right)^2 = 0$ because of (4.14) and (4.16).Thus, substituting (4.25) into (4.24), we get

$$d\theta_t = \left(\frac{B\sigma_x^2}{2z_t}\right)^{1/2} dw_t^{(\theta)}, \tag{4.26}$$

as resultant phase fluctuations, where $z_t = |\Psi_t|^2$, which is the intensity process introduced above, and $dw_t^{(\theta)}$ is a new Wiener process

$$dw_t^{(\theta)} = \frac{1}{i\sqrt{2}\,|\Psi_t|}\left(\Psi_t^* d\xi_t - \Psi_t d\xi_t^*\right).$$

Thus, the angular process θ_t has zero drift part for stationary, Rayleigh distributed wireless channel.

4.4 AR Model for Wireless Flat Channel and Zero Doppler Frequency

In this section, we will explore the close relationship between the presented SDE and an AR stochastic process.

4.4.1 Derivation of AR model

Let's consider discrete-time samplings for the SDE process in (4.16) with equal distance time series, $t_0, t_1, \cdots, t_k, \cdots$, where $t_{k+1} - t_k = \delta t$. After replacing the continuous time differential $d\Psi_t$ in (4.16) with the discrete-time difference $\left(\Psi_{t_{k+1}} - \Psi_{t_k}\right)$, replacing Ψ_t with the arithmetic average $\left(\Psi_{t_{k+1}} + \Psi_{t_k}\right)/2$[2], and replacing the Wiener process $d\xi_t$ with a complex discrete Gaussian process $\delta t^{1/2} \cdot \tilde{n}(k)$, we obtain

$$\Psi_{t_{k+1}} = \frac{1 - \frac{1}{4}B \cdot \delta t}{1 + \frac{1}{4}B \cdot \delta t}\Psi_{t_k} + \frac{B^{\frac{1}{2}}\sigma_x \cdot \delta t^{1/2}}{1 + \frac{1}{4}B \cdot \delta t} \cdot \tilde{n}(k), \tag{4.27}$$

where is $\tilde{n}(k)$ a standard complex Gaussian process with zero mean and unit variance. Equation (4.27) is a first-order AR process for the wireless channel. The AR coefficients are functions of the constant B, the sampling time interval δt, and the square root of variance of channel σ_x.

The multi-path Rayleigh scattering model [19], i.e. Eq. (4.3), has been used for stationary multi-path fading wireless channels for a long time. Tradi-

[2]Here, we use the "midpoint" corresponding to a Stratonovich integral for the numerical stability, in contrast to Ito's integral which uses the "left point". In the SDE (4.16), the constant nature of the volatility yields equivalence between the Stratonovich and Ito integrals – which justifies the "midpoint" discretization.

tionally, an AR process of order one has been assumed in Rayleigh scattering model. However, in the literature to date, there has not been a rigorous systematic derivation of the dynamics, which is where the proposed SDE theory becomes an essential extra ingredient. For the traditional AR model, there is no account given of the direct relationship between the AR coefficients and the underlying physical characteristics of multi-path wireless channels, namely a resultant amplitude arising as a superposition of a number of random phasors each evolving on a suitable time-scale. The AR model developed here is derived from these basic physical principles, using techniques from SDE theory to describe the continuous time evolution, and then passing to discrete time. Our development makes transparent the relations between the AR coefficients and the physical [correlation timescale] parameter B, the variance of the channel, and the discrete sampling interval, as demonstrated in (4.27). The physical origins of the AR coefficients are thus determined. By comparison, the AR coefficients can also be obtained (see [21]) statistically using Yule-Walker equations and autocorrelation of the process.

To simulate a Rayleigh distributed channel, Eq. (4.3) requires large N (thousands or more) paths, which results in a lot of computation. Instead of simulated these large N paths, we model the total behavior of all these paths by one stochastic process Ψ_t. To generate a single value of channel data at instant time t, we need to produce N random number $\varphi_t^{(k)}$ and x_k from (4.3), while only one complex random number $\delta\xi_t$ (two real random numbers) from (4.27). Thus the computation complexity of the SDE model (4.16) is about 1 of N (see (4.3)). Considering the large , the SDE model provides a very simple

way to simulate Rayleigh distributed wireless channel more efficiently.

Wong & Chang (1996) verified the first-order Markovian model for a Rayleigh fading channel in [16]. This reference concludes that the first-order Markovian chain is sufficient to model a Rayleigh fading channel for any application. The first-order Markovian assumption implies that, given the information of current state, any future state should be independent of the previous state. Our first-order AR model (discrete-time SDE) (4.27) derived from the essential scattered electrical field (multi-path) equation (4.3) complies with the first-order Markovian assumption. There is evidence, though not conclusive, for improving the model accuracy by increasing the model order [20]. Here we restrict ourselves to an AR model of order one. The rationale behind this is as follows. The SDE theory favors the dynamical description of a wireless channel for a stationary receiver, as developed in section 4.3. Moreover, its discretization is automatically an AR model of order one, and it preserves the Markovian property since the underlying SDE is Markov in this case. Jakes' model overlooks the statistical analysis of stationary channels (i.e. channels without Doppler shift). The familiar Bessel function autocorrelation $J_0(2\pi f_D \tau)$ obtained from Jakes' model results in a constant (one) for a stationary channel; thus Jakes' model is inappropriate to describe a stochastic process that we consider here in which the temporal channel behavior is due to the relative phase fluctuations. Although second or higher order AR models may be appropriate to obtain closer approximation to the autocorrelation of a wireless channel with a particular Doppler frequency, we are not concerned with such non-stationary wireless channels here. We present a novel approach to obtaining a first-order

AR model for a stationary wireless channel through systematic mathematical reasoning from first principles beginning with the well accepted multi-path scattered electric field model, i.e. Eq. (4.3). Simulated data will be shown to verify our AR model in the next part of this section.

4.4.2 Verifying the AR Model Using Simulated Data

With computer generated channel data Ψ_{t_k} from (4.3) and (4.2), we define a difference process as

$$\Delta_\alpha \Psi_{t_k} = \Psi_{t_{k+1}} - \alpha \Psi_{t_k}, \tag{4.28}$$

where

$$\alpha = \frac{1 - \frac{1}{4} B \cdot \delta t}{1 + \frac{1}{4} B \cdot \delta t}. \tag{4.29}$$

If we can verify that the difference process $\Delta_\alpha \Psi_{t_k}$ is a complex Gaussian process with zero mean and β^2 variance, where

$$\beta = \frac{B^{\frac{1}{2}} \sigma_x \cdot \delta t^{1/2}}{1 + \frac{1}{4} B \cdot \delta t} \tag{4.30}$$

then the AR process for wireless channel (4.27) will be confirmed.

Figure 4.2 confirms that the real and imaginary parts of the difference process $\Delta_\alpha \Psi_{t_k}$ are Gaussian processes that we expected. Thus, our derived AR process described in (4.27) is well verified.

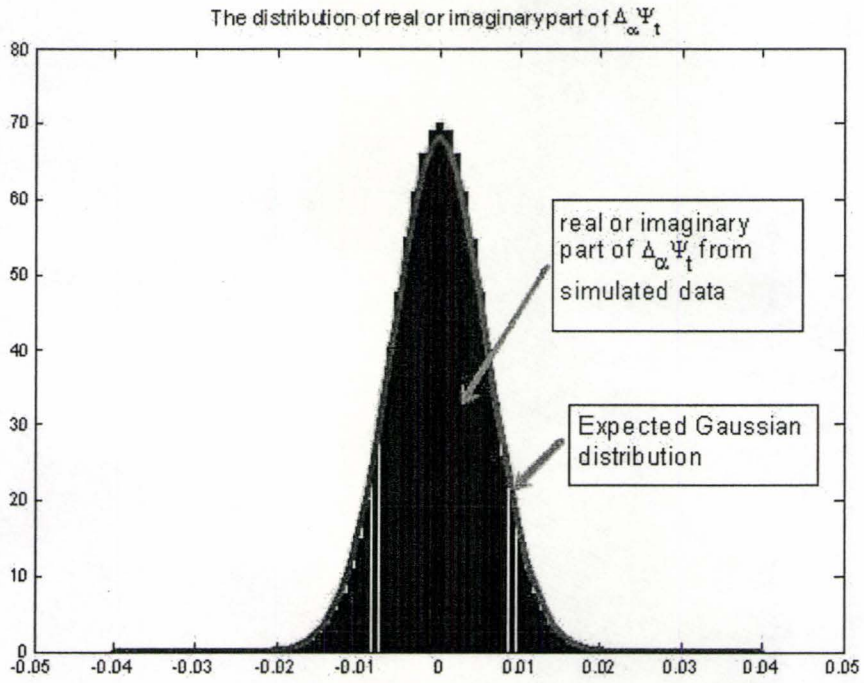

Figure 4.2: Comparison of the difference process from simulated channel data with the expected theoretical Gaussian distribution. Simulated channel data is generated with N=50, B=202 sec-1, sampling time δt= 10E-6 sec., σ^2=0.32. (cf. eq. (4.2), (4.3), (4.33), (4.34)).

4.5 Summary

In this chapter, we have presented a first-order stochastic AR model for a wireless channel which is based on SDE modeling of stationary Rayleigh fading wireless channels with "multipath reception" characterization. A rigorous and principled mathematical derivation of the origin of our stochastic AR model has been provided in detail. The AR model provides more channel information than previous AR models for stationary wireless channels. Moreover, simulated wireless channel data lend strong support to our first-order stochastic AR model. The essential features of the proposed stochastic AR model can be summarized as follows:

1. It can model stationary Rayleigh-distributed fading channels effectively.
2. It can efficiently generate synthetic Rayleigh-distributed channel data.
3. It is an instance of a first-order Markov chain.
4. The model developed follows from SDE theory under assumptions concerning the nature of multi-path fading channels.
5. The AR parameters express physical meanings.

4.6 Appendix

4.6.1 Proof of the stationarity for "multipath reception" ε_t in (4.3)

Since the relative phase $\varphi_t^{(k)}$ is based on a Wiener process as in (cf. (4.2)), $\varphi_t^{(k)}$ is a Markov process. Thus, $\exp\left[i\varphi_t^{(k)}\right]$ is also a Markov process. When $\varphi_0^{(k)}$ is chosen as random variable uniformly distributed upon $[0, 2\pi)$, the initial distribution of $\exp\left[i\varphi_t^{(k)}\right]$ will be uniformly distibuted on the unit circle $\{|z| = 1, z \in \mathbb{C}\}$, which is also the asymptotic distribution of $\exp\left[i\varphi_t^{(k)}\right]$. Under such initial conditions, the distribution of $\exp\left[i\varphi_t^{(k)}\right]$ does not change with time, so it is a (strict sense) stationary process. Thus, as a summation of scaled $\exp\left[i\varphi_t^{(k)}\right]$, ε_t is also a stationary Markov process if $\varphi_0^{(k)}$ is uniformly chosen on $[0, 2\pi)$.

4.6.2 Appendix: Proof of the SDE (4.12)

We provide a proof of the SDE (4.12). Corresponding to (3.31) and Ito's formula (3.35), the notations used in the section 4.3 are as follows. The phase $\varphi_t^{(k)}$ in Eq. (4.2) corresponds to in (3.31). Thus, comparing Eqs. (4.2) and (3.31) we have $b \to 0$ and $\sigma \to B^{1/2}$. The ε_t in Eq. (4.3) corresponds to F_t in (3.34) and identifying ε_t with $F_t = f(t, x_t)$ we identify:

$$
\begin{aligned}
dx_t &= d\varphi_t^{(k)} \\
\frac{\partial f}{\partial t} &= 0 \\
\frac{\partial f}{\partial x_t} = \frac{\partial(\sum x_k \exp\left[i\varphi_t^{(k)}\right])}{\partial \varphi_t^{(k)}} &= i x_k \exp\left[i\varphi_t^{(k)}\right] \qquad (4.31) \\
\frac{\partial^2 f}{\partial x_t^2} = \frac{\partial(i x_k \exp\left[i\varphi_t^{(k)}\right])}{\partial \varphi_t^{(k)}} &= -x_k \exp\left[i\varphi_t^{(k)}\right]
\end{aligned}
$$

Notice that the index k contributes to the summation in (4.3); thus (3.34) is extended to the multi-variate formula for the collection of component phases $\varphi_t^{(k)}, k = 1, 2, \cdots$, as

$$
dF_t = \frac{\partial f}{\partial t} \cdot dt + \sum \frac{\partial f}{\partial \varphi_t^{(k)}} \cdot d\varphi_t^{(k)} + \frac{1}{2} \sum \frac{\partial^2 f}{\partial (\varphi_t^{(k)})^2} \cdot (d\varphi_t^{(k)})^2 \qquad (4.32)
$$

Now, substituting all the relations in (E1) into the above equation, yields

$$
\begin{aligned}
d\varepsilon_t &= \sum i x_k \exp\left[i\varphi_t^{(k)}\right] \cdot d\varphi_t^{(k)} - \frac{1}{2} \sum x_k \exp\left[i\varphi_t^{(k)}\right] \cdot (d\varphi_t^{(k)})^2 \\
&= \sum x_k \left(i d\varphi_t^{(k)} - \frac{1}{2} (d\varphi_t^{(k)})^2 \right) \exp[j\varphi_t^{(k)}]
\end{aligned}
$$

and thus Eq. (4.12) is obtained.

4.6.3 Appendix: Proof of the SDE (4.13)

Assuming $dw_t^{(j)}$ and $dw_t^{(k)}$ for any j, k $(j \neq k)$ are independent. Introducing equation (4.2) into (4.12) and applying

$$\left(dw_t^{(j)}\right)^2 = dt,$$

we have

$$\begin{aligned} d\varepsilon_t^{(N)} &= \sum_{j=1}^{N} x_j \left(id\varphi_t^{(j)} - \frac{1}{2}(d\varphi_t^{(j)})^2 \right) \exp[j\varphi_t^{(j)}] \\ &= \sum_{j=1}^{N} x_j \left(iB^{1/2} dw_t^{(j)} - \frac{1}{2} B dt \right) \exp[j\varphi_t^{(j)}] \\ &= \sum_{j=1}^{N} x_j iB^{1/2} dw_t^{(j)} \exp[j\varphi_t^{(j)}] - \frac{1}{2} B dt \sum_{j=1}^{N} x_j \exp[j\varphi_t^{(j)}] \\ &= V - \frac{1}{2} B \varepsilon_t^{(N)} dt, \end{aligned} \tag{4.33}$$

where

$$V = \sum_{j=1}^{N} x_j iB^{1/2} dw_t^{(j)} \exp[j\varphi_t^{(j)}]. \tag{4.34}$$

Furthermore, we decompose V into real and imaginary parts as

$$\begin{aligned} V &= B^{1/2} \left[\sum_{j=1}^{N} x_j i \cos\left(\varphi_t^{(j)}\right) dw_t^{(j)} - \sum_{j=1}^{N} x_j \sin\left(\varphi_t^{(j)}\right) dw_t^{(j)} \right] \\ &= B^{1/2} \left[i \sum_{j=1}^{N} x_j \cos\left(\varphi_t^{(j)}\right) dw_t^{(j)} - \sum_{j=1}^{N} x_j \sin\left(\varphi_t^{(j)}\right) dw_t^{(j)} \right] \end{aligned} \tag{4.35}$$

The quantities $\sum_{j=1}^{N} x_j \cos\left(\varphi_t^{(j)}\right) dw_t^{(j)}$ and $\sum_{j=1}^{N} x_j \sin\left(\varphi_t^{(j)}\right) dw_t^{(j)}$ in the r.h.s. of (4.35) appearing above are scaled Wiener processes. We have

$$\sum_{j=1}^{N} x_j \cos\left(\varphi_t^{(j)}\right) dw_t^{(j)} = \sigma_c dw_t^{(c)} \tag{4.36}$$

where

$$\sigma_c^2 = \sum_{j=1}^{N} x_j^2 \cos^2\left(\varphi_t^{(j)}\right),$$

and

$$\sum_{j=1}^{N} x_j \sin\left(\varphi_t^{(j)}\right) dw_t^{(j)} = \sigma_s dw_t^{(s)} \tag{4.37}$$

where

$$\sigma_s^2 = \sum_{j=1}^{N} x_j^2 \sin^2\left(\varphi_t^{(j)}\right). \tag{4.38}$$

In (4.36) and (4.37), we claim that and are independent Wiener processes. Proof of independence follows.

Proof: From (4.35) and (4.36), (4.37), we have

$$\begin{aligned} V &= B^{1/2}\left[i\sigma_c dw_t^{(c)} - \sigma_s dw_t^{(s)}\right] \\ &= B^{1/2}\sigma_x\left[i\frac{\sigma_c}{\sigma_x} dw_t^{(c)} - \frac{\sigma_s}{\sigma_x} dw_t^{(s)}\right], \end{aligned} \tag{4.39}$$

where

$$\sigma_x^2 = \sigma_c^2 + \sigma_s^2 = \sum_{j=1}^{N} x_j^2. \tag{4.40}$$

We have

$$\begin{aligned}\left(\frac{\sigma_c}{\sigma_x}dw_t^{(c)}\right)\left(\frac{\sigma_c}{\sigma_x}dw_t^{(c)}\right) &= \frac{1}{2\sigma_x^2}\sum_{j=1}^{N}x_j^2\sin\left(2\varphi_t^{(j)}\right)\cdot dt \\ &= \frac{1}{2}dt\cdot\sum_{j=1}^{N}\alpha_j\sin\left(2\varphi_t^{(j)}\right), \qquad (4.41)\end{aligned}$$

where

$$\alpha_j = \frac{x_j^2}{\sigma_x^2}, \qquad (4.42)$$

and

$$\sum_{j=1}^{N}\alpha_j = 1. \qquad (4.43)$$

For $N\to\infty$, $\alpha_j\to 0+$, let $\left\{\varphi_t^{(\rho(j))}\right\}$ be a permutation of $\left\{\varphi_t^{(j)}\right\}$ so that $0\le\varphi_t^{(\rho(1))}<\varphi_t^{(\rho(2))}<\cdots<\varphi_t^{(\rho(N))}\le 2\pi$. Then in (4.41) we have

$$\begin{aligned}\sum_{j=1}^{N}\alpha_j\sin\left(2\varphi_t^{(j)}\right) &= \sum_{j=1}^{N}\alpha_j\sin\left(2\varphi_t^{(\rho(j))}\right) \\ &\simeq \frac{1}{2\pi}\int_0^{2\pi}\sin(2x)dx \\ &= 0, \qquad (4.44)\end{aligned}$$

From (4.41) and (4.44), we have

$$\left(\frac{\sigma_c}{\sigma_x}dw_t^{(c)}\right)\left(\frac{\sigma_c}{\sigma_x}dw_t^{(c)}\right)\to 0, \text{ for } N\to\infty. \qquad (4.45)$$

Thus, $dw_t^{(c)}$ and $dw_t^{(s)}$ are independent. Here, we use the fact that if $dw_t^{(c)}\cdot dw_t^{(s)}=0$, $dw_t^{(c)}$, $dw_t^{(s)}$ are independent (Ref. Karatzas & Shreve

[18]).

End

Furthermore, we have

$$\begin{aligned}\left(\frac{\sigma_c}{\sigma_x}\right)^2 &= \frac{1}{\sigma_x^2}\sum_{j=1}^{N} x_j^2 \cos^2\left(\varphi_t^{(j)}\right) \\ &= \sum_{j=1}^{N} \alpha_j \cos^2\left(\varphi_t^{(j)}\right) \\ &= \frac{1}{2} + \frac{1}{2}\sum_{j=1}^{N} \alpha_j \cos\left(2\varphi_t^{(j)}\right) \\ &= \frac{1}{2}\ N \to \infty. \end{aligned} \tag{4.46}$$

In the above, we use the fact that

$$\begin{aligned}\sum_{j=1}^{N} \alpha_j \cos\left(2\varphi_t^{(j)}\right) &\overset{N\to\infty}{=} \frac{1}{2\pi}\int_0^{2\pi} \cos(2x)dx \\ &= 0. \end{aligned} \tag{4.47}$$

Similarly, we have

$$\left(\frac{\sigma_s}{\sigma_x}\right)^2 \overset{N\to\infty}{=} \frac{1}{2}. \tag{4.48}$$

Introducing (4.46) and (4.48) into (4.39), we have

$$\begin{aligned} V &= \frac{B^{1/2}\sigma_x}{\sqrt{2}}\left[i dw_t^{(c)} - dw_t^{(s)}\right] \\ &= B^{1/2}\sigma_x \cdot d\xi_t, \end{aligned} \tag{4.49}$$

where

$$d\xi_t = \frac{1}{\sqrt{2}}\left[idw_t^{(c)} - dw_t^{(s)}\right]. \tag{4.50}$$

Since $dw_t^{(c)}$ and $dw_t^{(s)}$ are independent Wiener processes, $d\xi_t$ is a complex Wiener process. From (4.50), we deduce the following properties of $d\xi_t$:

$$|d\xi_t|^2 = dt, d\xi_t^2 = 0. \tag{4.51}$$

Now from (4.33) and (4.49), and for above ξ_t in (4.51), we have shown

$$d\varepsilon_t^{(N)} = -\frac{1}{2}B\varepsilon_t^{(N)}dt + B^{\frac{1}{2}}\sigma_x d\xi_t, \tag{4.52}$$

i.e. (4.13).

4.6.4 Appendix: Variance of Channel's envelope ε_t

From the definition of in (4.3), we have

$$\begin{aligned}
\mathbf{Var}\left(\varepsilon_t^{(N)}\right) &= \mathbf{E}\left(\left|\varepsilon_t^{(N)} - \mathbf{E}\left(\varepsilon_t^{(N)}\right)\right|^2\right) \\
&= \mathbf{E}\left(\varepsilon_t^{(N)} \cdot \left(\varepsilon_t^{(N)}\right)^*\right) \\
&= \sum_{k=1}^{N}\sum_{j=1}^{N} x_j x_k \mathbf{E}\left(\exp\left[i\varphi_t^{(j)} - i\varphi_t^{(k)}\right]\right).
\end{aligned} \tag{4.53}$$

For $j \neq k$,

$$\mathbf{E}\left(\exp\left[i\varphi_t^{(j)} - i\varphi_t^{(k)}\right]\right) = 0. \tag{4.54}$$

The above (4.53) is thus simplified as

$$\mathbf{Var}\left(\varepsilon_t^{(N)}\right) = \sum_{j=1}^{N} x_j^2. \tag{4.55}$$

From (4.40) and (4.55), we have

$$\sigma_x^2 = \mathbf{Var}\left(\varepsilon_t^{(N)}\right). \tag{4.56}$$

(See main text under (4.13))

Chapter 5

Multipath Flat Fading Channel With Doppler Frequency

5.1 Introduction

In chapter 4, we have discussed the statistical analysis the multipath flat fading channel without Doppler frequency shift, and successfully derive / obtain a first-order AR model to represent such channel. In this chapter, we will consider a more general case, i.e. wireless flat fading channel with Doppler frequency shift.

Analysis and modeling such channels are essential to wireless communication systems. The traditional statistical analysis, such as autocorrelation and power spectrum, based on Clarke's model [26] is not appropriate to describe real multipath flat channels. In this chapter, we will extend the traditional Clarke's model incorporating the effect of fluctuations in the component

phases, and perform the statistical analysis. For a general flat fading channel with Doppler frequency, a first order AR model is not a appropriate, while we use a state-space model to represent the flat fading channel very well.

Statistical analysis and modeling of wireless channels is essential to wireless communication systems. Clarke's model [26] and the corresponding statistical analysis of mobile radio reception has been widely accepted in numerous wireless applications. Since the component phases in Clarke's model are assumed to be constant in time, the well-known results of statistical analysis based on this model, such as the autocorrelation and Doppler power spectrum (Jake's spectrum [19]), are not appropriate to describe real wireless channels for which the random environments (radio propagation paths) are time-varying and accordingly for which the channel is non-constant in the absence of Doppler frequency shift. In comparison with measured spectra, Jakes' spectrum has limitations - it is unbounded and does not incorporate the effect of temporal phase fluctuations.

In the section 5.2 of this chapter, we extend the traditional Clarke's model incorporating the effect of fluctuations in the component phases, and perform the statistical analysis which results in a closed-form expression of the autocorrelation of the fading. The theoretical power spectral density function, which is the Fourier transform of the resultant autocorrelation of the fading, is shown to fit the practical measured spectra, which is in contrast to the traditional theoretical flat fading channel spectra (Jakes' spectrum). The proposed model and statistical results should have important implications for detailed spectral analysis and channel simulations for real wireless communications systems in

random fluctuating electromagnetic propagation environments.

Section 5.3 discusses the dynamic modeling of a general multipath flat channel. We develop here a state-space model (SDEs) that represents a wireless channel with these modified spectral characteristics. This is achieved by developing the relationship between a continuous-time state-space model and the theory of the rational transfer function. A novel method for the design of a rational transfer function of a linear system is proposed. The system input is a Gaussian white noise process, which generates a wireless channel with a desired arbitrary power spectrum. We represent the rational transfer function via the *Observable Canonical Form* (OCF) to obtain the continuous-time state-space model. A discrete-time version of the state-space model is then provided to represent and simulate a discrete-time flat fading wireless channel.

Section 5.4 introduces some other approaches to multipath fading channel simulation. One is based on Clarke's scattering model and operated in the time-domains; the second is based on transforming the frequency domain to the time domain with IFFT realization, the third is based on a filtering-method in the time-domain. Comparing with these available approaches, the presented state-space approach in section 5.3 is simplest to realize. The summary and conclusions for this chapter are drawn in section 5.6.

5.2 Statistical Analysis of A Wireless Flat Channel With Doppler Frequency

In a wireless mobile communication system, the signal incoming to the receiver contains a large number of reflected radio waves - this phenomenon is referred to as multipath propagation. The received signal has randomness in its amplitude, phase, and angle of arrival, giving rise to the multipath fading for the resultant received envelope or amplitude. In this section, we integrates the dynamics of phase fluctuations and terminal motion into the modeling of wireless mobile channels and discusses the resultant effect on the channel's autocorrelation and power spectrum.

For a time-varying channel with terminal motion, it has been traditionally assumed that when there is no relative motion between the receiver and transmitter, the entirety of all reflected radio waves generate a "stationary" channel, i.e. the received signal is constant in time, so that the channel appears to be time-invariant. For a deeper perspective of such assumptions in mathematical terms, we firstly revisit the familiar traditional Clarke's model for a wireless flat fading channel (ref:[26]), expressed as

$$\varepsilon_t = \sum_{n=1}^{N} x_n \exp[j(2\pi f_n t + \varphi^{(n)})], \tag{5.1}$$

where the x_n is the electric field strength of the nth path, the f_n are the Doppler shift components corresponding to nth path and the relative component phases $\{\varphi^{(n)}\}$ are assumed to be constant in time. The quantity ε_t rep-

resents the complex envelop of N signal rays with assuming that all rays are arriving from a horizontal direction and come from arbitrary angles surrounding the receiver. (Notice that the carrier frequency, i.e. ω_0, has been removed in (5.1). Eq. (5.1) is implicit in both Clarke's and Jakes' models.) From Clarke's model, i.e. (5.1), it is clear that the complex envelope ε_t is constant when $f_n = 0$, i.e. when there is no relative motion between the receiver and the transmitter. Thus, the model accords with the traditional assumptions. Based on Clarke's model, i.e. (5.1), the autocorrelation is derived in terms of the zeroth-order Bessel function of the first kind (cf.[26]), i.e. $P_0 J_0(2\pi f_D \tau)$ (P_0 is the average power of the received signal, and f_D is the maximum Doppler frequency shift). Correspondingly, according to the Wiener-Khintchine theorem, the power spectral density (PSD) of the flat channel in Clarke's model is equal to the Fourier transform of the aforementioned autocorrelation, thus

$$S(f) = \begin{cases} \frac{P_0}{\pi f_D \sqrt{1-(f/f_D)^2}} & |f| < f_D \\ 0 & |f| > f_D \end{cases}, \tag{5.2}$$

which is traditionally referred to as *Jakes' spectrum*. The maximum Doppler frequency arises as

$$f_D = \frac{v}{c} \cdot f_c, \tag{5.3}$$

where v is the speed of the mobile receiver, c is the (constant) speed of light in air, and f_c is the carrier frequency of the transmitted signal. Observe that, despite the divergence of Jakes' spectrum as the frequency f tends to $\pm f_D$, the spectrum has finite energy.

However, in a real mobile radio communication environment, even without

relative motion, the received signal still fluctuates in time, i.e. the channel is time-varying because the electromagnetic propagation environment is still time-varying. This implies that the relative component phases of reflected radio waves $\{\varphi^{(n)}\}$ are also time-varying. Therefore, the traditional Clarke's model is not sufficient to describe such situations, and the results of the statistical analysis based on the traditional Clarke's model (5.1) must be modified to include the effect of explicit time dependence in the component phases. For example, the autocorrelation of the fading (cf. [26]), which is the zeroth-order Bessel function of the first kind, i.e. $J_0(2\pi f_D \tau)$ (f_D is the maximum Doppler frequency shift) reduces to a constant when the maximum Doppler frequency shift is zero, so it is inappropriate to provide a reasonable statistical description for a wireless channel which is still time-varying even without Doppler frequency shift (no motion between transmitter and receiver).

The traditional U-shape theoretical Doppler power spectrum (Jakes' spectrum), the Fourier transform of the Bessel function $J_0(2\pi f_D \tau)$, has limitations in terms of representing a practically measured spectra. For example, the traditional U-shape theoretical spectrum cannot specify the peak value and has a fixed spectral width, i.e. $2f_D$ (f_D is the maximum Doppler frequency shift), whereas the real measured spectrum will reach a peak near the maximum Doppler frequency and then decay to zero (see Figure 5.3 in section 5.2.2).

Based on the above discussion, we see that it is meaningful to develop an extended Clarke's multipath model for flat fading channels such that it allows the relative phases to fluctuate in time and accordingly generates a new theoretical power spectrum closer to the practical measurement than the Jakes'

spectra. The scattered electric field model with dynamic relative phases and a fixed Doppler frequency shift, independent of signal ray ($f_n = f_0$, for all n), is presented in [12], where statistical analysis of the model, such as the auto-correlation and power spectrum, is also discussed. The multipath model with dynamic phases and zero Doppler shift for flat channel is presented in [27], where a stochastic differential equation (SDE) and a first-order autoregressive (AR) process are obtained to describe the dynamics of the channel. In this section 5.2, we shall focus on a novel multipath flat fading channel model, introducing fluctuating component phases into the traditional Clarke's model, and provide a rigorous statistical analysis of the proposed fading model. We argue that this extended channel model and its statistical properties are essential for accurate spectral analysis and channel simulations in wireless communications.

This section 5.2 is organized as follows. Firstly in subsection 5.2.1, we present a channel model extended from the traditional Clarke's model [26], allowing the relative component phases to fluctuate in time. Then, in subsection 5.2.2, statistical analysis is applied to the model, obtaining closed-form expressions for the autocorrelation of fading and the corresponding power spectral density. Simulation of discrete channel data is provided in subsection 5.2.3.

5.2.1 Fading Model For Mobile Radio Reception

In this subsection, we extend Clarke's model [26] for mobile radio reception, by considering explicitly time-varying component phases. Similarly to the

mathematical embodiment of Clarke's model in the form of Eq. (5.1), we let

$$\varepsilon_t = \sum_{n=1}^{N} x_n \exp[j(2\pi f_n t + \varphi_t^{(n)})] \tag{5.4}$$

represent the complex envelope of N signal rays arriving at a moving receiver, where x_n is the strength of the nth signal ray which has a relative Doppler shift f_n and a relative component phase $\varphi_t^{(n)}$ where the subscript indicates the time variation. All rays are assumed to arrive from a horizontal direction (cf. [26]). In the original Clarke's model, the component phases $\{\varphi_t^{(n)}\}$ are assumed to be time-invariant and i.i.d. random variables uniformly distributed over $[0, 2\pi)$ (i.e. $\varphi_t^{(n)}$ is written simply as $\varphi^{(n)}$). Here, we relax the assumption on the component phases such that they are time-dependent, and $\{\varphi_t^{(n)}\}$ is a collection of independent Wiener processes (see Appendix 5.5.1 on page 111) with uniform random initialization on the interval $[0, 2\pi)$, with the dynamical property that (cf. [12])

$$d\varphi_t^{(n)} = B^{1/2} dw_t^{(n)}, \tag{5.5}$$

in which dw_t represents the infinitesimal increments in a Wiener process w_t (Ref. [14]) and $d\varphi_t^{(n)}$ represents the infinitesimal increments in the relative phases $\varphi_t^{(n)}$. Here, B is a positive constant with the dimension of frequency, which determines the correlation time scale of the component phase process (see Eq. (5.18)). Note that, for any instant of time t, the amplitude of the complex envelope ε_t is still Rayleigh distributed due to the independence assumption amongst the component phases $\{\varphi_t^{(n)}\}$. With the assumption of phase fluctuations according to (5.5), Field & Tough [12] successfully ap-

plied a random walk model (where Doppler shift is fixed independent of the path/scatterer) to the analysis of radar sea clutter in Ref. [13].

The proposed dynamical model for mobile radio reception should be applicable to a broad range of wireless communication environments, such as GSM/CDMA, satellite communication, etc.

5.2.2 Statistical Analysis of Fading Model

In this subsection, we focus on the statistical analysis of the fading phenomenon based on the model presented in section 5.2.1. The autocorrelation of the fading will be discussed first, followed by the power spectrum.

Autocorrelation

The autocorrelation of the complex envelope ε_t is written as

$$R_\varepsilon(\tau) = \mathbf{E}[\varepsilon_t \varepsilon^*_{t+\tau}]. \tag{5.6}$$

where the asterisk denotes complex conjugation, $\mathbf{E}[\cdot]$ denotes the statistical expectation, and τ is a time lag. We begin by computing the cross-correlation between a pair of signal rays, which is given by

$$\begin{aligned} &\mathbf{E}[x_n e^{j(2\pi f_n t + \varphi_t^{(n)})} \cdot x_m e^{-j(2\pi f_m (t+\tau) + \varphi_{t+\tau}^{(m)})}] \\ &= \mathbf{E}[e^{j2\pi f_n t} \cdot e^{-j2\pi f_m (t+\tau)}] \mathbf{E}[x_n e^{j\varphi_t^{(n)}} \cdot x_m e^{-j\varphi_{t+\tau}^{(m)}}] \end{aligned} \tag{5.7}$$

in which we can assume that the Doppler shift (determined by the angle of the propagation relative to the direction of motion, see (5.12) below) is independent of the component phase and amplitude in the component paths or 'signal rays' because the motion of the terminal has no statistical relation with that of the scatterer motion. So, the Doppler envelope is independent of phase. We also neglect the effects of small changes in distance/time-delay on the amplitude $\{x_n\}$ of the component signal rays (cf. footnote on p. 43). Due to the assumption of independence of any pair of signal rays, we have

$$\mathbf{E}[x_n e^{j\varphi_t^{(n)}} \cdot x_m e^{-j\varphi_{t+\tau}^{(m)}}] = \begin{cases} 0 & if \quad m \neq n \\ \mathbf{E}[x_n^2] \cdot \mathbf{E}[e^{j(\varphi_t^{(n)} - \varphi_{t+\tau}^{(n)})}] & if \quad m = n \end{cases} \tag{5.8}$$

Substituting (5.8) into (5.7), we arrive at

$$\begin{aligned} &\mathbf{E}[x_n e^{j(2\pi f_n t + \varphi_t^{(n)})} \cdot x_m e^{-j(2\pi f_m (t+\tau) + \varphi_{t+\tau}^{(m)})}] \\ &= \begin{cases} 0 & if \quad m \neq n \\ \mathbf{E}[x_n^2]\mathbf{E}[e^{-j2\pi f_n \tau}]\mathbf{E}[e^{j(\varphi_t^{(n)} - \varphi_{t+\tau}^{(n)})}] & if \quad m = n \end{cases} \end{aligned} \tag{5.9}$$

Using the result of (5.9) with (5.4) substituted into (5.6), we obtain the autocorrelation of the complex envelope as

$$\begin{aligned} R_\varepsilon(\tau) &= \mathbf{E}[\sum_{n=1}^{N} x_n e^{j(2\pi f_n t + \varphi_t^{(n)})} \sum_{m=1}^{N} x_m e^{-j(2\pi f_m (t+\tau) + \varphi_{t+\tau}^{(m)})}] \\ &= \sum_{n=1}^{N} \mathbf{E}[x_n^2]\mathbf{E}[e^{-j2\pi f_n \tau}]\mathbf{E}[e^{j(\varphi_t^{(n)} - \varphi_{t+\tau}^{(n)})}]. \end{aligned} \tag{5.10}$$

Here, we let

$$P_0 = \sum_{n=1}^{N} \mathbf{E}[x_n^2] \tag{5.11}$$

which is the average received power.

If the direction of radiation of nth signal path and the terminal motion are at angle ψ_n, based on the knowledge of the physics the component Doppler shift for a component propagation path is given by

$$f_n = f_D \cos\psi_n \tag{5.12}$$

where f_D is the maximum Doppler shift, which occurs for signal rays that are in the same direction as the motion of the terminal (cf. Eq. (5.3)). With the assumption that ψ_n are uniformly distributed over the interval $[0, 2\pi)$, we see that the average Doppler frequency shift will be zero, i.e.

$$E[f_n] = \frac{1}{2\pi}\int_0^{2\pi} f_D \cos\psi d\psi = 0. \tag{5.13}$$

Substituting (5.11) and (5.12) into (5.10), finally we obtain

$$R_\varepsilon(\tau) = P_0 \mathbf{E}[e^{-j2\pi f_D \tau \cos\psi_n}]\mathbf{E}[e^{j(\varphi_t^{(n)} - \varphi_{t+\tau}^{(n)})}]. \tag{5.14}$$

The first expectation expression on the right hand side of (5.14), i.e. $\mathbf{E}[e^{-j2\pi f_D \tau \cos\psi_n}]$, has a simple closed-form derived previously by R.H. Clarke [26], namely

$$\begin{aligned} \mathbf{E}[e^{-j2\pi f_D \tau \cos\psi_n}] &= \frac{1}{2\pi}\int_0^{2\pi} e^{-j2\pi f_D \tau \cos\psi} d\psi \\ &= J_0(2\pi f_D \tau) \end{aligned} \tag{5.15}$$

where $J_0(x)$ is the zeroth-order Bessel function of the first kind. The right hand side of (5.15) is the traditional expression of autocorrelation of the fading in time with unit average power.

Based on our essential modification that the component phases are Wiener processes, governed by (5.5) rather than mere constants, we obtain

$$\begin{aligned} \varphi_t^{(n)} - \varphi_{t+\tau}^{(n)} &= \int_t^{t+\tau} B^{1/2} dw_t^{(n)} \\ &= -B^{1/2}(w_{t+\tau}^{(n)} - w_t^{(n)}) \end{aligned} \tag{5.16}$$

where $w_t^{(n)}$ is a standard Wiener process as before. Thus, $w_{t+\tau}^{(n)} - w_t^{(n)}$ is Gaussian distributed random variable with zero mean and variance of $|\tau|$, i.e.

$$w_{t+\tau}^{(n)} - w_t^{(n)} \sim \frac{1}{\sqrt{2\pi|\tau|}} \exp(-\frac{x^2}{2|\tau|}) \tag{5.17}$$

where $\sim$ indicates the distribution of a random variable according to some probability density function. Observe that, according to this description, the component phase differences are *unbounded*. However, via exponentiation according to (5.4), it is the phase *wrapped* processes that determine the received envelope, and in this respect each (wrapped) phase difference is uniformly distributed on the unit circle in the complex plane (cf. discussion above Eq. (5.5). Using (5.16) and (5.17), we derive that

$$\begin{aligned} \mathbf{E}[e^{j(\varphi_t^{(n)} - \varphi_{t+\tau}^{(n)})}] &= \mathbf{E}[e^{-jB^{1/2}(w_{t+\tau}^{(n)} - w_t^{(n)})}] \\ &= \int_{-\infty}^{\infty} e^{-jB^{1/2}x} \frac{1}{\sqrt{2\pi|\tau|}} e^{-\frac{x^2}{2|\tau|}} dx \\ &= e^{-B|\tau|/2} \end{aligned} \tag{5.18}$$

Substituting (5.15) and (5.18) into (5.14), we finally obtain the close form expression for the autocorrelation of the fading as

$$R_\varepsilon(\tau) = P_0 e^{-B|\tau|/2} J_0(2\pi f_D \tau) \tag{5.19}$$

Comparing this result with the traditional expression for the autocorrelation of the fading, our expression derived from our extended Clarke's model, i.e. multipath radio reception with component phase fluctuations, has an extra exponential decaying term, whose exponential index is proportional to the time delay. Thus, we observe that the combined autocorrelation of complex radio reception consists of two terms, one is the familiar Bessel function, i.e. $J_0(2\pi f_D \tau)$, resulting from Doppler shift, and the additional term arising from our extended model is the exponential decay function, i.e. $e^{-B|\tau|/2}$, arising from the component phase fluctuations and which exists independently of the motion of the receiver. In the case that $B \to 0$, i.e. absence of fluctuations in component phases, the exponential term $e^{-B|\tau|/2}$ approaches unity, so that the presented closed-form expression of autocorrelation of the fading (5.19) approaches the traditional autocorrelation for Clarke's model. Figure 5.1 plots the autocorrelation function of the complex envelope as a function of the normalized parameters $B\tau$ and $f_D\tau$ appearing in (5.19).

As a special case, when the maximum Doppler shift f_D is zero, the autocorrelation $R_\varepsilon(\tau)$ in (5.19) reduces to an exponential decaying function. Ref. [27] discusses this special case mathematically in terms of a first-order autoregressive (AR) model. It is well known that a first-order AR process has an

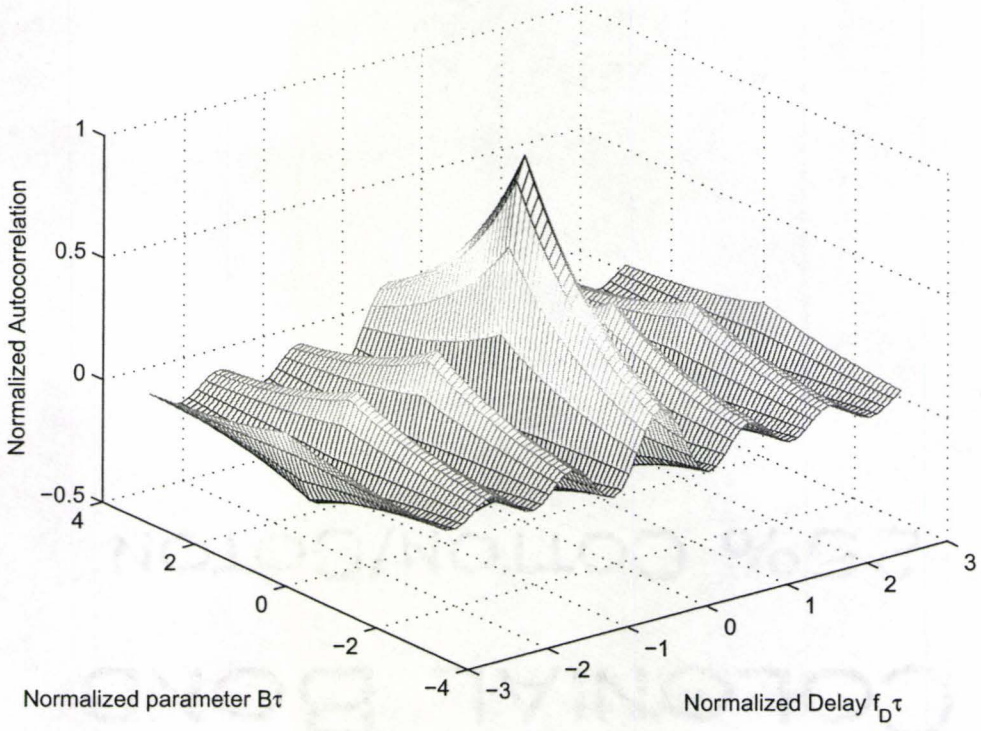

Figure 5.1: Autocorrelation of the complex envelope of the received signal according to the proposed extended Clarke's model

exponential decay property for its autocorrelation. In the case of real wireless applications, the time-varying electromagnetic propagation environment makes the channel fluctuate even if there is no relative motion between transmitter/receiver (i.e. zero maximum Doppler shift). The traditional Clarke's model is inappropriate for such cases because it implies that channels with zero Doppler are (random but) constant in time. Thus, our proposed multipath model embodied in Eqs. (5.4) and (5.5), together with the closed-form expression of the autocorrelation in (5.19), can be viewed as an extension of Clarke's work for more general cases of wireless channels.

Power Spectrum

The power spectrum of the fading process, denoted as $S_\varepsilon(f)$, is determined, via the Wiener-Khintchin theorem, as the Fourier transform of the autocorrelation function of the complex envelope, thus

$$\begin{aligned} S_\varepsilon(f) &= \mathcal{F}\{R_\varepsilon(\tau)\} \\ &= \mathcal{F}\{P_0 e^{-B|\tau|/2} J_0(2\pi f_D \tau)\} \\ &= P_0 \mathcal{F}\{e^{-B|\tau|/2}\} \otimes \mathcal{F}\{J_0(2\pi f_D \tau)\} \end{aligned} \tag{5.20}$$

where $\mathcal{F}\{\cdot\}$ is the Fourier transform operator and the sign $\otimes$ denotes convolution defined as

$$x(\tau) \otimes y(\tau) = \int_{-\infty}^{\infty} x(\tau - \lambda) y(\lambda) d\lambda \tag{5.21}$$

Specifically, we have

$$\mathcal{F}\{e^{-B|\tau|/2}\} = \frac{B}{(B/2)^2 + (2\pi f)^2} \quad B > 0 \tag{5.22}$$

and

$$\mathcal{F}\{J_0(2\pi f_D \tau)\} = \begin{cases} \frac{1}{\pi f_D \sqrt{1-(f/f_D)^2}} & |f| < f_D \\ 0 & |f| > f_D \end{cases} \tag{5.23}$$

Substituting (5.22), (5.23) and (5.21) into (5.20), we obtain the final expression for the power spectrum of the fading process as

$$S_\varepsilon(f) = \int_{-f_D}^{f_D} \frac{B}{(\frac{B}{2})^2 + [2\pi(f-\lambda)]^2} \frac{P_0/\pi}{\sqrt{f_D^2 - \lambda^2}} d\lambda \tag{5.24}$$

Eq. (5.23) is also the traditional representation of the power spectrum of the flat fading channel for unit average power, which is also referred to as *Jakes' spectrum.* Similar to the discussion of autocorrelation above, in the limit $B \to 0$, the power spectrum $S_\varepsilon(f)$ will approach the traditional Jakes' power spectrum, as apparent from the expression for $S_\varepsilon(f)$ in (5.20). Figure 5.2 is a plot of the power spectrum expressed in (5.24) for unit average power, i.e. $P_0 = 1$ with $B > 0$.

From (5.23), we see that the traditional representation of the power spectrum for the flat channel (Jakes' spectrum) takes infinite value at the maximum Doppler shift f_D in the frequency (f) axis and is zero outside of the interval $[-f_D, +f_D]$; thus it cannot specify the peak value near the maximum Doppler shift and at what frequency and how fast the spectrum decays beyond the peak value. Indeed, the spectra gathered from practical measurements are al-

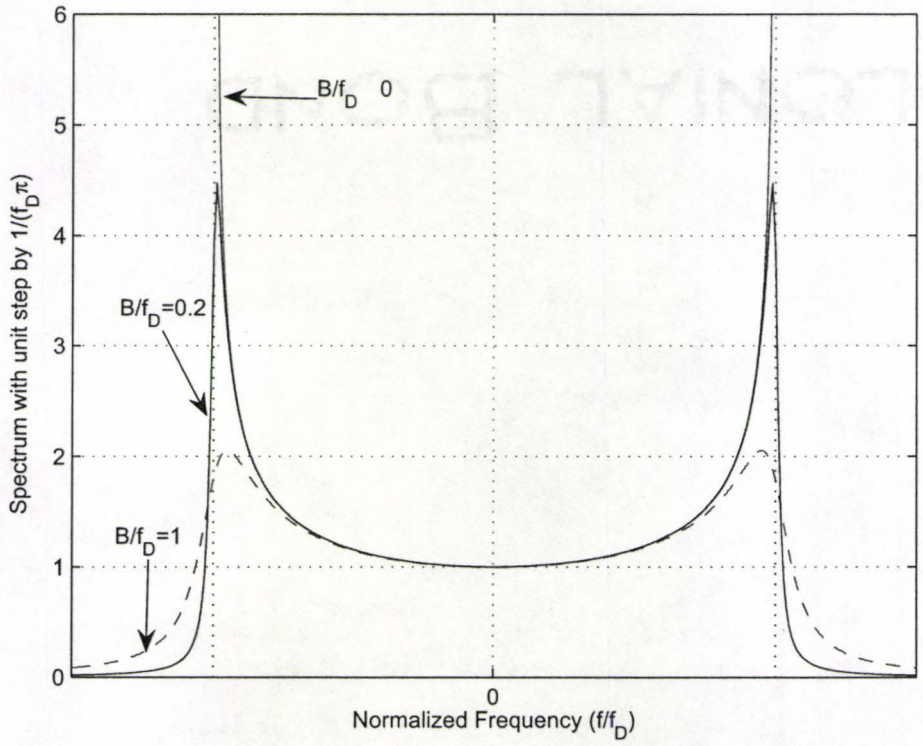

Figure 5.2: Power spectrum of the fading process for the proposed model (Traditional power spectrum for Clarke's model is also plotted as a special case for $B \rightarrow 0$.)

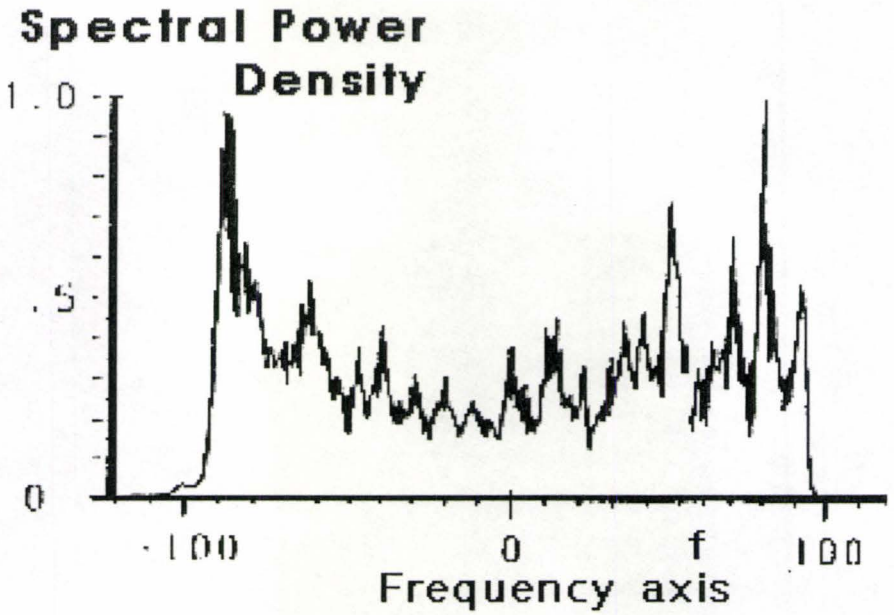

Figure 5.3: Measured Doppler Spectrum at 1800 MHz. Source: Research group of Prof. Paul Walter Baier, U. of Kaiserslautern, Germany (cf. [36])

ways finite and exhibit peaks near the maximum Doppler frequencies [34][35], decaying to zero as shown in figure 5.3 for a typical measured power spectrum for a flat channel. The frequency (f-axis) in figure 5.3, although not addressed in the literature previously, incorporates the effects of both phase fluctuations and Doppler components f_n, and so the terminology 'power spectrum' is more appropriate than 'Doppler spectrum'. By selecting the parameters B and P_0, we exhibit a specific theoretical power spectrum as close as possible to the measured spectrum of figure 5.3, which is shown in figure 5.4 and indepedently in figure 5.5. Comparing the theoretical spectra and the measured spectra in figure 5.4, it is apparent that our spectra $S_\varepsilon(f)$ formed by (5.24) approaches more closely the measured spectra as compared to the U-shape Jakes' spectrum.

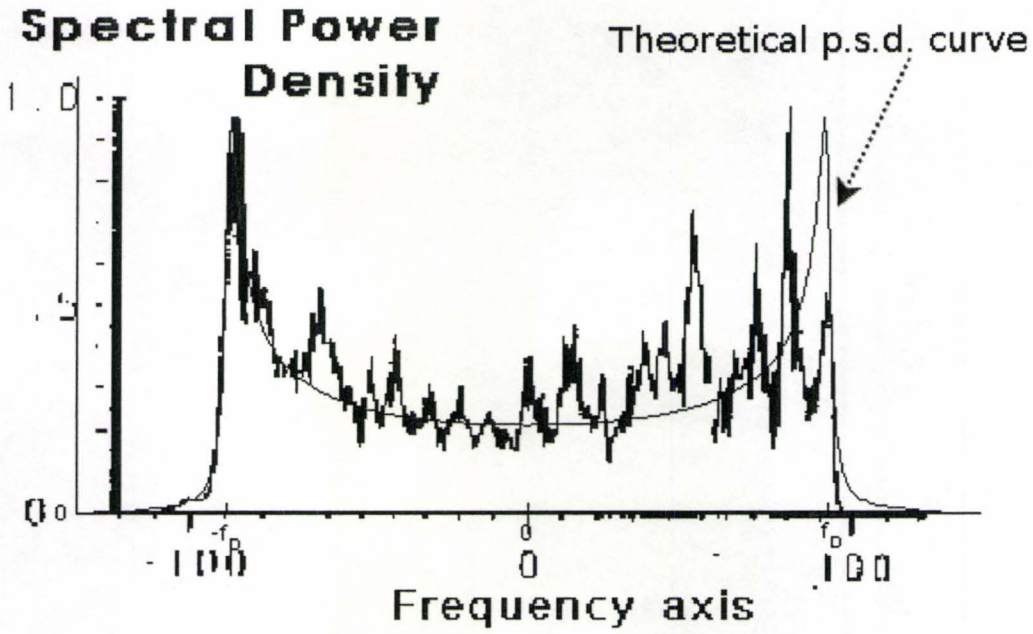

Figure 5.4: Comparing the theoretical power spectrum density with the measured power spectrum density. Theoretical spectrum: $B/f_D = 0.2$, $P_0/f_D = 0.2\pi$. Source of measured spectrum: Research group of Prof. Paul Walter Baier, U. of Kaiserslautern, Germany (cf. [36])

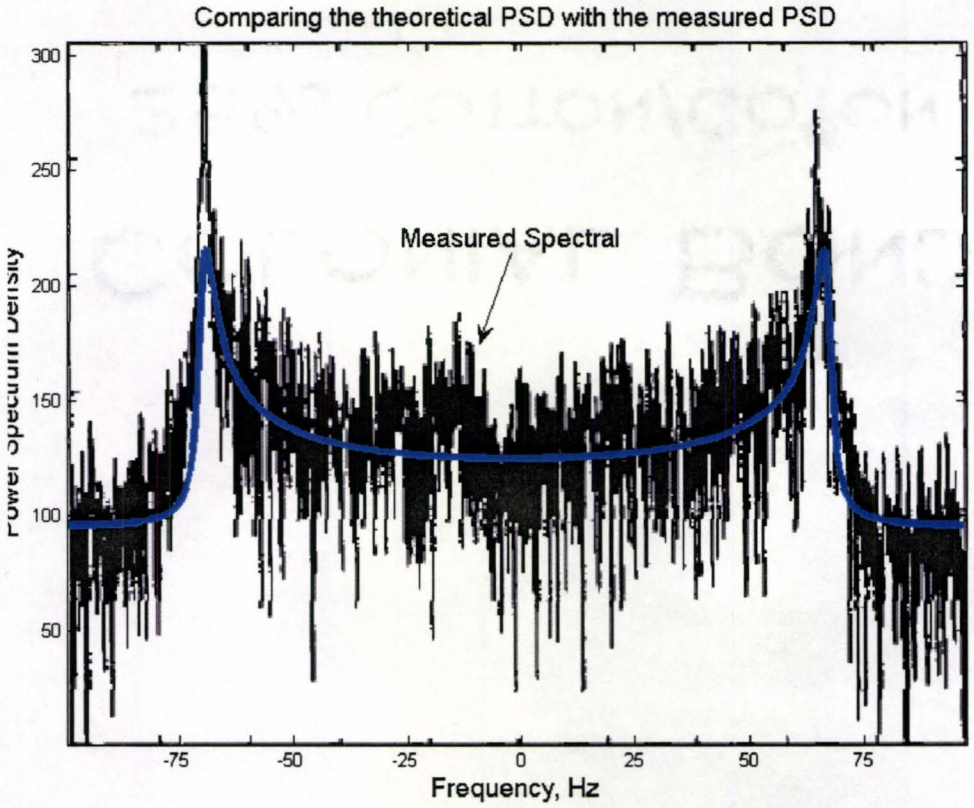

Figure 5.5: Comparing the theoretical power spectrum density with the measured power spectrum density. Theoretical spectrum: $B/f_D = 0.25$, $P_0/f_D = \pi$. Source of measured spectrum: cf. [29]

From figure 5.2, we observe how the value of B affects the shape of the spectra $S_\varepsilon(f)$ in respect of the peak value and peak width. Here, the definition of peak width depends on the practical requirements; one possible definition is the widely used 3dB width familiar in engineering applications.

In order to generate/simulate a power spectrum with a specified peak value and peak width based on our proposed multipath model we may firstly compute the value of B to satisfy the peak width requirement, and then adjust the value of P_0 to achieve the desired peak value. Such procedure has been used to obtain the theoretical power spectrum density curve shown in figure 5.4. Alternatively, estimation of the parameter B from measured data could be obtained by applying statistical information geometric techniques [38]. The *Fisher* information (geodesic) distance $d(\cdot,\cdot)$ between the measured and theoretical spectra can be minimized (over B) according to

$$\min_{(B)} d\left(\hat{S}^{(obs)}, \hat{S}^{(B)}\right) = \cos^{-1} \int \sqrt{\hat{S}^{(obs)}(\omega)\hat{S}^{(B)}(\omega)}d\omega \qquad (5.25)$$

($\omega = 2\pi f$) in which the $d(\cdot,\cdot)$ is regarded as a functional of the spectra that depends on the parameter B and where $\hat{}$ denotes normalization. The accurate setting of B obtained in this way should be of crucial importance in channel modeling.

In most mobile communication systems, the technique of channel coding is used for better reproduction of transmitted signals in a channel noise environment. For a wireless system with channel coding, it should be of interest to measure the performance of variant channel codings against the corrup-

tion of Rayleigh channels with different channel characteristics, i.e., maximum Doppler shift f_D, phase fluctuation parameter B, etc. Channel coding introduces correlation within the blocked information sequence, thus the channel correlation property will affect the channel decoding procedure. Such research topics are not covered in this thesis, and will be explored in our future research.

5.2.3 Simulation and Verification

In this subsection, we verify the closed-form expression for the autocorrelation of the fading process, i.e. (5.19), through the simulated data generated from the fundamental fading model (5.4) with component phase fluctuations, i.e. (5.5), and physical relation between Doppler shift f_n and angle of arrival ψ_n, i.e. (5.12). Our objective here is to verify our theoretical results, rather than provide a detailed channel generator/simulator, and so we are not concerned with the precise choice of the angles ψ_n in (5.12) and the number N of signal rays in (5.4) provided that their number N is large and the angles ψ_n are chosen uniformly on $[0, 2\pi)$. The routine of the computer simulation of discrete channel data is as follows:

For $k = 0, 1, 2, \cdots$, with $\{\psi_n\}$ is uniformly chosen from $[0, 2\pi]$, do

$\varepsilon_k = \frac{1}{N} \sum_{n=1}^{N} \exp[j(2\pi k f_D \Delta T \cos\psi_n + \varphi_k^{(n)})]$

$\varphi_{k+1}^{(n)} = \varphi_k^{(n)} + (B\Delta T)^{1/2} g_k^{(n)}, \quad g_k^{(n)} \sim \mathcal{N}(0, 1)$

Initialization: $\varphi_0^{(n)}$ is uniformly chosen from $[0, 2\pi]$.

Here, ΔT is the sampling period, $\{g_k^{(n)}\}$ are i.i.d. normal distributed with zero mean and unit variance.

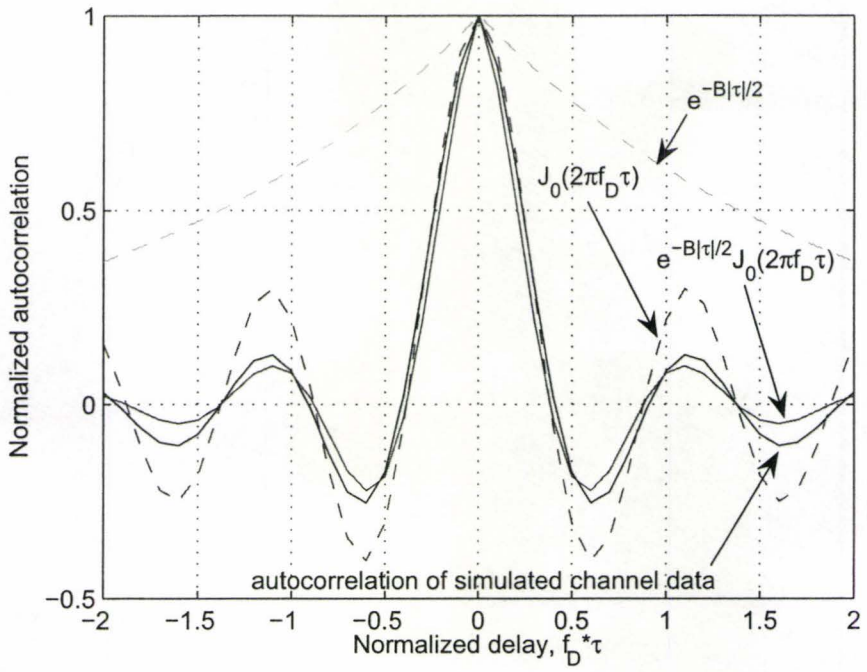

Figure 5.6: Verification of the close form autocorrelation in (5.19) from the simulated channel data with $B = 100$Hz, $N = 200$, $f_D = 100$Hz, $\Delta T = 10^{-3}$s, and $4 \cdot 10^6$ samplings.

The autocorrelation calculated from the simulated discrete channel data is plotted in figure 5.6, which confirms our theoretical derivation of the close form expression of autocorrelation of the fading as in (5.19).

5.2.4 The Implications of Modified Clarke's model to Wireless System Design

We have discussed the statistical characteristics of the presented extended Clarke's model and compared the resultant theoretical PSD with the measured spectrum. The modified channel model provides not only help on more

accurate assessment of system design but also important reference to receiver design. With regard to modelling a channel, we can predict the performance of modulation and coding algorithms by analysis or simulation (cf. [24]).

Random FM

In a communication system, discriminators function as the time derivative of the phase of the received signal, one component of which is *random FM*, the derivative (more precisely, in the presence of phase fluctuations, the difference time series) of the phase of the complex gain, i.e. ε_t in (5.4), where it appears as an additive disturbance with respect to phase. The power spectrum of random FM that is given in the standard Jakes model [19] can be used to calculate the probability of error, corresponding to the bit-error-rate (BER), when neglecting the additive measurement noise. This probability of error induced by random FM is also termed "Error Floor" because it cannot reach zero for any signal-to-noise ratio (SNR), however large (provided the Doppler f_D is non zero). When a more accurate channel model is introduced, such as the extended Clarke's model presented herein, we may produce more accurate theoretical power spectrum of random FM, resulting more accurate calculation of "Error Floor". This would be a very interesting topic in future research. The higher maximum Doppler frequency shift, the higher "Error Floor" will be. Thus, random FM is an important factor to receiver's design.

Level Crossing Rate

The level crossing rate (LCR) is a measure of the rapidity of the fading. It quantifies how often the fading crosses some threshold. The LCR is very important for system and receiver design because it determines how to choose a burst error correcting code, how to verify the burst error correcting code, how to choose the depth of interleaving to break up bursts, etc. [24]. With our proposed extended Clarke's model, more accurate statistical characteristics, e.g. power spectral density function, are impled that will provide a more accurate LCR calculation. This will be another potential interesting topic in future research.

5.3 Dynamic Modeling of A Wireless Flat Channel With Doppler Frequency

Various multipath models have been proposed since the 1960s. The most common model is the one proposed by Clarke [26], where the statistical characteristics of the signal at the mobile receiver are deduced from basic principles of electromagnetic scattering / propagation. Although Clarke's flat fading channel model and Jakes' classic spectrum have been widely used and accepted in many wireless communication standards (such as International Mobile Telecommunications-2000 (IMT-2000), which is the global standard for third generation (3G) wireless communications), they are nevertheless not sufficient to fully describe a wireless channel. In many cases of mobile radio communication, the received signal fluctuates in time even in the absence of

Doppler frequency shift (i.e. when there is no relative motion between the receiver and transmitter), resulting in a time-varying channel. This time variation is due to the fluctuations in the component phases that arise from the time-varying random propagation environments. This feature of the wireless channel cannot be accounted for by Clarke's model, which takes the channel to be constant if there is no relative motion between the receiver and the transmitter. The classic U-shape Jakes' power spectrum given in (5.2) is band limited and has infinite value at the maximum Doppler frequency f_D and is zero outside of $[-f_D, f_D]$. This is quite distinct from the measured Doppler power spectrum of a flat channel (see Figures 5.3 and 5.2). Since Jakes' spectrum cannot give a meaningful Doppler spread bandwidth and is unbounded, it is not appropriate as a theoretical basis for channel spectrum analysis and simulations where temporal phase fluctuations are significant (e.g. in applications to indoor wireless mobile communications).

By introducing time-varying component relative phases, section 5.2 (Ref. [28]) presents an extended Clarke's model for the flat channel. The extended Clarke's model (5.4) overcomes the deficiencies in the classic Clarke's model discussed above (section 5.2, also [28]). The process generated from the extended Clarke's model (5.4) is a (zero mean) Gaussian process (see Appendix 5.5.3), i.e. the Rayleigh property. In section 5.2, a theoretical power spectrum is derived based on the extended Clarke's model, and it is shown to approach more accurately the real measured spectra, as compared to the classic Jakes' spectrum. This novel theoretical power spectrum of the fading channel is expressed in the integral form (cf. p. 80). The classic Jakes' spectrum arises

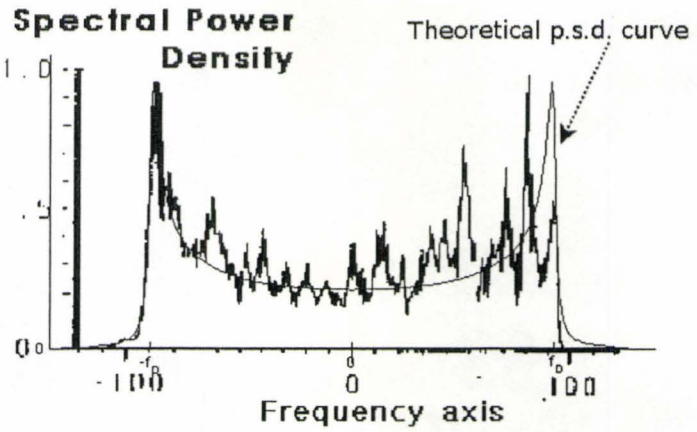

Figure 5.7: Comparing the theoretical PSD with the measured PSD. Theoretical spectrum:$B/f_D = 0.2$, $P_0/f_D = 0.2\pi$. Source of measured spectrum: Research group of Prof. Paul Walter Baier, U. of Kaiserslautern, Germany (cf. [36])

as a special case of the novel spectra in (5.24) in the limit $B \rightarrow 0$, which is illustrated in Figure 5.2. By carefully selecting the parameters B and P_0, section 5.2 exhibits a specific theoretical power spectrum based on (5.24) to approach as closely as possible to the measured spectrum in figure 5.3, which is reproduced here in figure 5.7. It is evident that the spectra $S_c(f)$ formed by (5.24) approximate the measured spectra more accurately as compared to the U-shape Jakes' spectrum.

It is familiar that a zero-mean stationary Gaussian random process can be modeled as the output of a linear system with input $W(t)$, a zero-mean white Gaussian noise with PSD equal to unity. Thus, to generate a Gaussian process (such as the one in (5.4)) for a flat fading channel, we need to find a linear system with transfer function $H(jw)$ satisfying

$$S_c(w) = |H(jw)|^2, \tag{5.26}$$

where $S_c(w)$ is the PSD of the flat fading channel being generated, which is assumed to be known from theory (typically of the form as derived in section 5.2) or measurement. Since the Rayleigh channel process is Gaussian, the matching of power spectrum of the output of above system to the wanted spectrum (such as modified Clarke's spectrum) is sufficient to yield the desired Rayleigh channel. This follows from uniqueness - a (zero mean) Gaussian process is fully captured by its autocorrelation function or equivalently (via the Wiener-Khintchine theorem) by its power spectral density. Generally, the PSD of a wireless channel is a non-rational function and we wish to approximate it by a rational proper function, i.e. as a ratio of two polynomials. The standard method for achieving this requires a non-linear optimization process for a square-error function of coefficients of the rational function, such as the Steiglitz method [31]. In this section, we will present a novel simple method to transform this non-linear optimization problem to a linear-equation-solving problem and produce an analytical solution.

There are numerous representations of a state space model corresponding to a rational transfer function, the OCF realization being a special instance that we study in this section (see 5.3.1). Concerning the model of the channel as the output of a linear system with a white Gaussian noise input, the state-space approach will result in a dynamical model of the fading channel, which happens to be expressed in terms of stochastic differential equations (SDEs). Thus, in this section, we will introduce a stochastic process to obtain a state-

space dynamical model (a set of SDEs) for the flat fading wireless channel.

This section is organized as follows. Firstly, in subsection 5.3.1, the state-space approach is applied to the transfer function, obtaining a multi-variable set of SDEs as the time-dependent dynamical model of the flat fading channel, and a corresponding discrete-time state-space model is derived for the direct application in digital communications. Verification of the presented approximation method and the simulation of a fading channel based on the presented discrete-time state-space model are provided in subsection 5.3.2. Two appendices are provided to explain in detail how to obtain the transfer function that is employed in the state-space approach. Firstly in Appendix 5.5.4, a novel method is presented to obtain a rational even function approximation to the power spectral density of a flat fading channel. Although this novel approach is used to approximate a PSD, with minor modification it can also be used as a general method for high-order recursive "shaping filter" design. Secondly, in Appendix 5.5.5, we discuss the relationship between a rational even function as a power spectral density and a corresponding linear transfer function.

5.3.1 State Space Model of Wireless Flat Fading Channel

From the discussion of Appendix 5.5.4 and Appendix 5.5.5, we have learned that, given a (arbitrary) power spectral density for a flat fading channel, we can approximate the PSD function by a rational even function and obtain a minimum-phase stable rational transfer function through numerical factorization. Thus, the fading channel can be modeled as the output of a corresponding linear system with an input of a white Gaussian noise with unit PSD. In this

subsection, we will present a state-space approach to modeling the flat fading channel.

Continuous-Time State-Space Model

As remarked previously, there are various forms to represent a rational transfer function in terms of a corresponding state-space model. We shall focus attention on the *Observable Canonical Form* (OCF) [33], others being related to OCF by a linear transformation. Given a general rational transfer function with input $X(s)$ and output $Z(s)$ in the Laplace s-domain (s is the transform variable) we express the transfer function as the ratio

$$\begin{aligned} H(s) &= \frac{p_{m-1}s^{m-1} + \cdots + p_1 s^1 + p_0}{s^m + q_{m-1}s^{m-1} + \cdots + q_1 s^1 + q_0} \\ &= \frac{Z(s)}{X(s)}, \end{aligned} \tag{5.27}$$

where the coefficients $p_{m-1}, \cdots, p_{m-(m-n)}$; $m > n$ may be set to zero so that the rational transfer function (5.79) (cf. Appendix 121) is a special case of (5.27). The OCF realization obtained from (5.27) is given by (see [33])

$$\dot{\mathbf{Y}}(t) = \mathbf{C} \cdot \mathbf{Y}(t) + \mathbf{d}x(t) \tag{5.28}$$

$$z(t) = \mathbf{g} \cdot \mathbf{Y}(t) \tag{5.29}$$

where $x(t)$ and $z(t)$ are the input and output in the time-domain of the given linear system. $\mathbf{Y}(t)$ is a new $m \times 1$ auxiliary state vector introduced to math-

ematically represent the output $z(t)$

$$\mathbf{Y}(t) = [y_0(t), y_1(t), \cdots, y_{m-1}(t)]', \tag{5.30}$$

in which the dimension of the vector $\mathbf{Y}(t)$ is the same as the highest order of the denominator of the transfer function (5.27). $\mathbf{d}$ is the $m \times 1$ vector

$$\mathbf{d} = [p_0, p_1, \cdots, p_{m-1}]', \tag{5.31}$$

and $\mathbf{C}$ is the $n \times n$ matrix

$$\mathbf{C} = \begin{bmatrix} 0 & 0 & \cdots & 0 & 0 & -q_0 \\ 1 & 0 & 0 & \cdots & 0 & -q_1 \\ 0 & 1 & 0 & \cdots & 0 & -q_2 \\ \vdots & & \ddots & & & \vdots \\ 0 & \cdots & 0 & 1 & 0 & -q_{m-2} \\ 0 & 0 & \cdots & 0 & 1 & -q_{m-1} \end{bmatrix}, \tag{5.32}$$

$$\mathbf{g} = [0, 0, \cdots, 0, 1]. \tag{5.33}$$

A flat fading channel can be viewed as the output of a linear system with transfer function $H(s)$ with a white Gaussian noise input of unit power spectral density (see (5.82) in Appendix 121). Now, to use the OCF to model a flat fading channel with a power spectrum $P(jw)$ satisfying

$$P(jw) = |H(jw)|^2, \tag{5.34}$$

($H(s)$ is given by (5.27)) we take the input $x(t)$ in the OCF realization (5.28) to be $W(t)$, a white Gaussian noise input with unit PSD, i.e.

$$\dot{\mathbf{Y}}(t) = \mathbf{C} \cdot \mathbf{Y}(t) + \mathbf{d} \cdot W(t) \tag{5.35}$$

Eqs. (5.35) and (5.29) thus constitute our desired continuous-time state-space model for the fading channel. If we multiply both sides of (5.35) by dt, we obtain

$$d\mathbf{Y}(t) = \mathbf{C} \cdot \mathbf{Y}(t)dt + \mathbf{d} \cdot W(t)dt, \tag{5.36}$$

in which, from the SDE theory [14],

$$W(t)dt = dw(t), \tag{5.37}$$

where $w(t)$ is a standard Brownian motion process [14]. Substituting (5.37) into (5.36), and combining with (5.29), we finally obtain the SDE representation of the flat fading channel model as

$$d\mathbf{Y}(t) = \mathbf{C} \cdot \mathbf{Y}(t) \cdot dt + \mathbf{d} \cdot dw(t) \tag{5.38}$$

$$z(t) = \mathbf{g} \cdot \mathbf{Y}(t), \tag{5.39}$$

where $z(t)$ is the actual fading channel process, and $\mathbf{Y}(t)$ is an auxiliary state vector of the linear system defined as in (5.30). Notice that a closed form solution is not generally available for the stochastic differential equation (5.38), in contrast to the deterministic case.

Discrete-Time State-Space Model

We now consider a sequence of discrete-time samplings for the SDE model in (5.38) and (5.39) with equal separation in time, $t_0, t_1, \cdots, t_k, \cdots$, where $t_{k+1} - t_k = \delta t$. For simplicity of notation, we replace sample time t_k by k for all variables, i.e., $\mathbf{Y}(t_k) \rightarrow \mathbf{Y}(k)$, $z(t_k) \rightarrow z(k)$. After replacing the continuous-time differential $d\mathbf{Y}(t)$ in (5.38) with the discrete-time difference $\mathbf{Y}(k+1) - \mathbf{Y}(k)$, replacing $\mathbf{Y}(t)$ in (5.38) with the arithmetic average $\frac{1}{2}(\mathbf{Y}(k+1) + \mathbf{Y}(k))$, and replacing the Wiener process $dw(t)$ with a discrete Gaussian process $\delta t^{1/2} \cdot n(k)$, we obtain

$$\mathbf{Y}(k+1) = \frac{2\mathbf{I} + \delta t\mathbf{C}}{2\mathbf{I} - \delta t\mathbf{C}} \cdot \mathbf{Y}(k) + \frac{2\delta t^{1/2}\mathbf{d}}{2\mathbf{I} - \delta t\mathbf{C}} \cdot n(k) \tag{5.40}$$

$$z(k) = \mathbf{g} \cdot \mathbf{Y}(k), \tag{5.41}$$

where $\mathbf{I}$ is a $m \times m$ identity matrix, $n(k)$ is a standard Gaussian process i.i.d. sequence with zero mean and unit variance, $\mathbf{C}, \mathbf{d}, \mathbf{g}$ are defined as before in (5.32), (5.31), and (5.33), and the matrix division in (5.40) is defined as (for square matrix $\mathbf{A}$ or vector $\mathbf{d}$ and square matrix $\mathbf{B}$)

$$\frac{\mathbf{A}(\mathbf{d})}{\mathbf{B}} \triangleq \mathbf{B}^{-1}\mathbf{A}(\mathbf{d}). \tag{5.42}$$

Eqs. (5.40-5.41) thus constitute the discrete-time state-space model for the wireless fading channel corresponding to a transfer function $H(s)$ as in (5.27).

The most obvious application of the state-space model is to simulate wireless flat fading channel. From (5.40-5.41), we can see that the computation

complexity increases linearly with the number of generated channel data, i.e., $m^2 \cdot O(N)$, where N is the total number of simulated data, and m is the highest order of the denominator of the transfer function (see (5.27)). Thus the state-space model is an appropriate choice for real-time implementation of a channel simulator.

It is worthwhile to observe that another direct application of the state-space model of the wireless flat fading channel is to form a *Kalman filter* in association with the received signal. We may write the discrete-time signal at the receiver for the flat fading channel as

$$r(k) = d(k)z(k) + n_r(k) \tag{5.43}$$

where $d(k)$ is the transmitted data, $r(k)$ is the received data, $n_r(k)$ is additive Gaussian noise at the receiver, and $z(k)$ is the channel state identical to that in (5.41). Substituting (5.41) into (5.43), we obtain

$$r(k) = \tilde{\mathbf{g}}(k) \cdot \mathbf{Y}(k) + n_r(k) \tag{5.44}$$

where

$$\tilde{\mathbf{g}}(k) = [0, 0, \cdots, 0, d(k)]. \tag{5.45}$$

Thus (5.40) and (5.44) constitute the respective *process* and *measurement* equations for the well known *Kalman filter*.

In many of wireless transmission-receiver system, we know that the more accurate estimation of channel we have, the better recovery of transmitted sig-

nal we obtain. Thus we often need a good selection channel model to approach the real channel so as to improve the estimation of channel state. Since the above state-space model can represent arbitrary flat fading Rayleigh channel with its PSD fitting into the desired PSD and it is easy to be integrated into algorithms for channel tracking and estimation, the presented accurate state-space model will be an appropriate choice for the performance and robustness of system design.

5.3.2 Verification & Simulations

In this subsection, we will first approximate a theoretical power spectral density given in (5.24) (cf. [28]) by a rational even function (5.60) through the method presented in Appendix 5.5.4. It should be noted that the presented method can also be applied to an arbitrary power spectral density function, either theoretical or experimentally observed. In the second part, we simulate the wireless flat fading channel via the discrete-time state-space model (5.40-5.41) developed from a system of SDEs. The PSD functions of simulated discrete channels are plotted in figure 5.12 and figure 5.13, which confirm our theoretical derivation of the close form expression of PSD function of the fading as in (5.24).

(Theoretical) Verification

For generality, we introduce a relative frequency f_r corresponding to a maximum Doppler frequency f_D, as

$$f_r = f/f_D. \tag{5.46}$$

We choose a theoretical PSD of the flat fading channel as in (5.24). Setting $B/f_D = 1$, $P_0/f_D = 3\pi$, the power spectrum function $S_c(f_r f_D)$ is thus determined, which arises as the $P(s)|_{s=j2\pi f_r f_D}$ in section 5.5.4, and is plotted in Figure 5.8. To obtain the square-error function (5.64), we set sampling points in the relative frequency $f_r = 0, 0.01, 0.02, \cdots, 1.3$. The pair (n, m) is used to determine the order of the polynomials $A(s)|_{s=j2\pi f_r f_D}$ and $B(s)|_{s=j2\pi f_r f_D}$ in (5.60-5.61). In the approximation of the power spectrum $S_c(f_r f_D)$ for the above parameters, we firstly obtain the vector $\mathbf{v}$ (see (5.77)), i.e. the coefficients of the polynomials $A(s)|_{s=j2\pi f_r f_D}$ and $B(s)|_{s=j2\pi f_r f_D}$ by the method provided in section 5.5.4; thus the rational even function is determined according to (5.61). To demonstrate the effect of the order of the rational even function $R(s)|_{s=j2\pi f_r f_D}$ on the approximation to the power spectral density $S_c(f_r f_D)$, we set the pair (n, m) successively to be $(1, 2)$, $(2, 3)$, and $(3, 4)$; for each pair (n, m), a rational even function $R(s|n, m)|_{s=j2\pi f_r f_D}$ is obtained and plotted against the objective power spectral density $S_c(f_r f_D)$, as shown in Figure 5.8. The neighborhood of the peak in Figure 5.8 is magnified for clarity in Figure 5.9 (with all parameters equal to those in Figure 5.8). More figures are provided in section 5.3.2 for the approach of rational even function

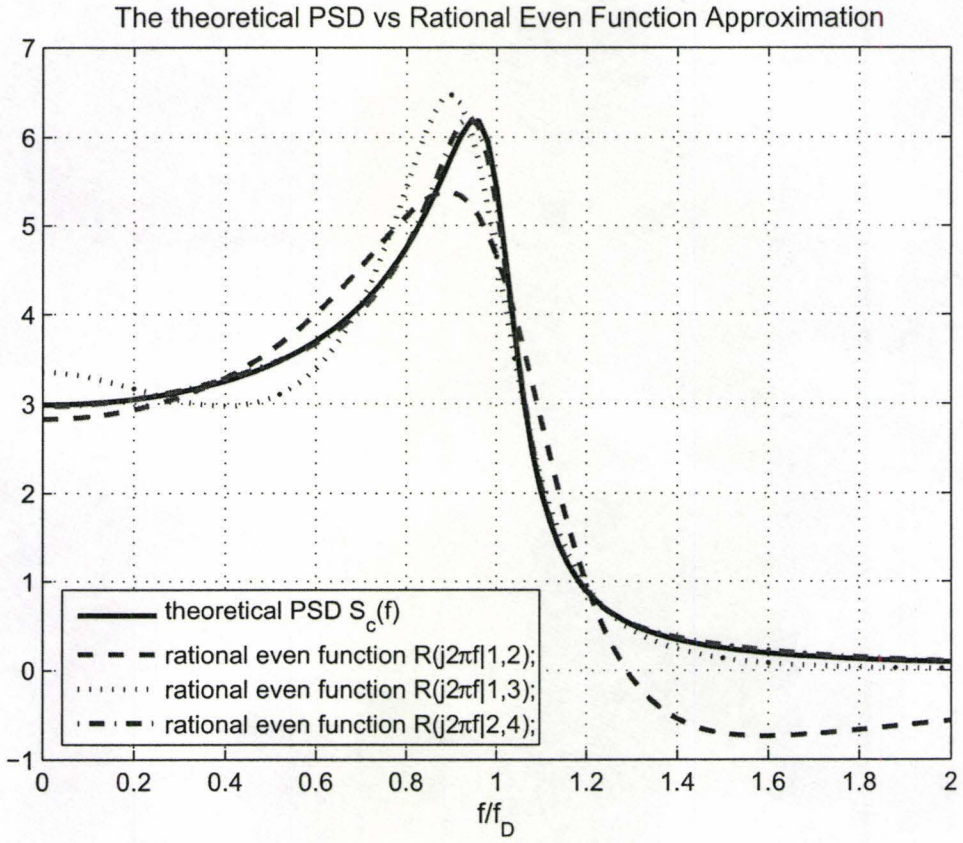

Figure 5.8: The theoretical PSD function $S_c(f)$ vs the rational even function $R(s)|_{s=j2\pi f}$, where $B/f_D = 1$, $P_0/f_D = 3\pi$, with various order of (n, m).

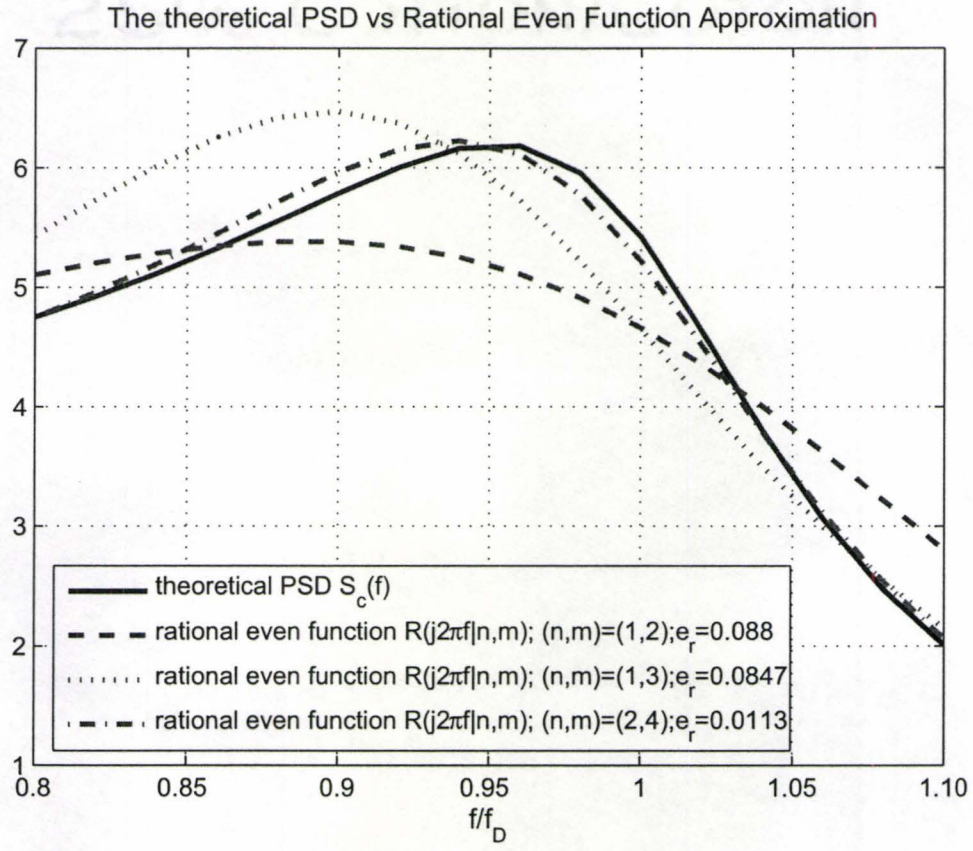

Figure 5.9: The theoretical PSD function $S_c(f)$ vs the rational even function $S(s)|_{s=j2\pi f}$, where $B/f_D = 1$, $P_0/f_D = 3\pi$ (peak area magnified), with various order of (n, m).

to variants of theoretical PSD curves.

From Figures 5.8 and 5.9, it is evident that a higher order pair (n, m) for the rational even function $R(s)$ achieves better approximation to the objective theoretical PSD function. For the order of pair (n, m), we choose the corresponding rational even function $R(s|n, m)$ to satisfy

$$e_r(n, m) < e_p \tag{5.47}$$

where e_p is a pre-defined error boundary, a constant in the interval $(0, 1)$, and e_r is a relative error defined as

$$e_r(n, m) = \frac{\int_0^{f_{max}} |R(j2\pi f|n, m) - P(j2\pi f)|\, df}{\int_0^{f_{max}} |P(j2\pi f)|\, df}. \tag{5.48}$$

The interval $[0, f_{max}]$ is the frequency range ($f_{max} = 1.3 f_D$ here) in which we wish to approximate the PSD function $P(s)|_{s=j2\pi f}$ (cf. section 5.5.4). Thus we have provided a criterion (5.47-5.48) to find a minimal order of rational even function $R(s)$ that is to approximate the power spectral density function $P(s)$. The computed values of $e_r(n, m)$ are also shown in Figure 5.9; it is evident that $e_r(2, 4)$ is much smaller than $e_r(1, 2)$ and $e_r(1, 3)$ in correspondence with the respective curves in Figure 5.9.

Simulations

We consider a wireless communication environment with carrier frequency f_c = 1800MHz, mobile receiver speed v = 60Km/h; thus the maximum Doppler frequency is $f_D = \frac{v}{c} f_c$ = 100Hz, and we set $B/f_D = 0.5$, $P_0/f_D = 3\pi$,

$(n, m) = (2, 4)$, the sampling time interval to be $\delta t = 1.0E - 5$s, and the sampling points in the relative frequency $f_r = 0, 0.01, 0.02, \cdots, 1.3$. The simulation process consists of the following five steps: first, the theoretical power spectral density $S_c(f)$ is obtained from (5.24); second, the approximated rational even function $R(s|2,4)|_{s=j2\pi f}$ is calculated according to the method presented in section 5.5.4; third, the transfer function $H(s)$ is obtained by factorizing the rational even function $R(s|2,4)|_{s=j2\pi f}$ (Eq. 5.79) in section 5.5.5; fourth, a discrete-time state-space model is generated based on the transfer function $H(s)$ obtained (see (5.40-5.41) in section 5.3.1); finally, the computed power spectra from the simulated fading channel process generated by (5.40-5.41) are plotted in Figures 5.10 & 5.11 (both have the same parameters). In Figure 5.10, the power spectral density of the state-space model is computed for one trial of the simulation (see (5.40-5.41)); in Figure 5.11, the average PSD of the state-space model is computed for 100 simulation trials. Both figures lend strong support to our presented methods – the rational even function approximation and the discrete-time state-space model of the flat fading channel – and illustrate the convergence to the theoretical PSD for a large number of trials in the simulation. More simulations are shown in figure 5.12 and figure 5.13 for different power spectral densities.

The most general approach of Rayleigh channel simulators is based on variant scattering models ([28, 43, 44, 45, 46, 47]), which is the sum of a number of sinusoids with uniformly distributed random phases. This method has high computational load because a large number of sin() or cos() functions

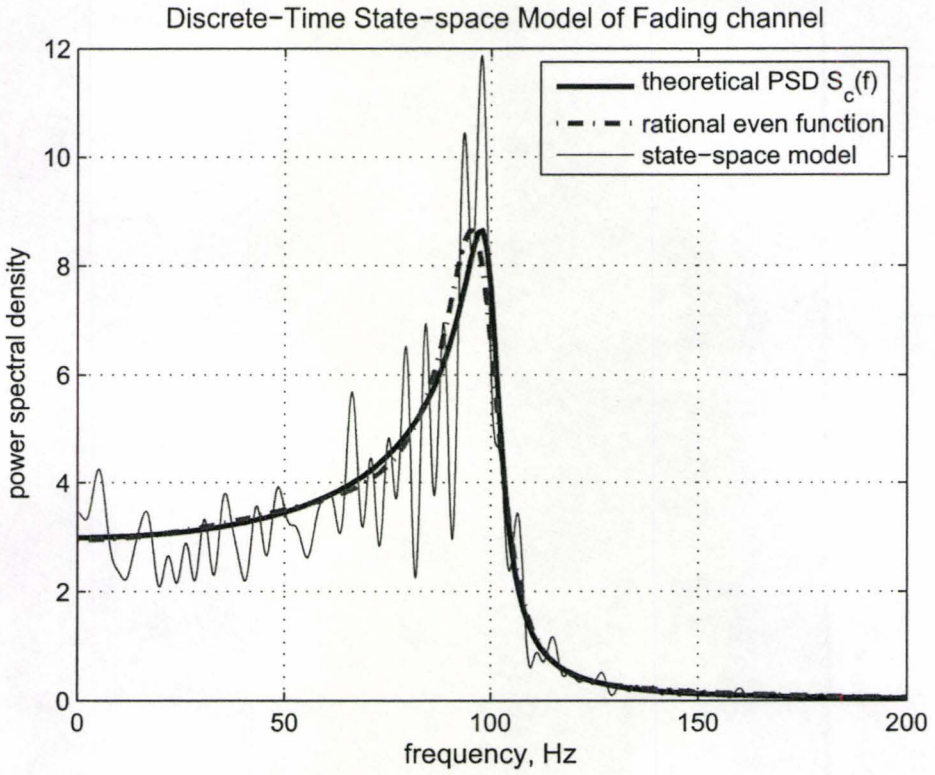

Figure 5.10: The computed PSD of the simulated fading channel from the state-space model (5.40-5.41), where the theoretical PSD, $S_c(f)$ and the approximated rational even function $R(s|2,4)|_{s=j2\pi f}$ are also provided for comparison. $B/f_D = 0.5$, $P_0/f_D = 3\pi$,$f_D = 100$Hz, $\delta t = 1e-5$s.

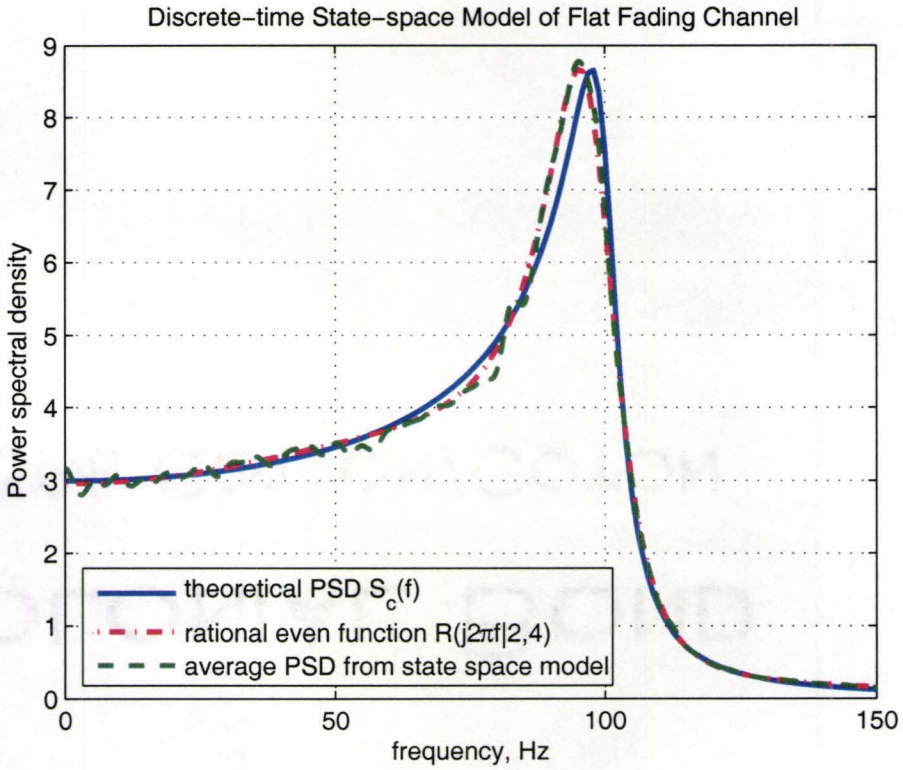

Figure 5.11: The average of 100 trials of the computed PSD of simulated fading channel from the state-space model (5.40-5.41), where the theoretical PSD, $S_c(f)$ and the approximated rational function $R(s|2,4)|_{s=j2\pi f}$ are also provided for comparison. $B/f_D = 0.5$, $P_0/f_D = 3\pi$, $f_D = 100$Hz, $\delta t = 1e-5$s.

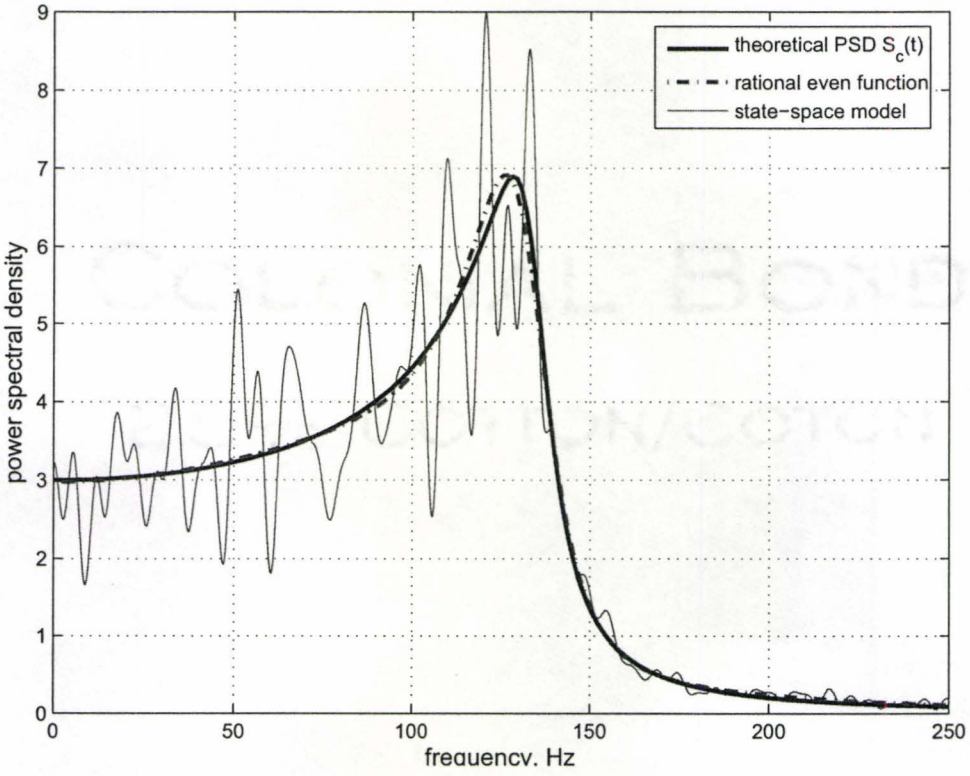

Figure 5.12: The computed PSD of the simulated fading channel from the state-space model with the theoretical PSD - $S_c(f)$ and the approximated rational even function $R(s|2,4)|_{s=j2\pi f}$. $B/f_D = 0.8$, $P_0/f_D = 3\pi$,$f_D = 133.3$Hz (i.e. mobile receiver speed $v = 80$Km/h), $\delta t = 1e-5$s.

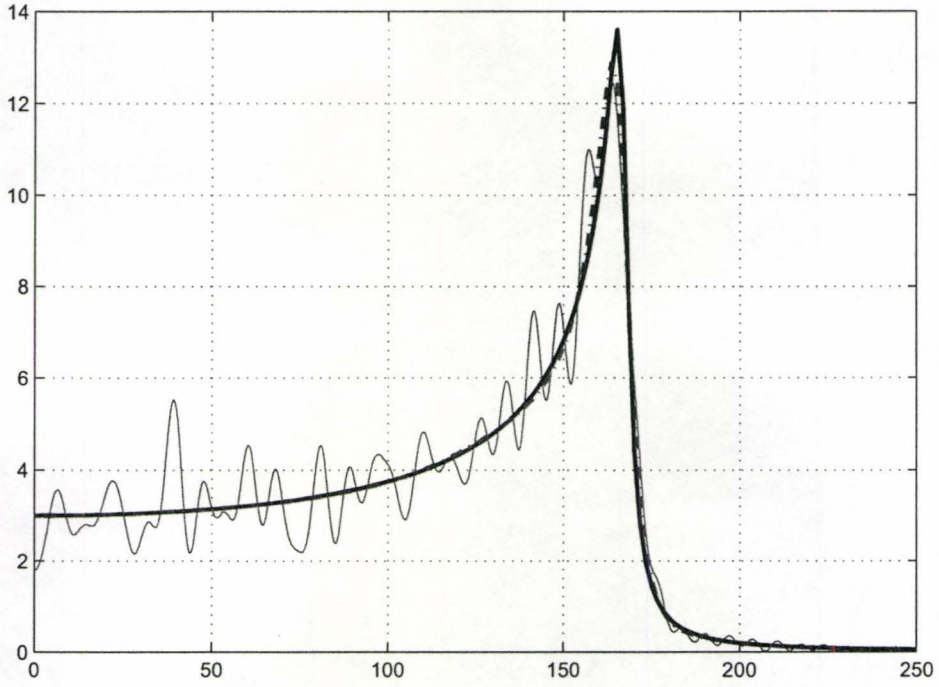

Figure 5.13: The computed PSD of the simulated fading channel from the state-space model with the theoretical PSD - $S_c(f)$ and the approximated rational even function $R(s|2,6)|_{s=j2\pi f}$. $B/f_D = 0.3$, $P_0/f_D = 3\pi$,$f_D = 166.7$Hz (i.e. mobile receiver speed $v = 100$Km/h), $\delta t = 1e-5$s.

are used in the simulation, so it is not ideal for real-time implementation[1]. In application to channel simulation, the state-space model presented above has much better computational efficiency than the aforementioned variant scattering models, and our model can be easily realized for fast real-time application without need of large amounts of memory, and moreover it is versatile to generate any narrow-band Rayleigh fading channel with arbitrary desired Doppler / power spectrum.

5.4 Approaches of Fading Channel Simulation

Currently, there are three main approach to simulate wireless multipath fading channels. The first approach is based on Clarke's scattering model as in Eq. (2.3), which is the sum of a number of sinusoids with uniformly distributed random phases. This approach was refined and improved in [43, 44, 45]. This method has much computational load because a large number of sin() or cos() are used in the simulation (see footnote on the current page).

The second approach to generate discrete Gaussian process with the PSD in Eq. (2.5) was presented in [50] and [51]. The idea was to use a complex Gaussian random number generator to produce a baseband line spectrum / frequency components from $-f_m$ to f_m, which is then multiplied with a discrete frequency mask equal to the square root of the spectral shape in Eq. (2.5). Both the baseband line spectrum as the noise source and the discrete frequency mask have the same number of points. The resulting multiplied

[1]The function sin()or cos() has to be executed / called for every single value on demand which contains a number of real number multiplex operations because these two function has infinite values so that they cannot be stored in limited memory of computer system.

sequence takes an inverse fast Fourier transform (IFFT), which also produce a Gaussian random process by the virtue of the linearity of the IFFT, and obtain a desired power spectrum as in Eq. (2.5), and hence also the autocorrelation of Eq. (2.4). There is much less computational complexity in this approach than the first approach. IFFT is the heaviest effort in this approach, which costs only $O(N \log_{\varepsilon} N)$ operations, where N is the number of independent complex Gaussian samples from line spectra / frequency components. A big disadvantage of this approach is that it require all channel data to be generated one for all and stored before they are sent through the channel, which means that the channel data cannot be produced continuously and large amount of memory is necessary to generate a long series of channel data.

The third approach adopts the filtering method in time-domain. A sequence of independent Gaussian random variables (flat PSD) in time domain pass through a linear filter with frequency response equal to the square root of the desired channel power spectrum, then the resulting output sequence remains Gaussian processes and has the desired power spectrum. The computational efficiency is in the same level as the second approach, which is about $2N \log_2 N$.[52][53]. The infinite impulse response (IIR) filter design is the core part of this approach, some complicated method, i.e., the Steiglitz method, is used, which makes this approach not easy for implementation of the real-time application.

A new approach presented in this thesis use state-space model to generate any arbitrary fading channel data with a desired Doppler / power spectrum. Being a core part of this approach, a novel method is presented for a fast de-

sign of a continuous-time IIR filter as the transfer function which is the square root of the desired power spectrum of the fading channel. The computational efficiency is the best among the available approaches, which increases linearly with the order of N, i.e. $m^2 \cdot O(N)$, where m is the highest order of the denominator of the transfer function. This approach does not need large amount of memory to store the temporary data as the second approach does.

5.5 Appendix

5.5.1 Appendix: Verify the relative phase $\varphi_t^{(k)}$ a Wiener process

At any instant of time t, we assume that the relative phase $\varphi_t^{(k)}$ (see (5.4)) has an equal chance to increase or decrease by a fixed step size ε (where $\varepsilon > 0$), such that the increment of phase, i.e. $\delta\varphi_t^{(k)}$ ($\delta\varphi_t^{(k)} \triangleq \varphi_{t+\delta t}^{(k)} - \varphi_{t+\delta t}^{(k)}$) is a random variable, which takes values from the discrete set $\{\varepsilon, -\varepsilon\}$ with equal probability, and the increments from one time step to the next are independent. With this basic reasonable assumption, when considering the continuum limit that the step size ε and the time increment δt tend to zero, subject to the scaling relation $\varepsilon^2 = B\delta t$, the relative phase $\varphi_t^{(k)}$ is thus a (scaled) Wiener process.[2]

[2]The construction of a Wiener process from a discrete random walk in this way follows by applying the central limit theorem to the displacement after n steps during some fixed time t, where $n \to \infty$, $\delta t \to 0$. The resulting displacement is $\mathcal{N}(0, t)$ normal distributed and, by construction, satisfies the independent increments property - thus, the limit of the discrete random walk corresponds to the standard (continuum) definition of the Wiener process [14].

5.5.2 Appendix: Approach of the square-error function Q in (5.63) by $\tilde{Q}$ in (5.64)

When the rational function $R(s)$ in (5.61) represents a PSD, the denominator $B(s)$ cannot not be zero for any $s = j2\pi f$, $f \in [0, +\infty)$, so that for any finite positive $f \in [0, f_{max}]$, $0 < f_{max} < \infty$, the value of the function $A(s)/B(s)$ is finite. Thus,

$$0 < a < |B(s)|^2 < b, \quad \forall f \in [0, f_{max}] \tag{5.49}$$

where a, b are positive constants.

From (5.64), we have

$$\tilde{Q} = \sum_{i=1}^{L} B^2(s_i) \left(\frac{A(s_i)}{B(s_i)} - P_i \right)^2. \tag{5.50}$$

Comparing (5.49) and (5.50), we have

$$a \sum_{i=1}^{L} \left(\frac{A(s_i)}{B(s_i)} - P_i \right)^2 < \tilde{Q} < b \sum_{i=1}^{L} \left(\frac{A(s_i)}{B(s_i)} - P_i \right)^2. \tag{5.51}$$

Substituting (5.61) and (5.63) into (5.51), we obtain

$$a \cdot Q < \tilde{Q} < b \cdot Q. \tag{5.52}$$

From (5.52) it is evident that, when the quadratic square-error $\tilde{Q} \to 0$, the original square-error Q will also tend to zero.

5.5.3 Appendix: Proof of Gaussian process for ε_t in the extended Clarke's model (5.4)

According to (5.4), set

$$\Phi_t^{(n)} = 2\pi f_n t + \varphi_t^{(n)} \tag{5.53}$$

$$r_t^{(n)} = a_n \exp[j\Phi_t^n] \tag{5.54}$$

where the index n refers to the n-th path and $\{r_t^{(n)}\}$ are random variables. Considering a time series $\{t_1, t_2, \cdots, t_k\}$ for any $k \geq 1$, denote

$$\mathbf{v}_n \triangleq [r_{t_1}^{(n)}, r_{t_2}^{(n)}, \cdots, r_{t_k}^{(n)}]^T, \tag{5.55}$$

where $\mathbf{v}_n$ is column random vector. We also denote a sampled channel state as a vector, i.e.,

$$\Upsilon \triangleq [\varepsilon_{t_1}, \varepsilon_{t_2}, \cdots, \varepsilon_{t_k}]^T. \tag{5.56}$$

Based on (5.53) (5.54) and (5.4), we have

$$\varepsilon_{t_i} = \sum_{n=1}^{N} r_{t_i}^{(n)}, \tag{5.57}$$

for $i = 1, 2, \cdots, k$. If we vectorize (5.57) with the index $i = 1, 2, \cdots, k$ and use (5.55) and (5.56), we obtain

$$\Upsilon = \sum_{n=1}^{N} \mathbf{v}_n, \tag{5.58}$$

where the vector random variables $\{\mathbf{v}_n\}$ are independent of each other, due to the assumption of independence of each path. Then by the central limit theorem (for vectors) Υ is a multivariate Gaussian, i.e., ε_t is a (zero mean) Gaussian process.

5.5.4 Appendix: The Approximation of a PSD Function by a Rational Even Function

In this section, we will discuss how to approximate a (arbitrary) power spectral density by a rational even function. The method provided in this section will produce an analytic solution which can easily be extended to a general method for the design of an arbitrary "shaping filter".

The Rational Even Function

We know that the ideal power spectral density is a non-negative real even function. If we want to use the rational function to approach the PSD function, it has to be the form

$$R_w(w) = K^2 \frac{w^{2n} + \alpha_{n-1}w^{2n-2} + \cdots + \alpha_1 w^2 + \alpha_0}{w^{2m} + \beta_{m-1}w^{2m-2} + \cdots + \beta_1 w^2 + \beta_0}, \tag{5.59}$$

where $K \neq 0$,$w = 2\pi f$, the coefficients $\alpha_k, \beta_k, k = 0, 1, \cdots$, are all real and $m > n$.

To simplify the discussion in what follows, we rewrite (5.59) replacing the variable w by $-js$ (s being the parameter of the Laplace transform) and re-

name the coefficients of the polynomial as

$$R(s) = \frac{a_n s^{2n} + a_{n-1} s^{2n-2} + \cdots + a_1 s^2 + a_0}{s^{2m} + b_{m-1} s^{2m-2} + \cdots + b_1 s^2 + b_0} \tag{5.60}$$

$$= \frac{A(s)}{B(s)}, \tag{5.61}$$

where the numerator $A(s)$ and the denominator $B(s)$ are both real even polynomials. Eqs. (5.59) and (5.60) are called 'rational even functions'.

The Traditional Method of Approximation

From section 5.5.4, we know that a power spectral density function can be approximated by a rational even function $R(s)$, which is expressed according to (5.60). We suppose that the power spectral density of the fading channel is $P(jw)$ (or $P(s)$ in the s-domain for the Laplace transform) which is obtained from measurement or known to us from theory (such as in (5.24) above). We now choose $L+1$ (arbitrary) frequency points within the interval $[0, f_{max}]$ (where $0 < f_{max} < \infty$), $f_0, f_1, \cdots, f_L, \in [0, f_{max}]$, which correspond to the values of the variable s_i in the s-domain

$$s_i = j2\pi f_i, i = 0, 1, \cdots, L. \tag{5.62}$$

Notice that these frequency points, $f_0, f_1, \cdots, f_L$ are generally chosen to be equally-spaced, although we are not limited to such. At these $L+1$ frequency points, we have $L+1$ values of the PSD $P(j2\pi f_0), P(j2\pi f_1), \cdots, P(j2\pi f_L)$, and $L+1$ values of the rational function $R(j2\pi f_0), R(j2\pi f_1), \cdots, R(j2\pi f_L)$.

For simplicity of notation, we represent the values of $P(j2\pi f_i)$ as $P_i, i = 0, 1, \cdots, L$ and $R(j2\pi f_i)$ as $R_i, i = 0, 1, \cdots, L$.

Traditionally, to approximate the power spectral density function $P(s)$ by a rational even function $R(s)$, we would define a square-error as

$$Q = \sum_{i=1}^{L} (R_i - P_i)^2, \tag{5.63}$$

and then minimize the value of Q corresponding to the coefficients of polynomials of the numerator $A(s)$ and the denominator $B(s)$ for the rational function $R(s)$, i.e., $a_0, a_1, \cdots, a_n$; $b_0, b_1, \cdots, b_{m-1}$ (see Eq. (5.60)). Unfortunately, this square-error is a highly non-linear function of the coefficients $a_i, i = 0, \cdots, n; b_i, i = 0, \cdots, m-1$, which is difficult to analyze mathematically. Steiglitz [31] uses a numerical method presented by Fletcher and Powell [32] to solve a discretised version of the minimization problem of the square-error akin to (5.63), where numerical iterative computation is required and the computation process is complex. Furthermore, the Steiglitz method for such a general optimization problem cannot guarantee a global solution. However, this particular non-linear optimization problem involving the square-error function (5.63) can be transformed to a simple minimization problem of a corresponding quadratic square-error function, as discussed in detail in the following.

A Novel Method of Approximation

The rational even function $R(s)$ is a ratio of two polynomial functions $A(s)$ and $B(s)$ according to (5.60-5.61). Thus, if the rational function $R(s)$ approaches the power spectral density $P(s)$, the polynomial $A(s)$ will approach the product $P(s) \cdot B(s)$. Accordingly we define a square-error function

$$\tilde{Q} = \sum_{i=1}^{L} (A(s_i) - P_i \cdot B(s_i))^2, \tag{5.64}$$

where s_i is defined previously in (5.62). If we define a vector $\mathbf{v}$ with components equal to the $n+m+1$ unknown coefficients in the above square-error function

$$\mathbf{v} = (a_0, a_1, \cdots, a_n, b_0, b_1, \cdots, b_{m-1})', \tag{5.65}$$

the square-error $\tilde{Q}$ is a quadratic function of the vector $\mathbf{v}$, i.e. $\tilde{Q}(\mathbf{v})$. Although the minimization of the original square-error Q in (5.63) does not imply the minimization of $\tilde{Q}$ in (5.64), observe that if $\tilde{Q}$ in (5.64) tends to zero then Q in (5.63) also does (see Appendix). The problem now is to find a best value of $\mathbf{v}$, say $\mathbf{v}^*$, to minimize the quadratic function $\tilde{Q}(\mathbf{v})$, which is mathematically tractable.

Firstly, we take partial-derivatives of $\tilde{Q}$ with respect to each individual component of $\mathbf{v}$ and set them to zero, i.e.

$$\frac{\partial \tilde{Q}}{\partial a_k} = 0, \quad k = 0, \cdots, n \tag{5.66}$$

$$\frac{\partial \tilde{Q}}{\partial b_k} = 0, \quad k = 0, \cdots, m-1. \tag{5.67}$$

Substituting (5.60) and (5.61) into (5.66), re-arranging and moving the constant term to the right hand side yields a system of $n+1$ equations

$$\sum_{i=1}^{L}\sum_{l=0}^{n} a_l s_i^{2(l+k)} - \sum_{i=1}^{L} P_i \cdot \sum_{l=1}^{m-1} b_l s_i^{2(l+k)} = \sum_{i=1}^{L} P_i s_i^{2(m+k)}, \tag{5.68}$$

where $k = 0, 1, \cdots, n$. Similarly with (5.67) we obtain a system of m equations

$$-\sum_{i=1}^{L} P_i \sum_{l=0}^{n} a_l s_i^{2(l+k)} + \sum_{i=1}^{L} P_i^2 \sum_{l=1}^{m-1} b_l s_i^{2(l+k)} = -\sum_{i=1}^{L} P_i^2 s_i^{2(m+k)}, \tag{5.69}$$

where $k = 0, 1, \cdots, m-1$.

Combining (5.68) and (5.69), we now have $n+m+1$ linear equations with $n+m+1$ unknown coefficients represented as components of the vector $\mathbf{v}$. For compactness we represent these $n+m+1$ linear equations in the matrix form

$$\mathbf{P} \cdot \mathbf{v} = \mathbf{r}, \tag{5.70}$$

where $\mathbf{r}$ is a $(n+m+1) \times 1$ vector

$$\mathbf{r} = \left[\sum P_i s_i^{2m}, \sum_{i=1}^{L} P_i s_i^{2(m+1)}, \cdots, \sum_{i=1}^{L} P_i s_i^{2(m+n)}, \right.$$
$$\left. -\sum_{i=1}^{L} P_i^2 s_i^{2m}, -\sum_{i=1}^{L} P_i^2 s_i^{2(m+1)}, \cdots, -\sum_{i=1}^{L} P_i^2 s_i^{2(2m-1)} \right]', \tag{5.71}$$

and $\mathbf{v}$ is also a $(n+m+1) \times 1$ vector defined as before in (5.65). $\mathbf{P}$ is a

$(n+m+1) \times (n+m+1)$ matrix, which has a block form

$$\mathbf{P} = \begin{bmatrix} \mathbf{P}_{11} & \mathbf{P}_{12} \\ \mathbf{P}_{21} & \mathbf{P}_{22} \end{bmatrix}, \tag{5.72}$$

where $\mathbf{P}_{11}$ is a $(n+1) \times (n+1)$ matrix

$$\mathbf{P}_{11} = \begin{bmatrix} \sum_{i=1}^{L} 1 & \sum_{i=1}^{L} s_i^2 & \cdots & \sum_{i=1}^{L} s_i^{2n} \\ \sum_{i=1}^{L} s_i^2 & \sum_{i=1}^{L} s_i^4 & \cdots & \sum_{i=1}^{L} s_i^{2(n+1)} \\ \cdots & \cdots & \cdots & \cdots \\ \sum_{i=1}^{L} s_i^{2n} & \sum_{i=1}^{L} s_i^{2(n+1)} & \cdots & \sum_{i=1}^{L} s_i^{2(2n)} \end{bmatrix}, \tag{5.73}$$

$\mathbf{P}_{12}$ is a $(n+1) \times m$ matrix

$$\mathbf{P}_{12} = -\begin{bmatrix} \sum_{i=1}^{L} P_i & \sum_{i=1}^{L} P_i s_i^2 & \cdots & \sum_{i=1}^{L} P_i s_i^{2(m-1)} \\ \sum_{i=1}^{L} P_i s_i^2 & \sum_{i=1}^{L} P_i s_i^4 & \cdots & \sum_{i=1}^{L} P_i s_i^{2m} \\ \cdots & \cdots & \cdots & \cdots \\ \sum_{i=1}^{L} P_i s_i^{2n} & \sum_{i=1}^{L} P_i s_i^{2(n+1)} & \cdots & \sum_{i=1}^{L} P_i s_i^{2(m+n-1)} \end{bmatrix}, \tag{5.74}$$

$\mathbf{P}_{21}$ is a $m \times (n+1)$ matrix

$$\mathbf{P}_{21} = -\begin{bmatrix} \sum_{i=1}^{L} P_i & \sum_{i=1}^{L} P_i s_i^2 & \cdots & \sum_{i=1}^{L} P_i s_i^{2n} \\ \sum_{i=1}^{L} P_i s_i^2 & \sum_{i=1}^{L} P_i s_i^4 & \cdots & \sum_{i=1}^{L} P_i s_i^{2(n+1)} \\ \cdots & \cdots & \cdots & \cdots \\ \sum_{i=1}^{L} P_i s_i^{2(m-1)} & \sum_{i=1}^{L} P_i s_i^{2m} & \cdots & \sum_{i=1}^{L} P_i s_i^{2(n+m-1)} \end{bmatrix}, \quad (5.75)$$

$\mathbf{P}_{22}$ is a $m \times m$ matrix

$$\mathbf{P}_{22} = \begin{bmatrix} \sum_{i=1}^{L} P_i^2 & \sum_{i=1}^{L} P_i^2 s_i^2 & \cdots & -\sum_{i=1}^{L} P_i^2 s_i^{2(m-1)} \\ \sum_{i=1}^{L} P_i^2 s_i^2 & \sum_{i=1}^{L} P_i^2 s_i^4 & \cdots & \sum_{i=1}^{L} P_i^2 s_i^{2m} \\ \cdots & \cdots & \cdots & \cdots \\ \sum_{i=1}^{L} P_i^2 s_i^{2(m-1)} & \sum_{i=1}^{L} P_i^2 s_i^{2m} & \cdots & \sum_{i=1}^{L} P_i^2 s_i^{2(2m-2)} \end{bmatrix}. \quad (5.76)$$

After obtaining the vector $\mathbf{r}$ and matrix $\mathbf{P}$ from the available values p_i and s_i, $i = 1, \cdots, L$, we can solve the linear equation (5.70) and obtain the analytical solution for the vector $\mathbf{v}$, which consists of all unknown coefficients of the rational even function $R(s)$ in (5.60),

$$\mathbf{v} = \mathbf{P}^{-1} \cdot \mathbf{r}. \quad (5.77)$$

We know that the quadratic function $\tilde{Q}(\mathbf{v})$ in (5.64) has a unique solution for its minimum; thus the matrix $\mathbf{P}$ is invertible ($\mathbf{P}$ is invertible also because

each sub-matrix by block form of $\mathbf{P}$ has the form of real Hermitian). Having obtained the solution for the vector $\mathbf{v}$, the desired rational even function $R(s)$, which here is specifically designed to approach the power spectral density $P(s)$, is finally obtained.

5.5.5 Appendix: Rational Transfer Function

A wireless fading channel can be viewed as the output of a linear system with input a white Gaussian noise process of unit power spectral density. In this section, we demonstrate how to obtain a rational transfer function of the corresponding linear system with a given power spectral density, which is ideally represented by a rational even function.

From elementary complex variable theory, if z is a root of a real even polynomial, then $z^*, -z, -z^*$are also its roots. Thus, the rational function in (5.60) can be expressed as

$$R(s) = K^2 \frac{\prod_{l=1}^{n}(s+u_l)(-s+u_l)}{\prod_{k=1}^{m}(s+v_k)(-s+v_k)}, \tag{5.78}$$

where $Re(u_l) > 0$, $Re(v_k) > 0$. If we define

$$H(s) = C \frac{\prod_{l=1}^{n}(s+u_l)}{\prod_{k=1}^{m}(s+v_k)}, \tag{5.79}$$

where $C = \pm K$, and $H(s)$ is thus a minimum-phase stable rational function, i.e. the system and its inverse are causal and stable. Then, comparing (5.79) and (5.78), we have

$$R(s) = H(s) \cdot H(-s). \tag{5.80}$$

Considering the properties of roots of the numerator and denominator in the rational function $R(s)$, when we assign $s = jw$ to (5.80), we obtain

$$\begin{aligned} R(jw) &= H(jw) \cdot H(-jw) \\ &= |H(jw)|^2. \end{aligned} \tag{5.81}$$

It is a familiar fact that, for a linear system with transfer function $H(s)$, given a Gaussian wide-sense stationary (WSS) input process, the output is also a Gaussian WSS process with PSD

$$P_o(jw) = P_i(jw)|H(jw)|^2, \tag{5.82}$$

where $P_o(jw)$ and $P_i(jw)$ are PSDs of the respective output and input processes. From (5.81) and (5.82), we see that, if $R(jw)$ is the power spectral density of a wireless fading channel, such fading channel can be modeled as the output of a linear system with a white Gaussian noise input with unit PSD, and the transfer function of the linear system is $H(s)$ (the Fourier transform of the impulse response of the system).

Provided the rational even function $R(s)$ is known, we can obtain the transfer function $H(s)$ after finding the roots of the polynomials $A(s)$ and $B(s)$ as in (5.78-5.79). (This can be achieved through the available numerical root-finding methods provided by numerous scientific computing software packages, such as MATLAB.)

5.6 Summary

In this chapter we focus on the statistical analysis and dynamic modeling of general multipath fading channels with Doppler frequency shift and phase fluctuations with an introduction of some approaches to fading channel simulation.

We have proposed an extended Clarke's model through the consideration of fluctuations in the relative component phases. With rigorous statistical analysis, a closed-form expression for the autocorrelation of the fading is derived, which arises as the product of two terms, one is the exponential decay resulting from the fluctuations of the component phases due to the time-variation in the electromagnetic propagation environment, the other is the zeroth-order Bessel function of the first kind that results from the Doppler frequency shift due to the relative motion between the receiver and transmitter. By considering the fluctuations in the component phases, the power spectrum of the fading channel is quite distinct from the Doppler spectrum and it is our proposed model, as opposed to the traditional one, that accords with observed real experimental data. Simulated channel data also verify the autocorrelation derived from our extended Clarke's model. The peak value and width in the derived power spectrum can be adjusted to fit observed spectra, and we exhibited its shape to conform to the real experimentally measured spectra, in contrast to the situation for the traditional Jakes' spectrum. The statistical analysis and results should be essential to effective spectral analysis and channel simulation in real wireless communication systems immersed in time-varying propagation environments, e.g. in the design of a channel simulator based on the proposed

multipath channel model for obtaining a desired observed power spectrum.

We have presented a novel method for the approximation of an arbitrary power spectral density function by a rational even function. Comparing with the traditional methods, our presented method does not require intensive computation, and can guarantee a global solution (since the error function involved is quadratic), and has the advantage of an analytical solution determined by (5.77). The performance of this method increases with the order of rational function. The solution for the rational even function of order $(2, 4)$ provides a very tight approximation to the power spectral density and thus higher orders are not essential. This novel method, which is applied here to the power spectral density approximation, could also be adapted to the problem of "shaping filter" design without significant change.

Based on the success of the approximation of a rational function to the power spectral density of a fading channel, we obtained a corresponding transfer function describing a linear system, which is used to generate a fading channel process as its output with a standard Gaussian white noise process as the input. A continuous-time state-space model, described in terms of stochastic differential equations, can be used to represent this linear system. With some manipulation upon time-discretization, we finally obtain a discrete-time state-space model for the flat fading channel, which is illustrated and verified by our simulation. As a simulator of a flat fading channel with an arbitrary power spectral density, the presented discrete-time state-space model based on the novel rational function approximation method is fast, accurate, stable and flexible to the adjustment of parameters, and so has potential for

application in various aspects of wireless communications, such as channel estimation/tracking and channel coding, etc. The significance of the corresponding state space model to channel simulation is that matching its spectral characteristics yields the desired channel uniquely.

One direct application for the state-space model of a flat fading channel is as a channel simulator. There are several approaches for the design of channel simulators. One is based on Clarke's scattering model, while a second is based on transforming the frequency domain to the time domain with IFFT realization. Lastly, a third is based on a filtering-method in the time-domain. Among these available approaches, the presented state-space approach is simple to realize and fast in computation.

Chapter 6

Conclusion

This thesis is devoted to understanding the characteristics of multipath channels. It provides a novel extended channel model and associated statistical analysis, including the introduction of an advanced mathematical tool - stochastic differential equation (SDE), to obtain a fast representation of a state-space model for an arbitrary flat fading channel using a novel linear transfer function design.

The well-known Jakes' spectrum for a flat fading channel has been widely used in wireless communication for more than thirty years. Although used as a theoretical power spectrum in many industry standards, Jakes' spectrum deviates from the measured channel spectrum. Further, Jakes' spectrum cannot adjust its U-shape, in which it has an infinite value around the maximum Doppler frequency. In contrast, the general measured channel spectrum has varying curve shapes and has a vertex around the maximum Doppler frequency. Thus, it is necessary and valuable to provide a new theoretical power spectrum

that more closely approaches the measured power spectrum. In considering the fluctuations of the component phases through a random walk model, absent in the classic Clarke's scattering model, we present a new scattering model for flat fading channel. In this model, the derived power spectrum is able to adjust its shape and vertex value through the control of one special parameter. The resultant power spectrum is more ideal than Jakes' U-shape spectrum as a theoretical power spectrum representing the power spectrum of a wireless channel.

It has long been known that a simple and effective channel model is very important in wireless system design because it has a close relationship with other techniques used in the processes of wireless data transmission and reception. A better channel model used in system design translates directly into better performance of the whole system. Based on the presented scattering model, we have proven that a first-order AR process is a suitable model for flat fading channel without a Doppler frequency shift. Traditionally, an AR process is also used as a dynamic model for a general flat fading channel, while the order of the AR process generally has to be very high to approach the desired fading process. State-space models have recently been used to simulate and model wireless channels [17], though obtaining the coefficients of state-space models for an arbitrary fading channel remains key, as discussed in section 5.3 (see also [30]). This unique challenge in identifying suitable coefficients will remain an interesting topic for future research on the completeness of the mathematical solution to this problem. One of state-space's most valuable benefits is its ability to integrate with other algorithms, such as channel es-

timation and pre-coding, for better performance or optimization. The most difficult part of the state-space approach to arbitrary flat fading channel is the rational transfer function design. This thesis presents a novel rational function designed for general purposes, which is used here specifically for power spectrum approximation. With the relatively low order of the rational function, the new method provides a satisfying accuracy with very fast realization.

This thesis discusses statistical characteristics and modeling for flat fading channel only. However, with appropriate expansion, the theory and methods mentioned in this thesis could be expanded to be used for frequency-selective channels, which are generally considered as a set of independent flat channels with possibly different statistical characteristics. Future work stemming from this thesis should continue to research the statistical characteristics and modeling of frequency-selective channels, as well as to introduce time-varying parameters in the state-space model for non-stationary fading channels.

Bibliography

[1] R. Stratonovich, Topics In The Theory Of Random Noise, v1 and v2, New York: Gordon and Breach, 1963.

[2] S. Rytov, Y. Kravtsov, and V. Tatarski, Priciples of Statistical Radiophysics, New York: Wiley, 2005, vol. 1.

[3] S. Rytov, Priciples of Statistical Radiophysics, New York: Wiley, 2005, vol. 4.

[4] J. La Frieda and W. Lindsey, "Transient analysis of phase-locked tracking system in the presense of noise," IEEE Trans. Inform. Theory, vol. 19, no. 2, pp. 155-165, March 1973.

[5] S. Primak, V. Kontorovich, and V. Lyandres, Stochastic methods and their applications to Communications: SDE Approach. Chichester: John Wiley & Sons, 2004.

[6] V. Kontorovich and V. Lyandres, "Stochastic differential equations: an approach to the generation ofcontinuous non-Gaussian processes," IEEE Trans. Signal Processing, vol. 43, no. 10, pp. 2372-2385, October 1995.

[7] S. Primak, J. Weaver, and V. Kontorovich, "Stochastic differential equations with random structures: a flexible tool for modeling communications problems," DCDIS, pp. 551-570, 2005.

[8] J. Weaver, S. Primak, and V. Kontorovich, "A time-varying stochastic framework for modeling wireless channels," J. Franklin Institute, vol. 344, no. 1, pp. 22-35, January 2007.

[9] Jakeman, E., "On the statistics of K-distributed noise," J.Phys. A13, 31-48 1980

[10] Tough, R.J.A., "A Fokker-Planck description of K-distributed noise," J. Phys. A20, 551-567 1987

[11] Jakeman, E. & Tough, R.J.A., "Non-Gaussian models for the statistics of scattered waves," Adv. Phys. 37, 471 1988

[12] Timothy R. Field and Robert J. A. Tough, "Stochastic dynamics of the scattering amplitude generating K-distributed noise," Journal of Mathematical Physics Vol 44(11) pp. 5212-5223. November 2003

[13] Field, T. R. & Tough, R. J. A., "Diffusion processes in electromagnetic scattering generating K-distributed noise," Proceedings: R. Soc. Lond. A, Mathematical, Physical and Engineering Sciences, Volume 459, Number 2037 / September 08, 2003, p2169 - 2193

[14] Oksendal, B., Stochastic Differential Equations- An Introduction with Applications, 5th Edition. Springer. 1998

[15] C.D. Charalambous, S.M. Djouadi, and S.Z. Denic, "Stochastic power control for wireless networks via SDE's: Probabilistic QoS measures," IEEE Trans. on Information Theory, vol. 51, No. 2, pp. 4396-4401, Dec. 2005.

[16] H. S. Wong, and P. C. Chang, "On Verifying the First-Order Markovian Assumption for a Rayleigh Fading Channel Model," IEEE Trans. On Vehicular Tech., vol 45, NO. 2, May 1996

[17] C. D. Charalambous, N. Menemenlis, "A state-Space Approach in Modeling Multipath Fading Channels via Stochastic Differential Equations," ICC 2001 - IEEE International Conference on Communications, no. 1, pp. 2251-2255, June 2001

[18] Ioannis Karatzas, Steven E. Shreve, Brownian Motion and Stochastic Calculus, Springer-Verlag, 2nd edition.

[19] W. C. Jakes, Jr., Microwave Mobile Communications. New York: Wiley, 1974.

[20] C.C. Tan, N.C. Beaulieu, "On First-order Markov Modeling for the Rayleigh Fading Channel," IEEE Trans. On Communications, vol.48, NO.12, Dec. 2000.

[21] G.E.P. Box, G.M. Jenkins, G.C. Reinsel, Time Series Analysis: Forecasting and Control, Prentice Hall, 1984.

[22] T. Eyceoz, A. Hallen, "Deterministic Channel Modeling and Long Range Prediction of Fast Fading Mobile Radio Channels," IEEE Communications Letters, vol.2, no.9, pp.254-256, Sept. 1998

[23] G.L. Stüber, Principles of Mobile Communication, Kluwer Academic Publisher, 1996.

[24] James K. Cavers, Mobile Channel Characteristics, Kluwer Academic Publishers, Norwell, MA, 2000

[25] T. R. Field and R. J. A. Tough, "Dynamical models of weak scattering," J. Math. Phys. 46, 013302 (2005).

[26] R. H. Clarke, "A Statistical Theory of Mobile Radio Reception," Bell Sys. Tech. J., vol. 47, no. 6, July-Aug. 1968, pp. 957-1000.

[27] T. Feng, T.R. Field, and S. Haykin, "Stochastic Differential Equation Theory Applied To Wireless Channels," IEEE Trans. on Communication, Volume 55, Issue 8, Aug. 2007, pp. 1478 - 1483 .

[28] T. Feng, T.R. Field, "Statistical Analysis of Mobile Radio Reception – an Extension of Clarke's Model," IEEE Trans. Comm., accepted for publication, August 2007 (in production)

[29] R.M. Buehrer, S. Arunachalam, K.H. Wu, A. Tonello, "Spatial channel model and measurements for IMT-2000 systems," IEEE VTC 2001 Spring, vol. 1, pp. 342-346

[30] T. Feng, T.R. Field, "A State-Space Model for Flat Fading Channels with a Novel Method of Rational Function Filter Design," submitted to IEEE Trans. Wireless Comm. (accepted for publishing with minor revision)

[31] K. Steiglitz, "Computer-aided design of recursive digital filter," IEEE Trans. on Audio & Electroacoust., vol. AU-18, pp. 123-129, June 1970.

[32] R.Fletcher and M. J. D. Powell, "A rapidly convergent descent method for minimization," Computer J., vol. 6, no. 2, pp. 163-168, 1963.

[33] Chi-Tsong Chen, Linear System Theory and Design. Third Edition, Oxford University Press US, 1998.

[34] Simon Haykin, and Michael Moher, Modern Wireless Communications,2005 Pearson Education, Inc.

[35] Mark A. Wickert, and Jeff Papenfuss, "Implementation of a Real-Time Frequency-Selective RF Channel Simulator Using a Hybrid DSP-FPGA Architecture," IEEE Trans. on Microwave Theory and Techniques, Vol. 49, NO. 8, Aug. 2001

[36] http://wireless.per.nl/reference/chaptr03/fading/scatter.htm

[37] Le Roux, Y.; Bertel, L. & Lassudrie-Duchesne, P., "Requirements for future models and simulators of the HF transmission channel," Eighth International Conference on HF Radio Systems and Techniques, 2000. (IEE Conf. Publ. No. 474), 353-356, 2000

[38] Wootters, W.K., "Statistical distance and Hilbert space," Phys. Rev. D **23**, p. 357 - 362, 1981

[39] Theodore S. Rappaport, Wireless Communications Principles & Practice, Prentice-Hall Inc., 1996

[40] Siamak Sorooshyari, Introduction to Mobile Radio Propagation and Characterization of Frequency Bands, Course Notes: Wireless Communication Technologies, Rutgers-The State University of New Jersey, USA.

[41] Gans, M. J., "A Power Spectral Theory of Propagatioin in the Mobile Radio Environment," IEEE Trans. on Vehicular Tech., Vol. VT-21, pp. 27-38, Feb. 1972

[42] Buehrer, R.M. Arunachalam, S. Wu, K.H. , Tonello, A., "Spatial Channel Model and Measurements for IMT-2000 System," Vehicular Technology Conference, 2001 Spring. IEEE VTS 53rd, vol.1 pp. 342-346, 2001.

[43] P. Dent, G. E. Bottomley and T. E. Croft. "Jakes Fading Model Revisited," Electronics Letters, 19 (13):1162-1163, June 1993.

[44] M. F. Pop and N. C. Beaulieu. "Design of Wide-sense Stationary Sum-of-sinusoids Fading Channel Simulators," in Proc. of IEEE ICC, Vol. 2, p. 709-716, April 2002

[45] Y. R. Zheng and C. Xiao. "Simulation Models with Correct Statistical Properties for Rayleigh Fading Channels," IEEE Trans. on Comm., 51(6):920-8, June 2003.

[46] Hoeher, P. "A statistical discrete-time model for the WSSUS multipath channel," IEEE Trans. on Veh. Technol., Vol. 41, p. 461 - 468, Nov. 1992

[47] G. D. Durgin, Theory of stochastic local area channel modeling for wireless communication, PhD Dissertation, Virginia Tech, Blacksburg, VA, Dec 2000, Online: http://scholar.lib.vt.edu/theses/available/etd-12012000-191046/unrestricted/etd3.pdf

[48] M. Patzold, "Level-crossing rate and average duration of fades of deterministic simulation models for rice fading channels", IEEE Trans. Veh. Technol., vol. 48, no. 4, July 1999.

[49] Mohammed M. Olama, Seddik M. Djouadi, and Charalambos D. Charalambous, "Stochastic Power Control for Time-Varying Long-Term Fading Wireless Networks," EURASIP Journal on Applied Signal Processing, vol. 2006, Article ID 89864, p. 1-13, 2006.

[50] Smith, J.I., "A computer generated multipath fading simulation for mobile radio", IEEE Trans. on Vehicular Tech., Vol. VT-24, No. 3, pp.39-40, Aug. 1975.

[51] D. J. Young and N. C. Beaulieu. "On the Generation of Correlated Rayleigh Random Variates by Inverse Discrete Fourier Transform," Proc. of ICUPC - 5th International Conference on Universal Personal Communications, vol. 1, Cambridge, Mass., p. 231-235, Sept. 29.-Oct. 2. 1996.

[52] Christos Komninakis and Joel F. Kirshman, "Fast Rayleigh Fading Simulation with an IIR Filter and Polyphase Interpolation," Satellite Communications, Jul 1, 2004.

[53] A. Anastasopoulos and K. M. Chugg. "An Efficient Method for Simulation of Frequency-selective Isotropic Rayleigh Fading," Proc. of Veh. Tech. Conf., Phoenix, Ariz., p. 539-543, May 1997.

[54] K. E. Baddour and N. C. Beaulieu. "Autoregressive Models for Fading Channel Simulation," IEEE Global Telecommunications Conference, Globecom 2001, 2:1187-1192, 2001

[55] Ossanna, Jr., Joseph F., "A Model For Mobile Radio Fading Due to Building Reflections: Theoretical and Experimental Fading Waveform Power Spectra," Bell System Technical Journal, pp. 2935-2971, November 1964.

[56] G.L. Turin, "Communication Through Noisy, Random-Multipath Channels," IRE Convention Record, Part 4, pp. 154-166, 1956

[57] T. Aulin, "A modified model for the fading signal at a mobile radio channel," IEEE Trans. on Vehicular Technology, VT-28(3):182-203, 1979.

[58] K. Pahlavan and A. H. Levesque, Wireless Information networks, New York, Wiley-Interscience, 1995.

[59] T.S. Rappaport, Wireless communications, Prentice hall, 1996.

[60] A.J.Coulson, A.G.Williamson, R.G.Vaughan, "A statistical basis for log-normal shadowing effects in multipath fading channels," IEEE Trans. Commun., vol.46 no.4, pp.494-502, Apr. 1998.